Distribution and sources of PAHs and trace metals in Bull Island, Dublin Bay

Aisling Cunningham BSc

Thesis submitted for the award of MSc

Dublin City University

Supervisor: Brian Kelleher

School of Chemical Sciences

September 2018

Table of Contents

Acknowledgements 3
Abbreviations of key terms 4
Abstract 5
1. Introduction 6
2. Materials and Methods 18
2.1 Study area 18
2.2 Sample locations 19
2.3 Sampling 20
2.4 Sample Preparation prior to extraction for PAH analysis 21
2.5 Accelerated solvent extraction (ASE) method 21
2.6 GC-MS analysis of PAHs 22
2.7 PAH Limit of quantification and Limit of detection 25
2.8 Particle size analysis (PSA) 25
2.9 Elemental analysis 25
2.10 Organic Matter, Moisture content, pH and EC 26
2.11 Metal analysis 26
2.12 Statistical Analysis and Mapping 27
3. Method Development 28
3.1 Extraction Solvent (DCM/Acetone vs DCM alone) 28
3.2 SIM vs TIC for quantification of 16 PAHs 28
3.3 PAH quantification from TLE vs quantification post SPE 29
4. Results 31
4.1 Physical and Chemical analysis of Sediments 31
4.1.1 Particle size analysis 31
4.1.2 Organic matter percentage 33
4.1.3 Total organic carbon and total organic carbon/Nitrogen (C:N) Ratio 34
4.1.4 EC and pH 36
4.2 Polycyclic Aromatic Hydrocarbon (PAH) Analysis of Dublin Bay Samples 38
4.3 Comparative Study of Dublin Bay Sediments 2016/2017 43
4.4 Metal and Elemental results 45
4.5 Statistical Testing 51
5. Discussion 61
6. Conclusion 72
7. Bibliography 74
8. Appendices 90

List of Figures

Figure 1: Position of Bull Island in Dublin Bay, the East coast of Ireland 6
Figure 2: Map of Bull Island, showing major rivers and streams flowing into the sampling zone.. 7
Figure 3: Structures and nomenclatures of 16 PAHs on the US EPA Priority PAH list (Yan et al. 2009). 10
Figure 4: PAH spatial distribution in µg/g in the outer Dublin Bay, image from Murphy et al. (2016). 12
Figure 5: Map of Bull Island showing four sampling zones and flow of tidal water into the study area 18
Figure 6: Map of inner Dublin Bay and identified sampling locations. 20
Figure 7: PAH certified reference standard (CRM) total ion chromatogram (TIC). 23
Figure 8: Naphthalene Mass Spectral fragmentation pattern (from 16 PAH CRM, Figure 7) (TIC). 24
Figure 9: Total lipid extract (TLE) in TIC mode. Example of Bull island sample 36 (no SPE carried out) 30
Figure 10: TIC of Neutral lipid fraction of Bull Island sample 36 (SPE carried out) 30
Figure 11: Percentage Clay distribution map 32
Figure 12: Percentage sand distribution map 32
Figure 13: Percentage silt distribution map 33
Figure 14: Percentage Organic Matter (OM) distribution map. 34
Figure 15: Percentage total organic carbon (%TOC) distribution map 35
Figure 16: Total organic carbon: nitrogen (C:N) ratio distribution map 36
Figure 17: Electrical conductivity distribution map (mS/cm) 37
Figure 18: pH distribution map 38
Figure 19: PAH distribution map (ng/g) 39
Figure 20: PAH isomer pair ratios cross-plot for source identification 42
Figure 21: Sampling Map 2 with 8 sites resampled in 2017 for comparative analysis 43
Figure 22: Calcium percentage distribution map 46
Figure 23: Iron percentage distribution map 47
Figure 26: Chromium distribution map (ppm) 50
Figure 27: Relative concentrations of heavy metals Iron, Aluminium and Calcium in sediment samples 51
Figure 28: PCA conducted on all variables analysed 53
Figure 29: Cluster analysis conducted on individual samples from Dublin Bay 54
Figure 30: PCA according to OM content 55
Figure 31: Total PAH concentration correlated with Pb concentration per organic matter group 58
Figure 32: Total PAH concentration correlated with TOC 58
Figure 33: Pb correlation with TOC 59

List of Tables

Table 1: Analysis carried out in this Bull Island study 17
Table 2: List of 16 PAHs, order of elution and average retention times 24
Table 3: Min and Max individual PAH values in sediments 40
Table 4: Comparative sum PAH levels in sediment samples in 2016 and 2017 44
Table 5: Average Heavy metal concentrations in DB samples (ppm) 45
Table 6: Range and average concentrations of lead and chromium studied in BI, ERL & ERM 51
Table 7: ANOVA results conducted on grouping identified in PCA for PAH results 55
Table 8: One-way ANCOVA analysis (OM vs PAH). 57
Table 9: Pearson's correlation table of all chemical parameters (right) 60

List of Appendices

Appendix 1: Sample GPS coordinates and description 90
Appendix 2: PSA results for Bull Island samples 92
Appendix 3: Organic matter (OM), nitrogen (N), Carbon (C), C: N ratio and TOC results for BI samples 93
Appendix 4: pH and EC values in BI samples 94
Appendix 5: Sum PAH values in BI samples 95
Appendix 6: Loading scores for all tested variables for component 1 and 2. 96
Appendix 7: Loadings scores for component 1 and 2, variables grouped by organic matter content (OM) 96

Acknowledgements

First of all, I thank my primary supervisor Dr. Brian Kelleher, for his continued enthusiasm in my work and encouraging me to pursue postgraduate research. Your ability to view the bigger picture and renew my focus on the task in hand has been magnificent and vital to my success. You believed that I could do it, even when I didn't believe in myself. I faced many hurdles, but the brainstorming and discussions with Dr. Alan Lee, especially towards the end of the project, were incredibly helpful. Working together was vital to the successes of the project. Thank you Murph, Sean and Shane for all of your knowledge and guidance. Thank you to Xavier Monteys from the GSI for your assistance throughout the project. Many thanks to the Irish Research Council and the Geological Survey of Ireland for funding this work.

My friends that I have met in DCU along the way, ye have been my rock! I genuinely could not have gotten up some mornings without the encouragement and friendship of my fellow postgrads and postdocs. Coffee mornings, lunchtime chats and gym sessions together made my days in DCU so much better. Being part of the PGAC was a great experience, I met so many new people and gained so much confidence in myself. I can't name you all, ye know who you are. The postgrad community was like a family to me and I won't forget any of you. You guys are all so awesome! I will really miss you all so much.

Thank you so much to all of the technicians in the School of Chemical Sciences. Veronica, Ambrose, Colm, Nicole, Vinnie, John, Damien and Mary. You all put my mind at ease about demonstrating, dealing with issues and when I was just having a tough ol' day. You guys are also awesome! Giddy Friday and chats at the hatch were the best.

To my lovely housemates, Aaron and Anthony, you guys kept me sane. Sometimes, we could not escape the science in the apartment, but what a lovely time we all had hanging out. Anthony, you have been my housemate, my mentor, my gym buddy, my colleague and most importantly, my friend. It's been so great sharing ideas with you and working together. I've learned so much from you.

And of course, my family and close friends in Bray and elsewhere, knowing that people support me and want me to achieve great things is what drove me to work hard and keep going. At times when I was feeling low, a text or time spent together was the best thing. Steve, Grainne Kim and Kris, I love you guys. Thank you Col for always being there for me, you're the cool Aunt that everyone else wants!

Mum, you inspire me to be the best that I can and to follow my dreams. Dad, you listen to me and encourage me. I'm sorry for the thousands of phone calls and messages, but neither of you would ever give up on me, even when I had given up on myself. Us four 'kids' would not be anywhere near where we are now if it wasn't for you two. I love you both.

I'm not sorry about mentioning you again, but I am so happy and thankful for your fantastic support, love and kindness in the last two years and beyond, Aaron. You always manage to make everything better and I love you for that. We can do it, together.

Abbreviations of key terms

Term	Abbreviation
Accelerated Solvent Extraction	ASE
Analysis of Covariance	ANCOVA
Analysis of Variance	ANOVA
Bull Island	BI
Certified reference material	CRM
Dublin Bay	DB
Elemental Analysis	EA
Electrical Conductivity	EC
Effect Range Low	ERL
Effect range medium	ERM
High molecular weight	HMW
Low molecular weight	LMW
Limit of Detection	LOD
Limit of Quantification	LOQ
Mass Spectrometer	MS
Neutral Lipid (fraction)	NL
Organic carbon	OC
Organic matter	OM
Polycyclic Aromatic Hydrocarbons	PAH
Principle Component Analysis	PCA
Persistent Organic Pollutants	POPs
Particle size analysis	PSA
Total Lipid Extract	TLE
Total Organic Carbon	TOC

Abstract

Aisling Cunningham

Distribution and sources of PAHs and trace metals in Bull Island, Dublin Bay

The objective of this project is to provide a coordinated, chemical and physical characterisation of the sediments and soils of Bull Island and its intertidal area. Data on organic pollutants and on characteristics such as particle size, metal content, pH and percentage organic matter has been recorded and mapped for future use. This data will now act as a baseline for future studies that investigate environmental change over time. Source and distribution of polycyclic aromatic hydrocarbons (PAHs) and metals including iron, chromium, calcium, aluminium and lead were analysed to further understand anthropogenic influence on the area. A range of methods were utilised to quantitatively assess the organic and inorganic input into the bay. Statistical analysis was carried out to determine relationships between variables tested and similarities between samples. Results show that PAHs present in the bay had a common source of combustion, indicating anthropogenic input. Organic matter content and Total Organic Carbon to total nitrogen ratios (C:N) showed that terrestrial material has a large influence on pollution concentration in the area. Principal component analysis (PCA) indicated strong linear relationships between PAH content and total organic carbon (TOC), and also a strong linear trend between lead and TOC. A PAH survey one year later indicates that these results vary over time and that consistent, temporal studies are required to understand the environmental dynamics of the area and to predict coastal change.

1. Introduction

Bull Island (BI) is situated in Dublin Bay on the east coast of Ireland (Figure 1). The area was chosen for study because it displays many of the contemporary management issues affecting Ireland's and international coasts, within a characteristic biogeophysical setting for Ireland. It is also unique in that it is classed as a man-made island as it formed in response to the construction of the Great South Wall in the 1700s and North Wall in the 1800s (Harris 1977).

Figure 1: Position of Bull Island in Dublin Bay, the East coast of Ireland

These walls were built to solve a long-time problem of silting at the mouth of the River Liffey (Figure 2) and increase access to Dublin Port (Lalor 1989; Koutsogiannopoulou & Wilson 2007). The movement of currents in the lagoon changed as a result and much of the silt was diverted from the river course and deposited on the North Bull resulting in the emergence of a true island parallel to the shore (Figure 1). Its growth and direction of expansion was greatly influenced by the volume of sediments, tidal direction, energy of the water system and water depth (Brooks et al. 2016). The evolution of the island involves a combination of constant

destruction and growth, with sediment levels in the sand and *salicornia flats* accreting by 2 mm - 5 mm/year (Harris 1977).

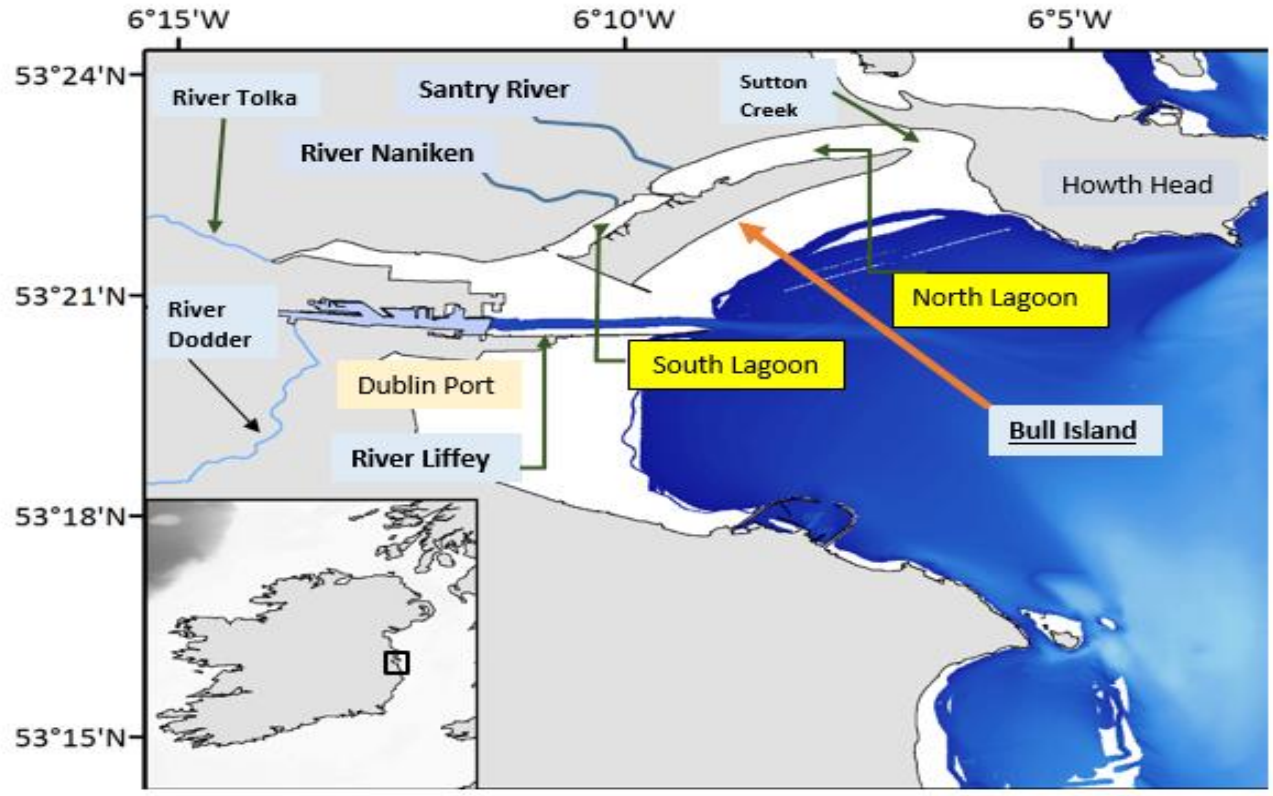

Figure 2: Map of Bull Island, showing major rivers and streams flowing into the sampling zone. Bull island is adjacent to Dublin Port and Howth head in this C-shaped inlet.

Bull Island is unique in its natural resources and attracts a variety of winter fowl annually. At peak feeding times, 40,000 birds have been seen at once on the island (Crowe et al. 2012). In 1981, UNESCO declared Bull Island a biosphere as it had been defined as having "*internationally important habitats and species*" (UNESCO 1995). By 2015, the area included in the biosphere had expanded and includes over 300 km^2 with a population of 300,000 people (Harris et al. 2014; UNESCO 2015). Bull Island is one of five most important wetlands in Ireland, with strong pressure on maintaining the natural habitat for its ecosystem and recreational functions (Crowe & Boland 2004).

Marine ecosystems such as BI provide important environmental functions such as sediment retention, nutrient removal and transformation (Costanza et al. 1997; Gunnell et al. 2013). These coastal systems are sensitive to anthropogenic influence that can lead to habitat destruction and loss, nutrient cycling perturbations and pollution (Bosch & Cooper 2009). BI is susceptible to riverine input from various rivers and smaller streams, with the Santry River being the most influencing on the island (Wilson 2003) (Figure 2). Salt marshes are under threat around the world from land reclamation, industrialisation, sedimentation and other factors (Gunnell et al. 2013).

Research conducted on BI varies from historical studies to pollution research (Wilson 1982 McBreen & Wilson 2006; Koutsogiannopoulou & Wilson 2007; Brooks et al. 2016; Murphy et al. 2016). Much of this research is in response to the attraction of the island for tourism (Brooks et al. 2016) and visiting bird species (Lalor 1989). The soil and sediment in BI is heterogeneous, with a range of sediments and particle sizes present (Brooks et al. 2016).

Hydrocarbon pollution can be from natural seepage (~ 47%) or anthropogenic sources (~ 53%) (Kvenvolden & Cooper 2003). Polycyclic aromatic hydrocarbons (PAHs) are a group of compounds most commonly associated with anthropogenic hydrocarbon pollution (Abdel-shafy & Mansour 2016; Sun et al. 2016; Murphy et al. 2016; Kim et al. 2017). They are persistent organic pollutants (POPs) and have been widely studied due to their ubiquitous and toxic nature in terrestrial and marine environments (Hung et al. 2008; Martinez et al. 2004; Raoux et al. 1999; Song et al. 2002; Wilcke 2000). PAHs are a concern due to their carcinogenic, mutagenic and teratogenic properties (Abdel-shafy & Mansour 2016; Krasnoschekova 1979) and adverse influence on marine biota (International Agency for Research in Cancer 1983; McCready et al. 2004; Woodhead et al. 1999).

As a result a group of 16 PAHs are listed as priority pollutants and their structures can be seen in Figure 3 (EU 1976; EU 1980). Anthropogenic PAH sources include combustion of

fossil fuels, vehicle emissions, petrochemical spills and burning of biomass (Hung et al. 2008; Simoneit 1989). PAHs interact with the marine system by gas exchange at the air water interface, or via dry soot deposition or precipitation. Once in the water they bind to particulate matter and accumulate in sediment (Oros & Ross 2004; Murphy et al. 2016). The Irish EPA enforce the EU's Water Framework Directive by monitoring over 200 priority substances including 8 PAHs (European Union and European Parliament 2000). These compounds are stable, lipophilic, hydrophobic and have been shown to survive in ancient sediments (Killops & Killops 2005).

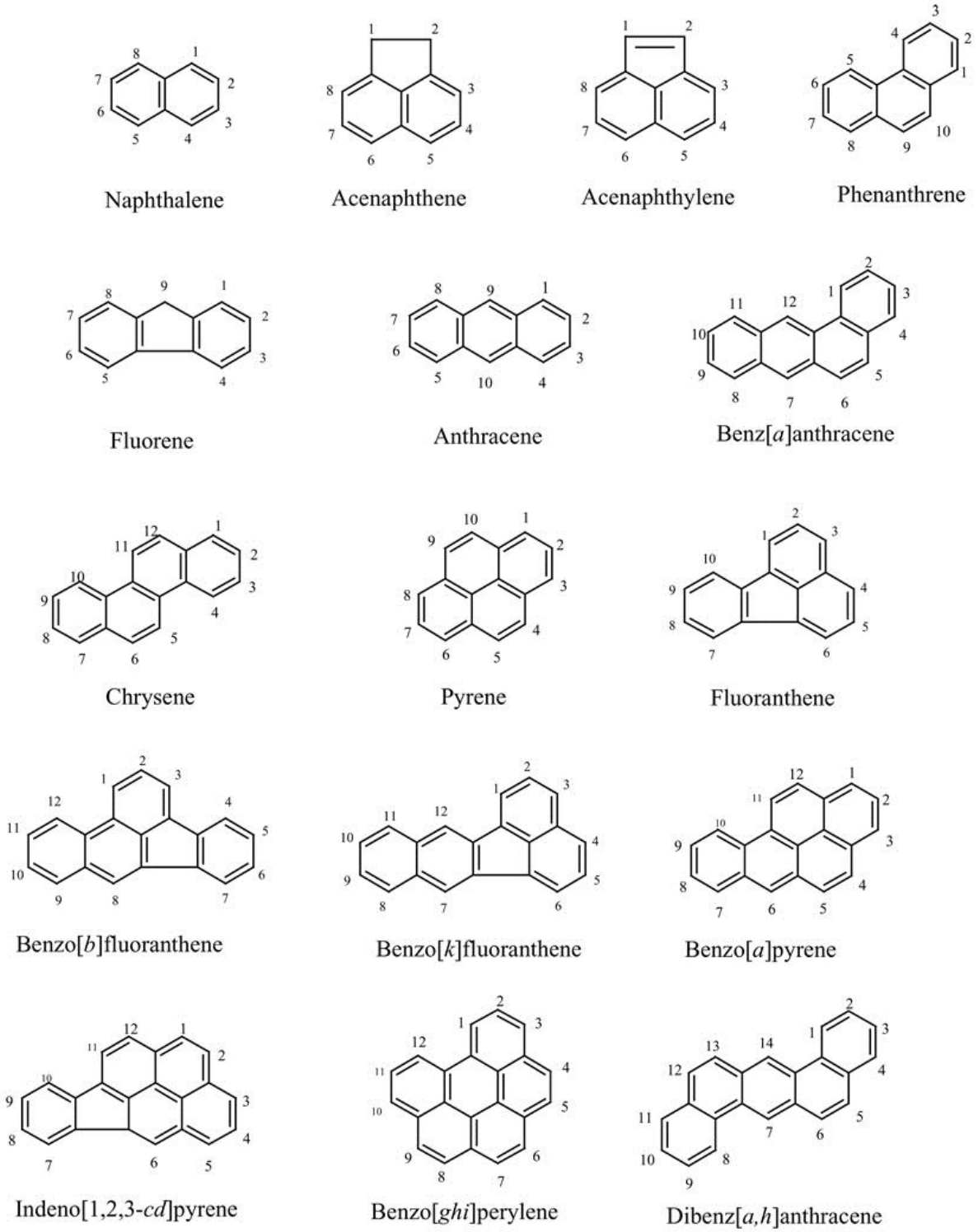

Figure.3: Structures and nomenclatures of 16 PAHs on the US EPA Priority PAH list (Yan et al. 2009).

The strong lipophilic tendencies of these compounds allows them to be stored in the fatty tissues of mammals and to travel through the food chain (Rengarajan et al. 2015). Although PAHs are mainly anthropogenically-produced, they can occur naturally in soils and events such as volcanic activity or natural seepage from oil and coal stores can release PAHs into the environment (Abdel-shafy & Mansour 2016). It has also been shown that salt marsh areas similar to BI have a high capacity for containment of PAHs due to the sequestration of organic contaminants in salt marsh plants (Gonçalves et al. 2016).

PAHs were recently analysed in the sediments of the greater Dublin Bay (Figure 4), adjacent to the sampling area in this study (Murphy et al. 2016). High molecular weight PAHs with 4 and 5-ringed compounds were prevalent. The source of PAHs in the bay was shown to be primarily from atmospheric deposition, with a PAH range from 12 ng/g to 3072 ng/g (Figure 4). The toxicity of PAHs in sediments can be evaluated by ERL (effect range low) and ERM (effect range medium) values suggested by Long et al (1998) of 0.55 µg/g and 3.17 µg/g respectively. Concentrations of PAHs in marine sediments over the ERM have potential for biological toxicity. In the study by Murphy et al. (2016), the average PAH levels for the bay were below the ERL but PAHs were not evenly distributed throughout the sampling area (Figure 4). 10 individual sample stations exceeded the ERL with some sample sites with a total PAH concentration of 3.072 µg/g which is close to the ERM.

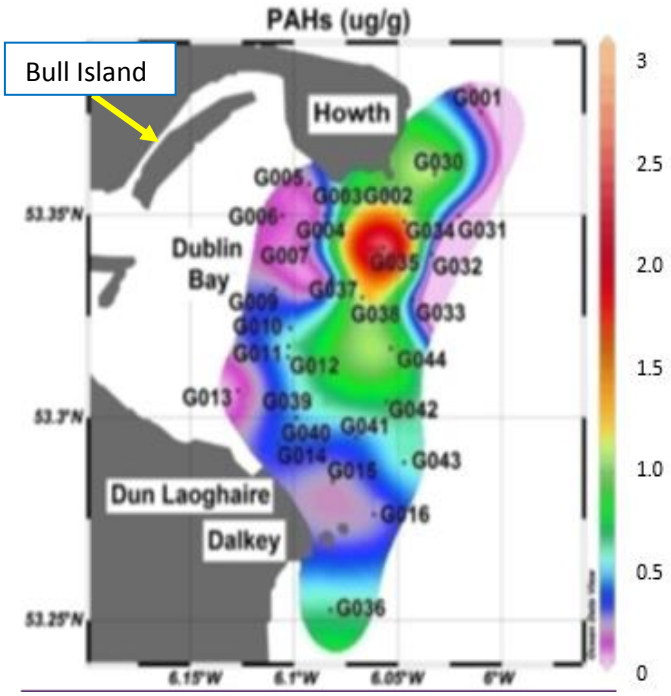

Figure 4: PAH spatial distribution in µg/g in the outer Dublin Bay, image from Murphy et al. (2016). Bull Island can be seen on this map, to the left of the sampled zone.

Furthermore, in a study of organic pollutants in Dublin City and its environs (Andersson et al. 2011) it was found that the soils of the inner city had highest concentrations of all 16 PAH compounds that were determined. PAHs were detected across the city, with maximum concentrations, over the ERM, occurring in the city centre (63,000 ng/g). This was attributed to historical sources of domestic coal burning and industrial emissions but it was deemed likely that PAH concentrations would decline gradually over time in response to the bituminous coal ban put in place in Dublin in 1990. Unfortunately, PAHs were not studied on Bull Island.

Metals are present in the marine sediments either naturally or through industrial activity (Rashdi et al. 2015; Reimann & Caritat 2000). Lead is an important environmental contaminant and is known to cause developmental complications in children, with lead-based paint being the most common source (Tiwari et al. 2013). Other sources include waste incineration (there is a new incineration facility in Dublin Port (https://www.dublinwastetoenergy.ie/)), sewage

sludge, fires, natural sources and electronic wastes. Both chromium and lead are listed as priority pollutants due to their known toxicity and have been shown to have carcinogenic properties, over a concentration of 0.015 ppm (Environmental Protection Agency Ireland, 2006; U.S. Department of Health and Human Services 2002).

Chromium is essential for humans in its Cr(III) form but is toxic in its other main, more soluble form; Cr(VI) (Vajpayee et al. 1999). Anthropogenic sources include the chemical industry, sewage sludge, waste incineration and some phosphorus fertilisers (Sedman et al. 2006). It also occurs naturally. The length of time that metals remain in sediment depends on many variables such as their chemical and sediment properties such as particle size (Molamohyeddin et al. 2017).

Andersson's study (2011) showed that Bull Island contained high levels of hexavalent chromium and lead (Andersson et al. 2011). Background levels of chromium and lead were established in non-contaminated sites as; 21-59 ppm and 30-120 ppm respectively. Samples from North Dublin, taken from Santry had lead levels of 663 ppm, more than 5 times that of the background levels. The Santry river flows into Bull Island (Figure 2), providing a possible source of lead to the island. These values are notably above the median values for lead (102 ppm) and chromium (59 ppm) in European soils (Luo et al. 2012) and lead also exceeded the recommended levels for soil of sustainable quality (85 ppm) (Dutch Ministry of Housing Spatial Planning and Environment (VROM) 2000). Lead can be found in a variety of matrices including plants (Sharma & Dubey 2005) and mammals (Neathery et al. 1975), with the accumulation of lead common in the upper layers of sediments (Auber and Pinta 1977).

High concentrations of anthropogenically-produced metals are expected in localised areas of urbanisation and industrialisation (Al-Masri et al. 2006) and as seen in the Dublin Soil Urban Geochemistry (SURGE) Project (the first in-depth baseline geochemical study of top

soils in the greater Dublin area), they generally decreased with distance away from industrialised areas (Glennon et al. 2014).

Iron plays a large role in the cycling of sulfur, phosphorus, carbon and many other trace elements in marine sediments as it can be present in several forms of reactive oxides (Wei-wei et al. 2018). Available iron in sediments can be toxic to human and marine life (Murad & Fischer 1988). The National soil database project mapped iron concentrations across Ireland and found average concentrations of iron between 20,100 ppm and 25,000 ppm in County Dublin (Fay. et al. 2007). Iron is a micronutrient that has an influence on ocean primary productivity and is an important component of the ocean's biogeochemical cycles (Tagliabue et al, 2017). It has also been strongly associated with the carbon cycle and organic ligands can control the concentration of dissolved iron in seawater. Furthermore, a major role for iron in the preservation of organic matter in sediments has recently been shown and it was suggested that since reactive iron can be stable over geological timescales, it could be an important factor in the long-term storage of carbon (Lalonde et al, 2012).

Calcium (Ca) is naturally ubiquitous and necessary for fundamental cellular functions within plant cells. It plays a specific role in cell division, plant defence and response to stress (Candan & Tarhan 2005), although very small concentrations of Ca^{2+} are necessary for these basic functions. Higher concentrations of Ca^{2+} can be detrimental in cells, causing oxidative stress and affecting chlorophyll necessary for photosynthesis (Candan & Tarhan 2005; Tanaka & Tsuji 1980). Aluminium (Al) is also naturally ubiquitous but can be toxic to aquatic life such as invertebrates at high concentrations by inhibiting metabolic processes (Rosseland et al. 1982). It can accumulate in plants leading to increased risk of transport of the metal up the food chain (Mossor-pietraszewska 2001). High concentrations of Al can depress the absorption of necessary elements into plants through the root systems (Fay. et al. 2007; Mossor-

pietraszewska 2001). The concentration of Al necessary to affect the growth of a specific plant depends on the susceptibility of the plant, the pH and other environmental stresses.

The effects of climate change have already been seen globally (IPPC 2014a), with predictions of higher rainfall and an increase in storms modelled for Ireland in the future (Dwyer 2012). Aeolian and marine movements are causing a continuous accretion of sand deposits in the sand dunes in BI whilst simultaneous erosion of the island's coastline is occurring (Gibson et al 2012). Coastal progradation was estimated by Gibson et al (2012) at ca.2.4 m/year in the south region of the island and 0.55 m/year on the northern parts of the island suggesting constant change in the area. In recent years, scientists and policymakers have pushed to highlight and protect carbon stored in coastal wetlands, known as *blue carbon* (Tollefston 2018). Blue carbon is the term for carbon sequestered by the world's ocean and coastal ecosystems. Tidal wetlands and coastal vegetated habitats have a very high capacity for the uptake and long-term storage of carbon (Kelleway et al. 2017). Estimating the quantity of carbon stored in coastal wetlands globally is challenging but understanding the rate of carbon sequestration, although difficult, would allow us to predict and manage the carbon storing capabilities of these ecosystems. We know that the high capacity for carbon storage is a result of at least three characteristics of coastal wetlands:

1. They can efficiently assimilate particulate carbon originating from within the ecosystem (autochthonous) and/or from external sources (allochthonous) (Kennedy et al. 2010).
2. Plants growing in these environments are very productive in converting CO_2 into plant biomass C (Alongi 2002; Nixon 1980) and;
3. The biogeochemical conditions within sediments lock carbon in by slowing the decay of organic material (Fourqurean et al. 2012; Kristensen et al. 2008; McLeod et al. 2011).

This means that carbon in such settings can accumulate for centuries but will be very much influenced by coastal change brought on by processes such as sea-level change, ocean acidification and increased flooding.

Coastal systems respond to natural and anthropogenic forces that pose significant threats to sustained societal and economic development such as climate change and sea level rise (IPCC 2012; Gibson et al. 2012). Combined processes drive increasingly intense storms, flooding events, and erosion, which adversely affect economic activity and have serious consequences for impacted communities, and which are expected to worsen over time (Kantamaneni et al. 2018; Bevacqua et al. 2018). BI has a large salt marsh zone (Figure 5). Salt marshes are very important environments globally as they provide a barrier between coastal waters and terrestrial land, a sink for pollutants and an ecosystem for wildlife (Sivaperuman & Venkatraman 2015).

Assessment and prediction of coastal vulnerability can only be achieved by the systematic and sustained monitoring of the physical, chemical and biological processes that occur in coastal zones. Integration of multi-disciplinary tools is required to address important societal challenges such as coastal vulnerability, port security and marine pollution (Angelini et al. 2018; IPPC 2014). Here we conduct a spatial characterisation of soils and sediments from BI that are then mapped to provide a snapshot of chemical and physical conditions on the island in 2016. These maps are then used, together with statistical analysis to look for information on the sources and fate of pollutants, natural organic matter and metals. Lastly, some sediments were sampled a year later and analysed for PAHs to investigate temporal change. A summary of analysis carried out is shown in Table 1.

Table 1: Analysis carried out in this Bull Island study

Physical analysis	Chemical analysis
• Particle Size Analysis (PSA):	• Total nitrogen content (%TN)
○ % Clay	• Electrical conductivity (EC)
○ % Silt	• PAHs
○ % Sand	• Total organic carbon content (%TOC)
• Average Particle Size	• Fe, Cr, Al, Cr, Pb, Ca
	• pH
	• Organic matter content (%OM)

2. Materials and Methods

2.1 Study area

Bull Island (Figures 1, 2, 5 and 6) is a 4.85 km long man-made sand island, situated in Dublin Bay on the East coast of Ireland. North BI grew parallel to the shore in a C-shaped inlet. The formation (and continual advancing) of the island involves a combination of constant destruction and growth. The sediments in Bull island and its surrounds are heterogeneous and can be divided into four zones; mudflat, salt marsh, the island and the intertidal zone (Figure 5). The inner area adjacent to the mainland is influenced by tidal action, with sandy beaches and mudflats becoming exposed at times of low tide (NPWS [National Parks and Wildlife Services] 2014). The water flow around BI is clockwise, North to South (Harris 1977; Brooks et al, 2016). This simple concept of water flow has been complicated due to the construction of the walls surrounding BI and also influenced by the headlands of the Bay (see Figure 5 for flow of tidal waters in the study area).

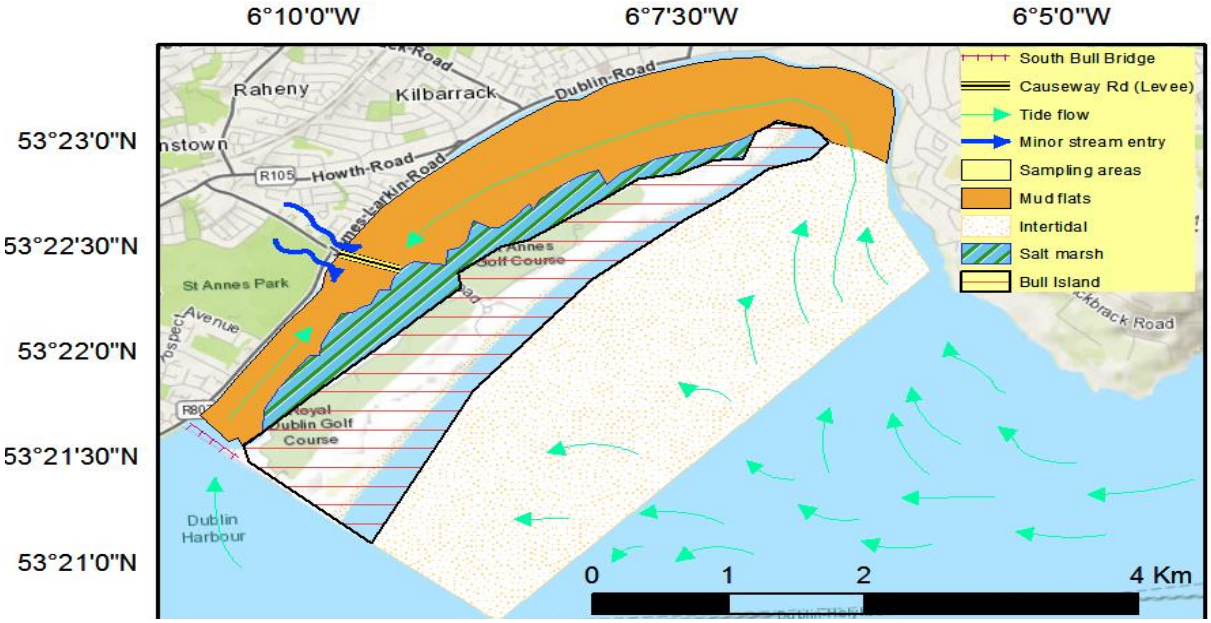

Figure 5: Map of Bull Island showing four sampling zones and flow of tidal water into the study area

Lagoons between BI and the mainland receive and supply water through two channels. The River Naniken flows into the southern lagoon, whereas the northern lagoon transfers water to and from Sutton Creek, with the Santry River having a small impact on the water flow in this area (Figure 2) (Brooks et al. 2016).

Two rivers enter the Irish Sea via Bull Island. The Santry and the Naniken River flow into the lagoon, accompanied by other, smaller streams (Figure 2). Nutrient input into the BI lagoon has been a major problem in the past, with the main sources including sewage discharge and input from rivers (Wilson 2005). The wastewater treatment plant in Ringsend is unable to accommodate the rising population levels, so although the sewage treatment process has improved in the last 10 years, the release of sewage poses a risk to flora and fauna in the biosphere (Dublin City Council (DCC) 2013). Bull Island is adjacent Dublin Port (Figure 2), the busiest port in Ireland, which contains several other industries including a wastewater treatment plant and a waste-to-energy incinerator.

2.2 Sample locations

Sampling locations were generated using ArcGIS (version 10.4) and R statistical programmes (Figure 6). The GRTS (Generalised Random Tessellation Stratified) package in R was used to generate the sampling locations (Stevens & Olsen 1999). Using ArcGIS, the sampling area was divided into four sampling areas; Bull Island, the mudflats, salt marsh and intertidal regions (Figure 5). Samples were then divided unequally into each sampling area. A higher number of samples was allocated to the mudflat and salt marsh areas where organic matter was expected to be higher, compared to the intertidal samples, beyond the island. Sample numbers were allocated as follows: mudflats 20, salt marsh 15, Bull Island 10 and intertidal 10. Coordinates and sample descriptions are listed in Appendix 1. As the large majority of the study area gets completely covered in tidal water, an error diameter of 5 metres

from each sampling point was chosen in order to allow for large objects, for example stones, and inaccessible sample points.

Figure 6: Map of inner Dublin Bay and identified sampling locations.

2.3 Sampling

The majority of samples were taken on foot, using a handheld Garmin eTrex 20x GPS and photos were taken of each sample area and given a unique sample code. A 10cm x 10cm x 10cm sample point was marked out using a trowel, which was rinsed well deionised water, then with acetone before each use to remove any traces of organic matter, that can cause contamination. At each sample point, 2 samples were taken. One sample from each site was stored in a pre-labelled plastic bag for physical, non-organic analysis and another was stored in an inert pre-furnaced jar, with a PTFE lined lid for organic analysis. All sampling equipment was cleaned between each sampling point to prevent any cross contamination of samples. Sampling of the intertidal area was carried out on a small research vessel. Samples were transported back to the lab and stored at -20°C until analysis.

2.4 Sample Preparation prior to extraction for PAH analysis

Samples of between 3 g and 7 g were air-dried (room temperature ~20°C), sieved (40 mm mesh) and homogenised prior to extraction. The mass of sample extracted depended on the organic matter (OM) content of individual samples. Sample weights between 3-5 g were suitable for higher OM samples (≥20% OM) and samples mostly consisting of sand, and 5-7 g of sample was extracted for samples of low OM content (≤20% OM), as more sample was required to show sufficient peaks of PAHs on the GCMS software. Final quantification was adjusted to reflect initial extraction quantities. All samples were extracted in triplicate. 40 ml amber glass collection vials were pre-furnaced before use. A new, unused PTFE-lined septum was used for each collection vial to avoid cross contamination.

2.5 Accelerated solvent extraction (ASE) method

Sediment samples were extracted using a Dionex Accelerated Solvent Extractor (ASE) (model 200) instrument. This automated system extracts organic compounds from sediment samples using HPLC and GC grade solvents (>99% purity). 33 ml extraction cells were used for analysis, using pre-furnaced sand as a packing material (furnaced at 500°C for 6 hours, to remove all organic matter). This automated system extracts organic compounds from sediment samples using HPLC and GC grade solvents (>99% purity). Dichloromethane (DCM) was heated to 100°C and drawn through 33 ml stainless steel extraction cells under high pressure (1500 psi) to enhance extraction. The extraction of PAHs involved an initial preheat of 1 min, heat at 100°C for 5 min and static for 6 mins and included a 60 % flush volume and a last purge of 60 seconds (Heemken, 1997). Each extraction cell was extracted for 1 full cycle, allowed to cool to room temperature, then stored upright at -30 °C until analysis. A PAH recovery experiment was carried out before further analysis of the samples via this method. Previously tested, PAH free sediment samples were spiked with the following deuterated PAH standards;

naphthalene (d8), acenaphthene (d10), anthracene and perylene (d12) giving a recovery range of 75 - 100 %. Recovery was determined using a range of sediment types (sand, mud and sandy mud) to gain an accurate recovery percentage for the heterogeneous samples from Dublin bay.

Post extraction, samples were dried, using a rotary evaporator to 1 ml in pre-furnaced round-bottom flasks at a temperature of 25°C. Once the volume of sample reached roughly 1 ml, the contents of the round-bottom flask were transferred to a 1 ml volumetric flask, using a furnaced glass syringe, to ensure that the samples were made up to exactly 1ml for quantitative purposes. Finally, the 1 ml samples were transferred into pre-labelled GC vials and a spatula tip full of activated copper was added to the extracts to remove sulphur**.** The 1 ml extracts were shaken for 24 hours in the dark and were then subsampled and stored for analysis.

2.6 GC-MS analysis of PAHs

Analysis of samples was carried out on a gas chromatograph mass spectrometer (GC-MS) (Agilent 5975C Quadrupole MSD with triple axis detector), along with an auto-sampler system. A HP5MS fused silica (Agilent) column was used (30 m x 0.25 mm i.d) with a film thickness of 0.25µm. Helium of ultra-high purity was the carrier gas and had a flow rate of 1ml/min. 1 µL of sample was injected the injector port, which was set at 250 °C with a 2:1 split injection, the initial oven temperature was 70 °C for 0.5 min and increased at 10 °C/min to 300 °C and held for 20min; with a total run time of 45 min. The GCMS interface and the ion source were set at 300 °C and 230 °C respectively. Selected ion mode (SIM) was used for identification of the 16 PAHs (this method was chosen post method development, explained in Section 3). A filament delay of 6 minutes was used. The mass spectrometer (MS) uses electron impact mode with ionisation energy of 70 eV and a mass scan range set from 30 to 650 Da. 5α-cholestane was the internal standard for all samples.

In BI sediment samples, the 16 priority PAHs were quantified using the cholestane internal standard and a calibration curve produced from a 16 PAH certified reference material (CRM) standard. Chromatogram analysis was carried out using Chemstation software (Agilent). NIST, Petrochem and Wiley spectral libraries were used to identify compounds. Structures were confirmed using the literature and Ion extracted chromatograms in Chemstation. SIM mode was used to quantify 16 PAHs. Limits of detection (LOD) and limits of quantification (LOQ) for the classes of PAHs ranging from 2 benzene rings to 6-benzene ringed compounds were calculated from these calibration curves. Figure 7 shows the 16 PAH CRM total ion chromatogram (TIC) and Figure 8 shows the mass spectral fragmentation pattern of naphthalene, a 2-ring PAH commonly occurring in BI samples. Table 2 shows the elution order and retention times of the priority 16 PAHs tested in this study.

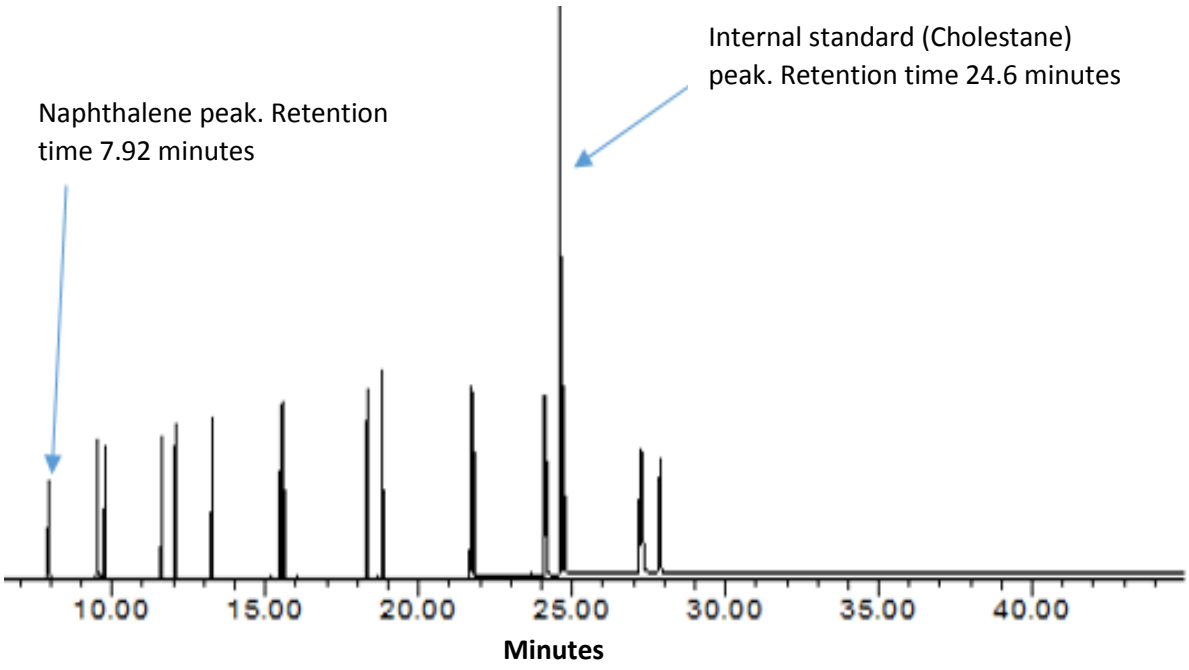

Figure 7: PAH certified reference standard (CRM) total ion chromatogram (TIC). The first peak at 7.94 minutes was identified as Naphthalene using the MS software. The second and third peaks are 2- and 3-methyl-napthalene that were not quantified in this study. The remainder of peaks are referred to in Table. 2.

Table 2: List of 16 PAHs, order of elution and average retention times

Order of Elution	Compound	Retention Time (minutes)
1	Naphthalene (peak 1 in Fig. 7)	7.94
2	Acenanaphthylene	11.59
3	Acenaphthene	12.05
4	Fluorene	13.25
5	Phenanthrene	15.43
6	Anthracene	15.53
7	Fluoranthene	18.25
8	Pyrene	18.8
9	Chrysene	21.62
10	Benz (a) anthracene	21.7
11	Benzo (k) fluoranthene	24.08
12	Benzo (b) fluoranthene	24.13
13	Benzo (a) pyrene	24.74
14	Indeno (1,2,3,- cd) pyrene	27.1
15	Dibenz (ah) anthracene	27.17
16	Benzo (ghi) perylene	27.71

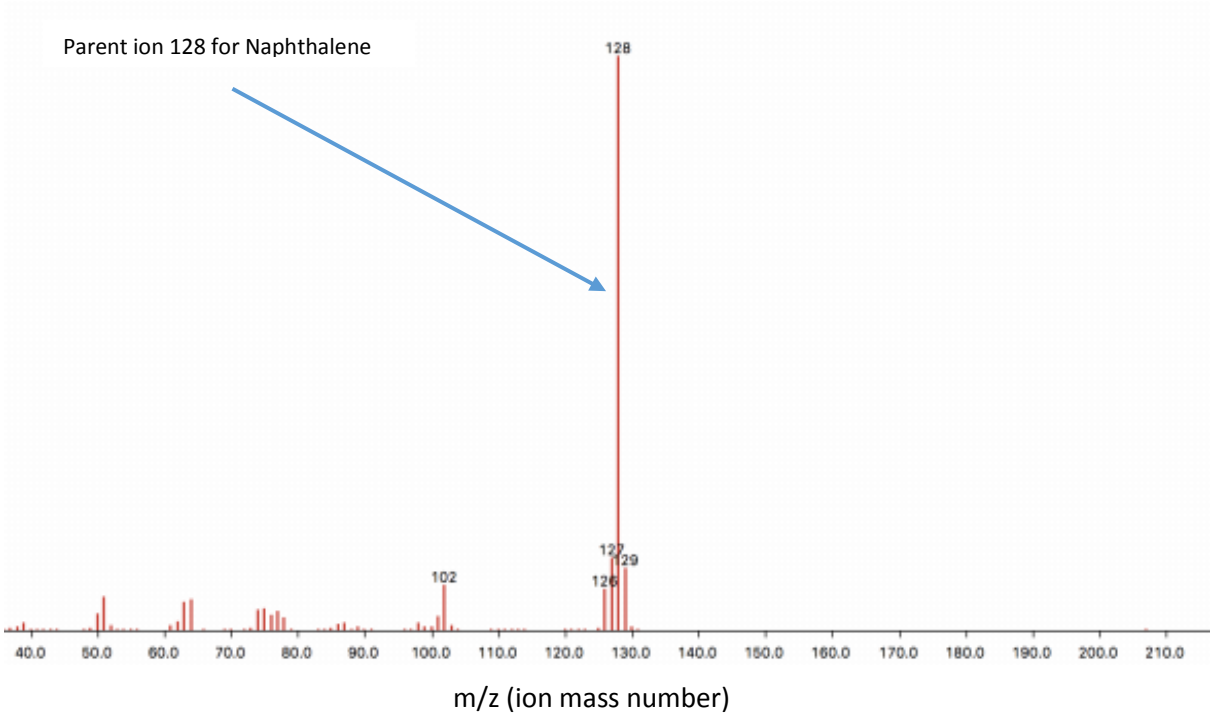

Figure 8: Naphthalene Mass Spectral fragmentation pattern (from 16 PAH CRM, Figure 7) (TIC).

2.7 PAH Limit of quantification and Limit of detection

The limit of quantification (LOQ) and limit of detection (LOD) was calculated for each group of PAH compounds according to the number of benzene rings (see Equation 1 and 2 below). A LOQ and LOD was determined for 2 ring PAHs using naphthalene, fluorene (3-ring), phenanthrene (4-ring), pyrene (5-ring) and benzo (ghi) perylene (6-ring). The LOQ for each PAH ranged from 22.50 ng/g (all 5 and 6-ring PAHs) to 67.50 ng/g (fluorene). The LOD ranged from 7.43 ng/g (all 5 and 6-ring PAHs) to 22.20 ng/g (fluorene). The LOQ and LOD were calculated using Equations 1 and 2 (ICH 2005);

$$\text{LOD} = \frac{\text{Average standard deviation of 5 peaks of a compound (e.g fluorene)} \times 3.3}{\text{slope of calibration curve}} \qquad \text{Equation 1}$$

$$\text{LOQ} = \frac{\text{average standard deviation of 5 peaks of a compound (as above)} \times 10}{\text{slope of calibration curve}} \qquad \text{Equation 2}$$

2.8 Particle size analysis (PSA)

PSA analysis was carried out on a Malvern Mastersizer 2000 laser diffraction particle size analyser system. This instrument determines particle size by independent laser class analysis and allocates the percentages of clay, silt and sand present in a given sample., along with the average grain size of a given sediment sample. Sediment types can vary between poorly sorted to well sorted grains. All BI samples were sand based, with a variance in the sorting and mud percentages. Sediment samples were sent to University College Cork for analysis.

2.9 Elemental analysis

An elemental analyser (EA) (Fisons model NA 1500 NCS, series 2) was used to determine the percentage composition of carbon, hydrogen and nitrogen (CHN). A reaction tube facilitates the measurement of these elements using Helium as the carrier gas. For CHN analysis, air dried, ground and sieved BI samples of 4.0 - 5.0 mg were weighed out and placed

into tin boats and inserted directly into the EA auto-sampler for analysis. The run time for 1 sample is 10min. Total organic carbon (TOC) was determined by acidifying the homogenised sediment samples with 2M HCL. 4.0 - 5.0 mg of sample was weighed into silver, acid resistant capsules, and placed into the oven at 80°C to remove all inorganic carbon, prior to placing onto the auto-sampler of the EA. All samples were analysed in triplicate.

2.10 Organic Matter, Moisture content, pH and EC

Organic matter percentage was determined by loss on ignition heating 3-5 g dry weight of sample in ceramic crucibles at 550°C for 8 hours (Hoogsteena et al. 2015). The samples were weighed using an analytical balance before and after being heated to determine the exact loss of mass. Percentage moisture was also determined using this method. Samples were run in triplicate. The 5:1 method of water to sediment was used for pH and elemental composition (EC) analysis (ISO 10390:2005). 5-parts deionised water to 1-part sample by volume was mixed then placed into a clean reagent bottle and shaken for 1 hour on a horizontal shaker at 160 strokes/min. Samples were allowed to settle, and pH was determined using a bench top pH probe. Samples were filtered before EC analysis.

2.11 Metal analysis

The metals aluminium (Al), calcium (Ca) and iron (Fe) chromium (Cr) and lead (Pb) were extracted for analysis after digestion in 2M Aqua Regia (nitric acid and hydrochloric acid mixture) for 2 hours at 108°C. For each sample 0.5 g of dried, ground with a pestle and mortar, and sieved (2 mm) sample was weighed out and 5 ml of Aqua Regia was added to the digestion tube. After digestion was complete samples were cooled and filtered through Whatman 1 filter paper. The samples were then diluted to 25 ml for heavy metals and 50 ml for metals. Analysis was conducted via ICP-OES (model Varian Vista MPX). Due to samples having very high

levels of silicates and carbonates samples were also analysed using XRF (model Niton XL3t) due to potential possible interferences when analysing for multiple elements with ICP.

2.12 Statistical Analysis and Mapping

The mapping of all parameters were produced using ArcGIS software (10.4) using inverse weighting distance interpolation techniques (IDW). IDW assumes that the sample points closer together have more of an influence on each other, in comparison to the points that a further away. Principle component analysis (PCA) was carried out using PAleontological STatistics (PAST) (V3.17) on all multi-variable data (Hammer et al 2001). PCA was used to relate data sets to determine relevant associations between components based on individual sample results. Due to the large variation in data, hierarchical cluster analysis was then applied to identify clusters with similar properties (results in section 4). ANOVA (analysis of variance test) was then conducted on these clusters using the mean average of PAH concentration to investigate a potential significant difference between each cluster. A further PCA was then conducted on sample groups after the individual samples were grouped based on OM content. This was done to investigate if samples with similar OM were closely related. One-way ANCOVA (analysis of covariance test, carried out after ANOVA) was then conducted to investigate if a linear relationship between OM and PAH existed and if not where there was a significant difference between OM and PAH concentration. Statistically significant correlations between PSA, PAHs, Metals, %OM and %TOC were established using Pearson's correlations in PAST and a stepwise regression analysis was conducted using R Statistics (version 3.4.3) to identify the variables that were most closely related to PAH concentration. Cross-plots were constructed in PAST software.

3. Method Development

Method development was carried out during the extraction stage of PAH analysis and also during quantifications. Extraction parameters and experimental variables were altered to quantify PAHs as accurately and efficiently as possible. The method development for this project involved three steps.

3.1 Extraction Solvent (DCM/Acetone vs DCM alone)

A variety of solvents have been used in past research to analyse PAHs in environmental samples (Saim et al. 1998; Arienzo et al. 2017). The samples in this project vary in geochemical properties such as particle size, organic matter, carbon content, pH and EC. Thus, some samples may not be optimally extracted with a particular solvent. Initially, samples were extracted using a 50:50 mix of Acetone/DCM as carried out by Saim et al. (1998). This resulted in a reaction of some samples with the mixture of solvents, causing a cloudy precipitate to form at room temperature. The same samples were further extracted using dichloromethane (DCM) alone as a comparison, with no precipitation forming, so DCM was chosen as the only solvent required for extraction of PAHs as it gave a cleaner extract. There are a number of variables that can be altered in the extraction using an ASE instrument, including solvent temperature, number of cycles in a run and extract volume. A recovery experiment determined that no other adjustments needed to be carried out to improve extraction.

3.2 SIM vs TIC for quantification of 16 PAHs

The samples collected from BI were very heterogeneous, visually. Samples varied in colour, from dark brown-black, thick, heavy mud samples, to light brown samples mainly composed of sand. It was clear that samples differed from the time of sampling and that analysis may prove difficult. Samples were first analysed on the GC in total ion chromatogram (TIC) mode, which shows all visible peaks detected. When samples were run in TIC mode there were

a large number of peaks, sometimes overlapping, which made it harder to identify the 16 PAHs. This is an acceptable method to use when quantifying a very clean sample, containing only a defined number of peaks that are separated well, for example TIC mode was sufficient when looking at the 16 PAH CRM as in Figure 7. In order to easily detect theses PAHs from the environmental samples, selected ion mode (SIM) was used with great success as the peaks were much easier to identify.

3.3 PAH quantification from TLE vs quantification post SPE

The accuracy of sample quantification can also be compared before and after a clean-up step such as solid phase extraction (SPE). Total lipid extracts (TLE) were fractionated into neutral lipid (NL) fraction by extraction with chloroform by solid phase extraction (SPE). The filter size was 40 µm and SPE Bond Elut NH_2 cartridges of 3 ml volume were used. Addition of chloroform extracts the NL fraction from the total lipid extract. Figure 9 and 10 show chromatograms of a TLE and NL extract from a Bull Island sample (sample ID: 36). The outcome of this comparison is that the SPE step reduced the background noise of the chromatogram slightly, but there was still a presence of other peaks that were extracted by chloroform into the neutral lipid fraction, other than the 16 PAHs. It was thus decided that it was not necessary to spend time carrying out SPE. It was decided that the first extraction of the TLE, analysed by SIM mode, is still a preferred method for this study, as peaks are visible and quantifiable as was seen in other studies (Yang et al. 2018; Wallace et al. 2017).

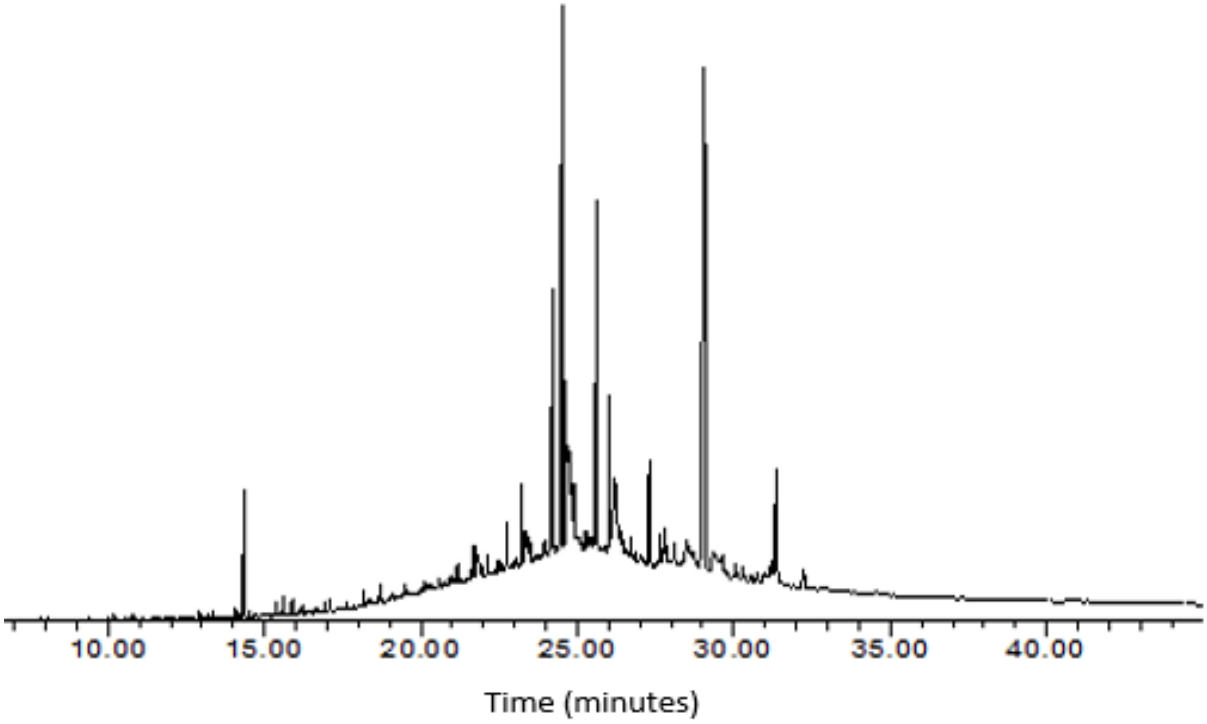

Figure 9: Total lipid extract (TLE) in TIC mode. Example of Bull Island sample 36 (no SPE carried out)

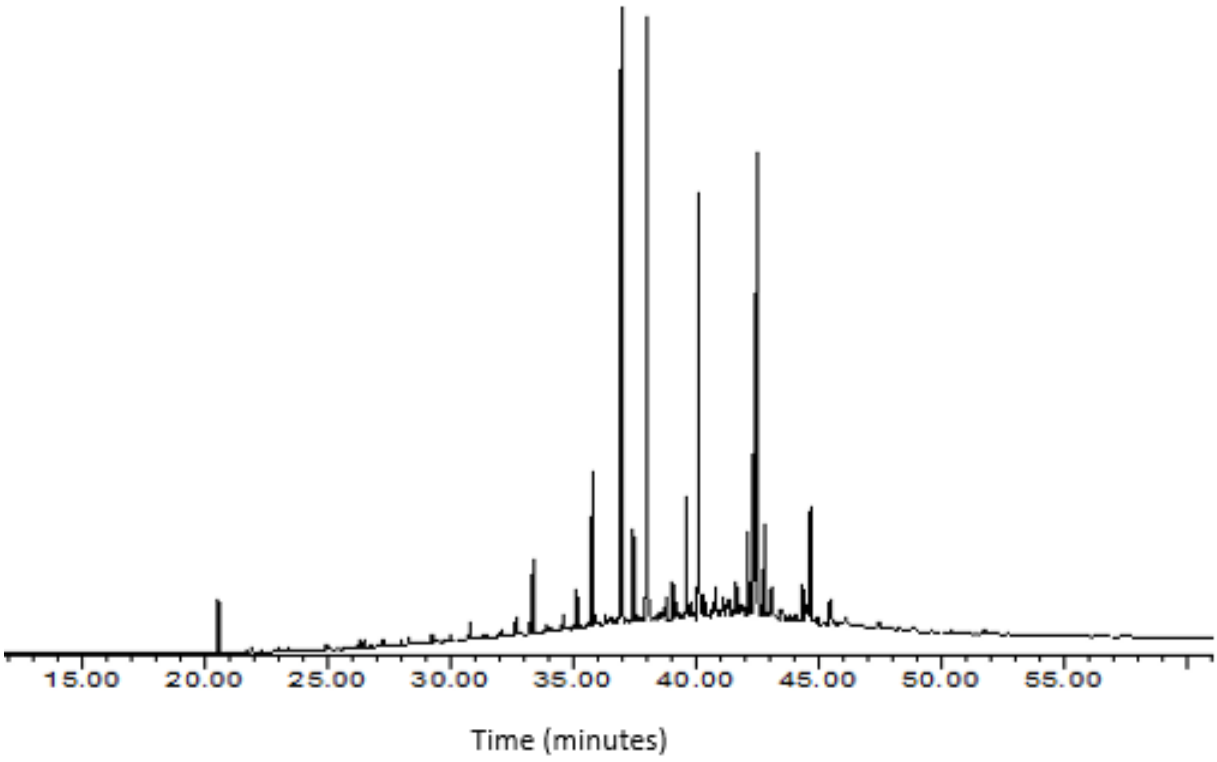

Figure 10: TIC of Neutral lipid fraction of Bull Island sample 36 (SPE carried out)

4. Results

4.1 Physical and Chemical analysis of Sediments

4.1.1 Particle size analysis

Particle size analysis (PSA) showed the percentage sand, silt and clay and the average grain size in the soils and sediments of Bull Island. The distribution of these properties can be seen in Figures 11, 12 and 13 (n=31) where PSA results were interpolated to predict sediment type beyond the sample point. Appendix 2 outlines the distribution of sediment grains in BI (mean grain size (µm), sorting, clay %, silt %, mud %, sand % and sediment description).

Percentage clay and silt in BI ranged from 0-14.1% and 0-43.75% respectively with the intertidal zone showing lower silt and clay % beyond BI and on the beach areas. Sand dominated the sediments, with 13 of 31 samples containing over 90 % sand and silt varied between 1-43 %. This was expected as BI is an island originating from the deposition of sand and silt. Samples ranged from poorly sorted muddy sand to well sorted sand, with mean grain size ranging from 106.9 µm to 506.9 µm.

Sand dominated the intertidal zone, with all samples containing ≥95% sand, except 65, in the intertidal zone that consisted of 80% sand, and the remaining 20% was clay and silt. In general, the mudflats and salt marsh were dominated by a combination of silt and clay, and the island consisted mostly of a combination of silt and sand. Samples 45, 46 and 47 taken from the island were ≥99% sand as they were taken from sand dunes. Samples 07, 15, 23, 6 and 41 contained the highest values for clay content, originating in the salt marsh and mudflat areas.

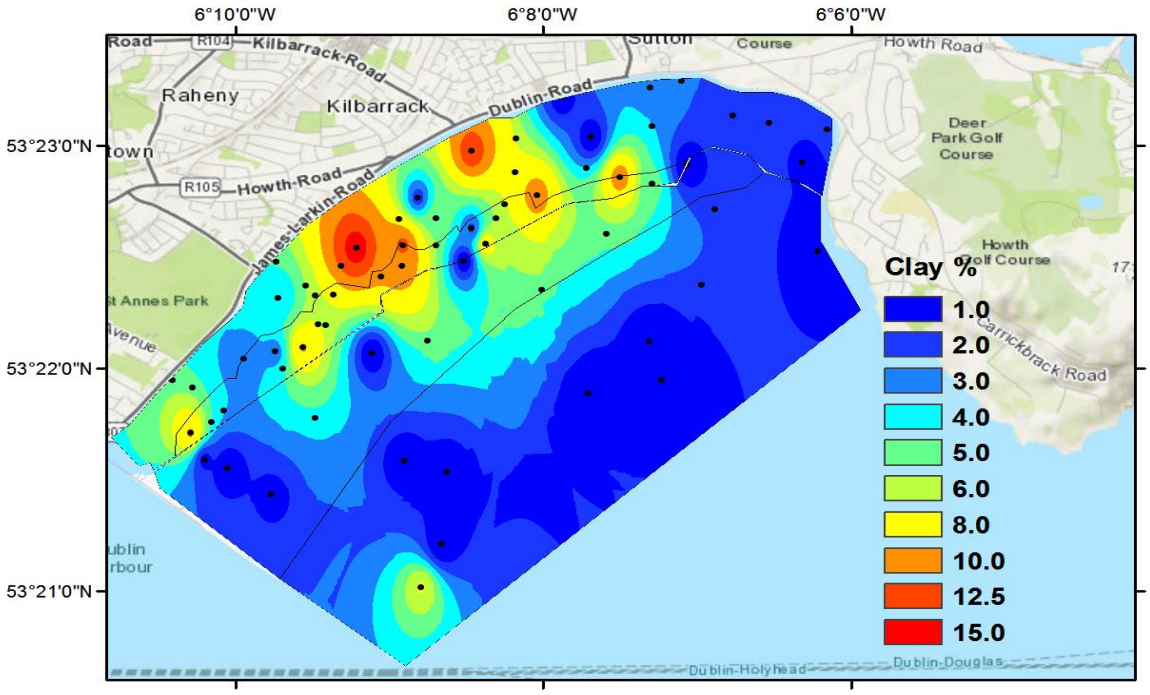

Figure 11: Percentage Clay distribution map

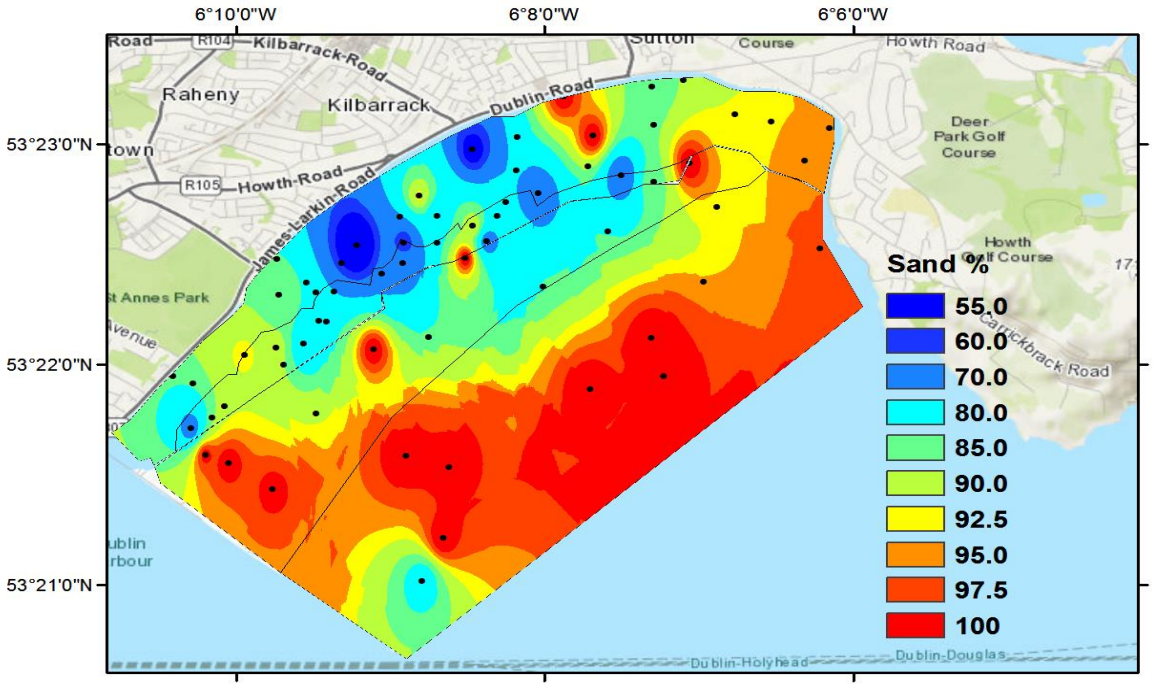

Figure 12: Percentage sand distribution map

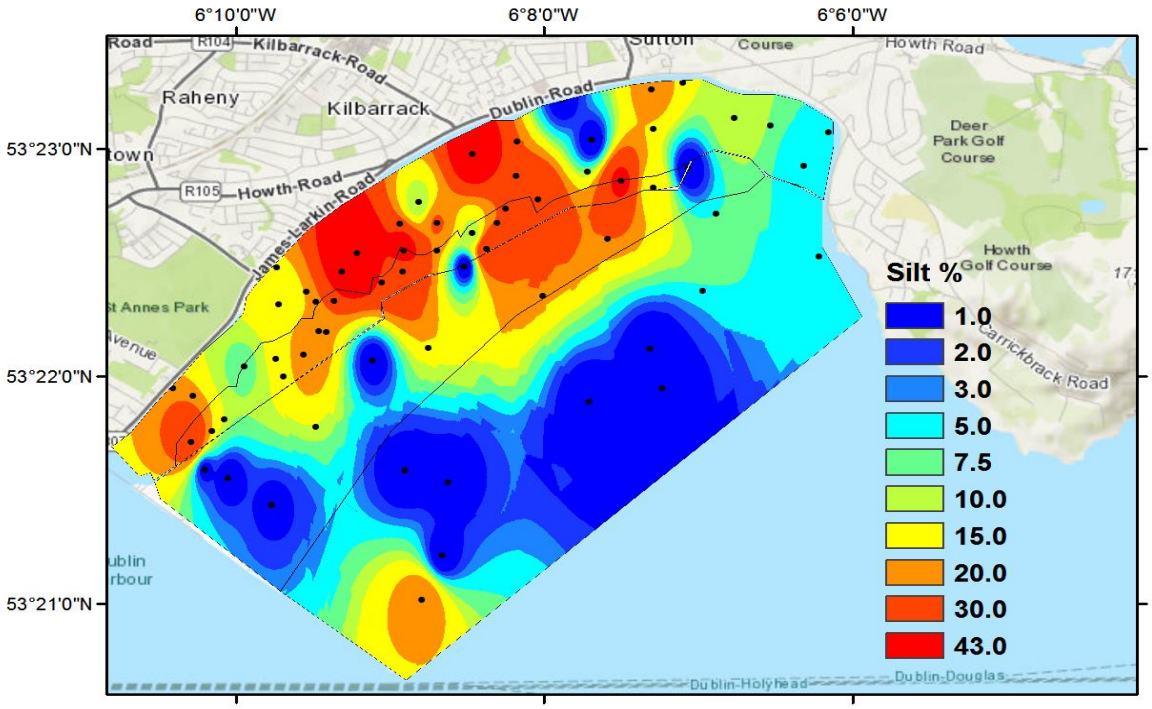

Figure 13: Percentage silt distribution map

4.1.2 Organic matter percentage

Organic matter (OM) percentage shows the percentage of animal and plant residues in various stages of decomposition in a sediment sample. Organic matter (OM) percentage in BI soils and sediments is mapped in Fig. 15 and varies between 0.50 – 62.0 % OM (Appendix 3). As expected there are higher concentrations of OM in the southern lagoon area and on BI, with consistently low OM in intertidal samples. The highest values of OM were at sample stations 29, 33, 37 and 39, all of which are in the salt marsh zone. Organic matter content is generally low in areas of high sand content (Fig. 8) and higher in areas with the higher volume of fine clay and silt-based sediments.

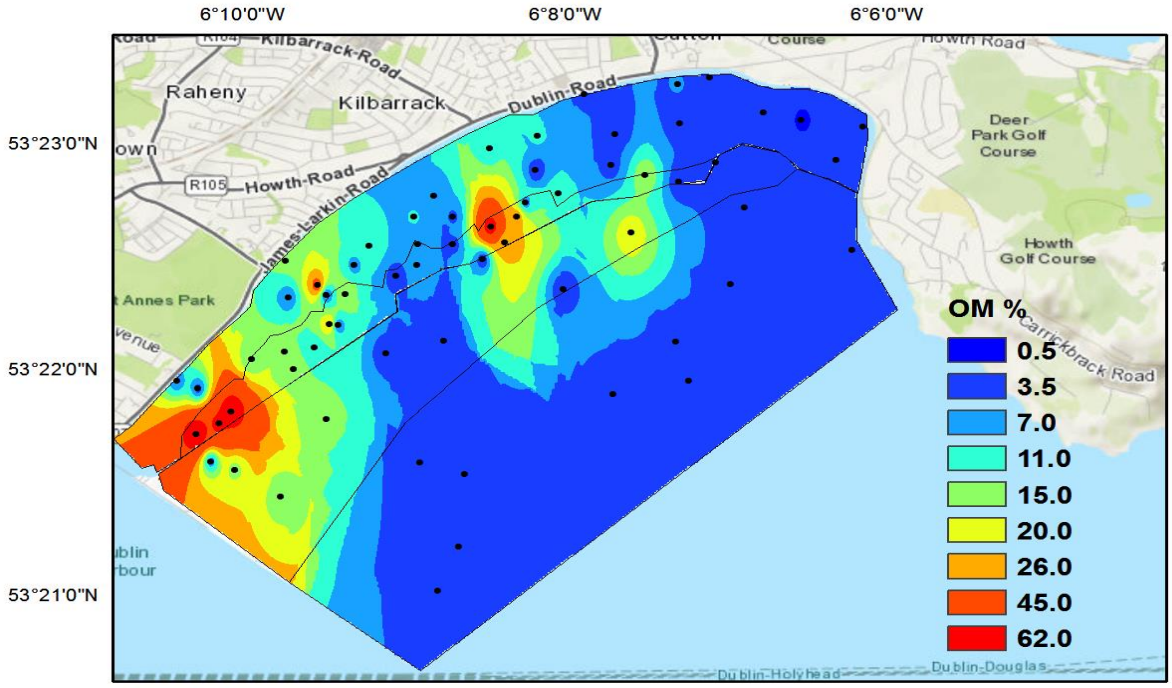

Figure 14: Percentage Organic Matter (OM) distribution map.

4.1.3 Total organic carbon and total organic carbon/Nitrogen (C:N) Ratio

The measurement of organic matter in sediments is not straight forward and varies in the analytical approach used. This is because quantification through simple weighing is not possible due to the strong association between organic matter and the inorganic component of sediments. The most common method used to quantify OM is through analysis of total organic carbon (TOC) where organic carbon is combusted to CO_2 after removal of inorganic material by acid treatment. Organic carbon is a major component of all organic matter and through years of empirical evidence total organic mass can be calculated, on average as twice that of TOC (Achterberg et al. 2009). The total organic carbon to nitrogen ratio (C/N ratio) in soils and sediments is a useful proxy that is employed in paleo-climatic (Ishiwatari & Uzaki 1987), agricultural (Friedel & Gabel 2001), composting (Barrington et al. 2002), marine and sedimentary research (Rumolo et al. 2011; Kähler & Koeve 2001). It is a powerful tool that can contribute to investigations of climate and carbon cycling, ecology, ocean and freshwater

circulation through time and optimal soil conditions for growth. In coastal environments where organic matter will come from several sources, the C/N ratio helps us establish whether OM is terrestrial (C:N ratios generally higher than 15) or marine (C:N between 4 and 15) in origin (Meyers 1997).

Total organic carbon (TOC) and total organic carbon/nitrogen ratio (C:N) were quantified using an elemental analysis instrument (see Appendix 3, n=59). TOC ranged from 0 - 15.95 % (Fig. 16) with samples of high sand content containing the lowest TOC and OM concentrations overall. The highest concentrations of TOC occurred in areas of ≤ 92.5 % sand, with a maximum TOC content of 3 % in areas where the sediment is 100 % sand. TOC was higher in sediments with more predominance of silt and clay particles, suggesting that the organic carbon adheres to the finer sediments or that there are depositional zones, as suggested with the OM content.

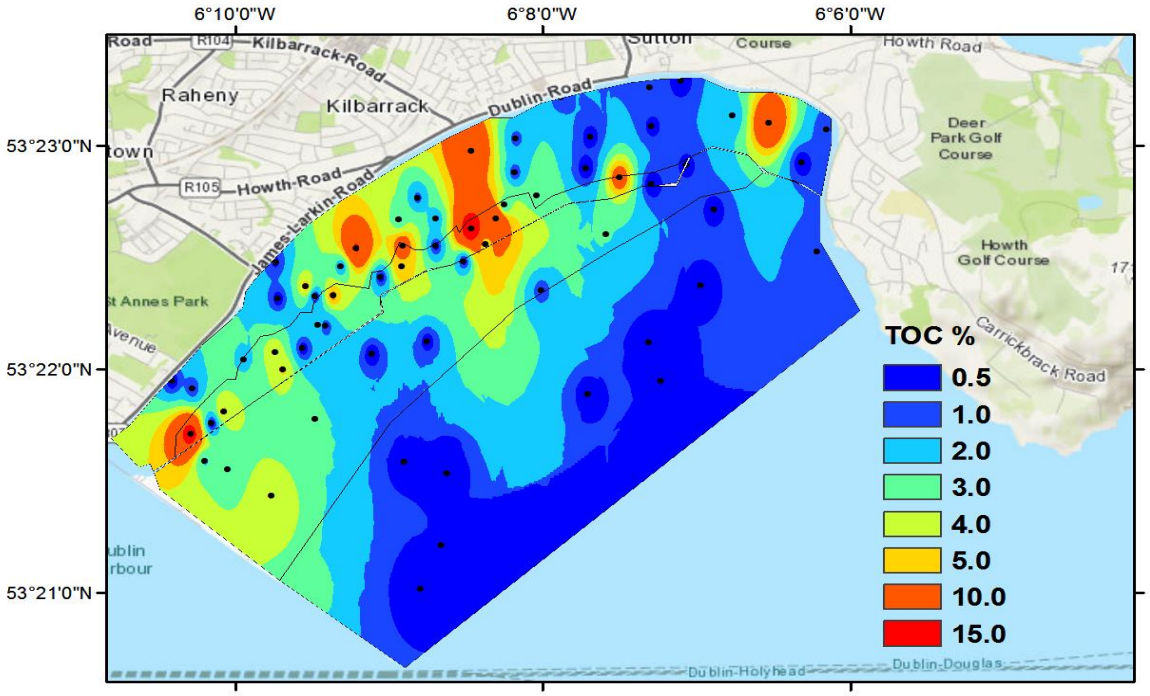

Figure 15: Percentage total organic carbon (%TOC) distribution map

The ratio of TOC to total nitrogen content (C:N) varied across the sampling area, between 2.0 - 43.2 (Fig. 16). The samples of C:N values over 35 occurred in areas of higher silt content, particularly along the roadway, on the right hand side of the levee road that intersects the middle of the island. The intertidal zone contained the lowest TOC:N values between 1.0 - 15.0, samples on the island and salt marsh contained a ratio of ≤35 and highest values were found in the mudflats. Overall, all four zones mapped in Fig. 16 have a large variance in C:N ratios, with the maximal numbers occurring in the salt marsh and mudflat zones, similar to the OM and TOC values.

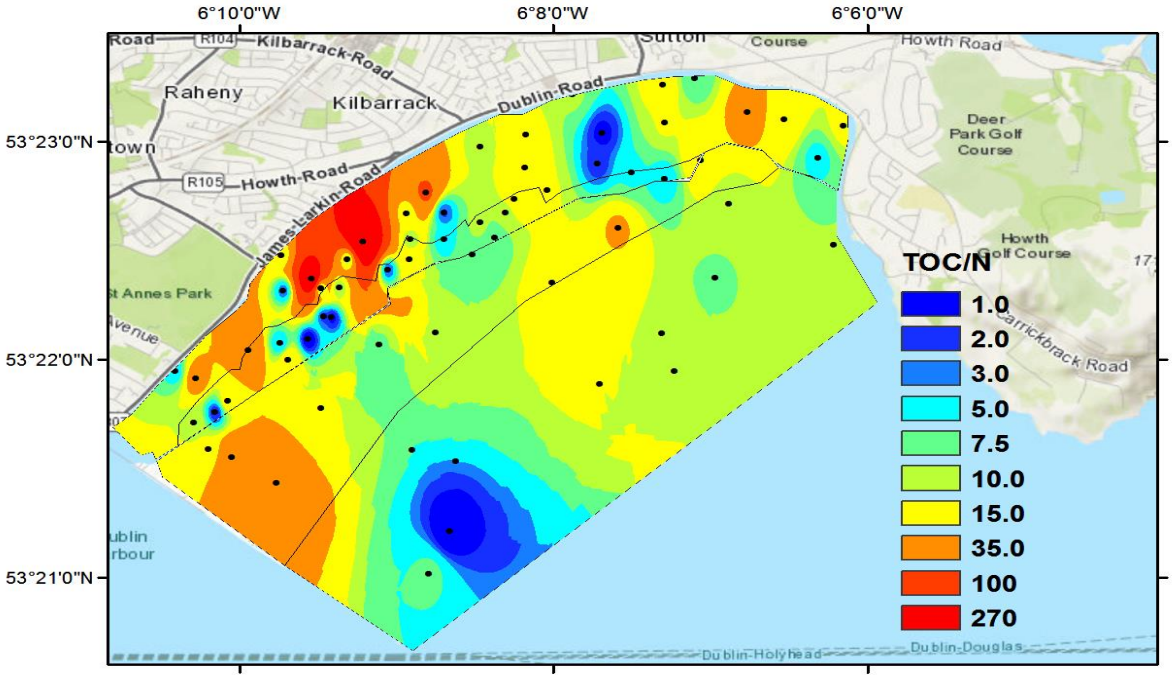

Figure 16: Total organic carbon: nitrogen (C:N) ratio distribution map

4.1.4 EC and pH

The electrical conductivity (EC) value relates to the concentration of conductive ions, which can indicate whether the area is heavily influenced by marine or freshwater, with a higher EC value being sourced from marine sources. A map of EC ranging from 0.06 - 9.24 mS/cm is

shown in Figure 18 (for data, see Appendix 4). The island showed lowest EC concentrations, where samples are not in direct contact with seawater. The intertidal zone EC values ranged from 1.0 to 6.0 mS/cm, whereas areas in the salt marsh and mudflats, specifically samples 15, 22, 32, 34, 35, 37, 39, 40 and 4 contained the highest values of 7.0 - 9.5 mS/cm. These 9 samples of higher EC content contained ≤85 % sand, indicating that these samples have higher amounts of finer sediments than the samples with low EC content.

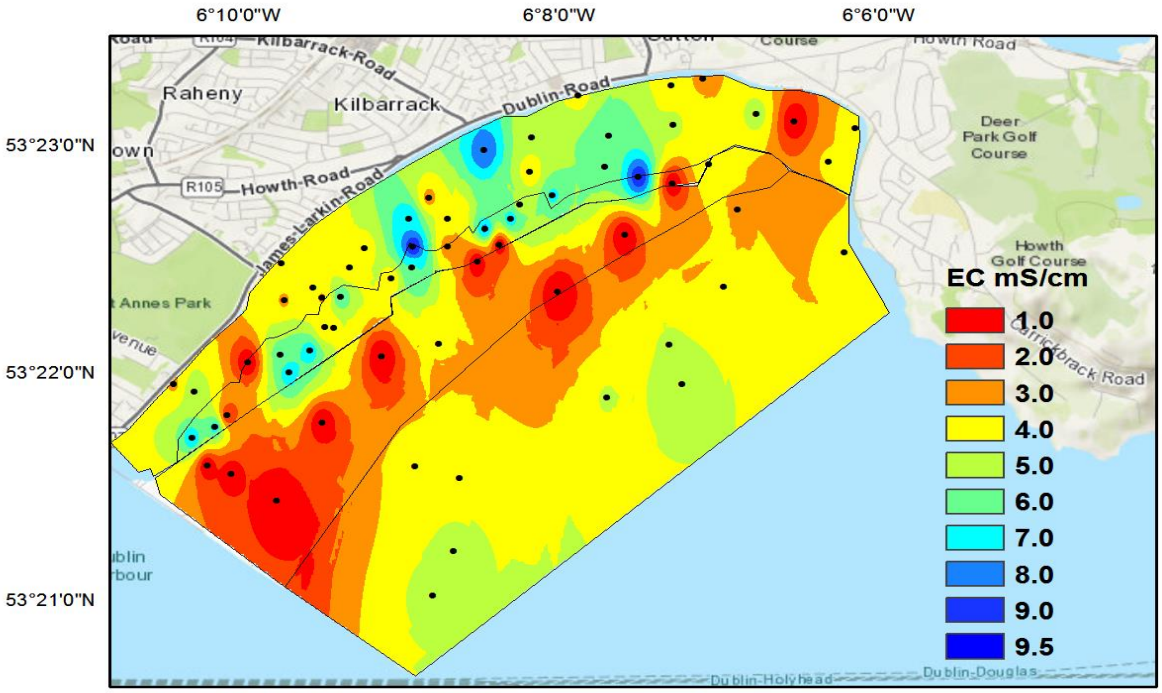

Figure 17: Electrical conductivity distribution map (mS/cm)

A map of pH is shown in Figure 18. The pH in the study area ranged from 6.30 - 9.90 with lower pH values at the southern lagoon area of the salt marsh and mudflats, and also in southern BI (see Appendix 4). The pH is slightly acidic in samples 16, 33, 36 and 37 and the range in the intertidal zone was moderately basic, with values between 8.0 and 9.9 pH units. Overall, the largest range in pH, which varies from slightly acidic to slightly basic (6.5 - 8.5) is in the south of the sampling area, where there is also a cluster of samples with high OM content and low sand content.

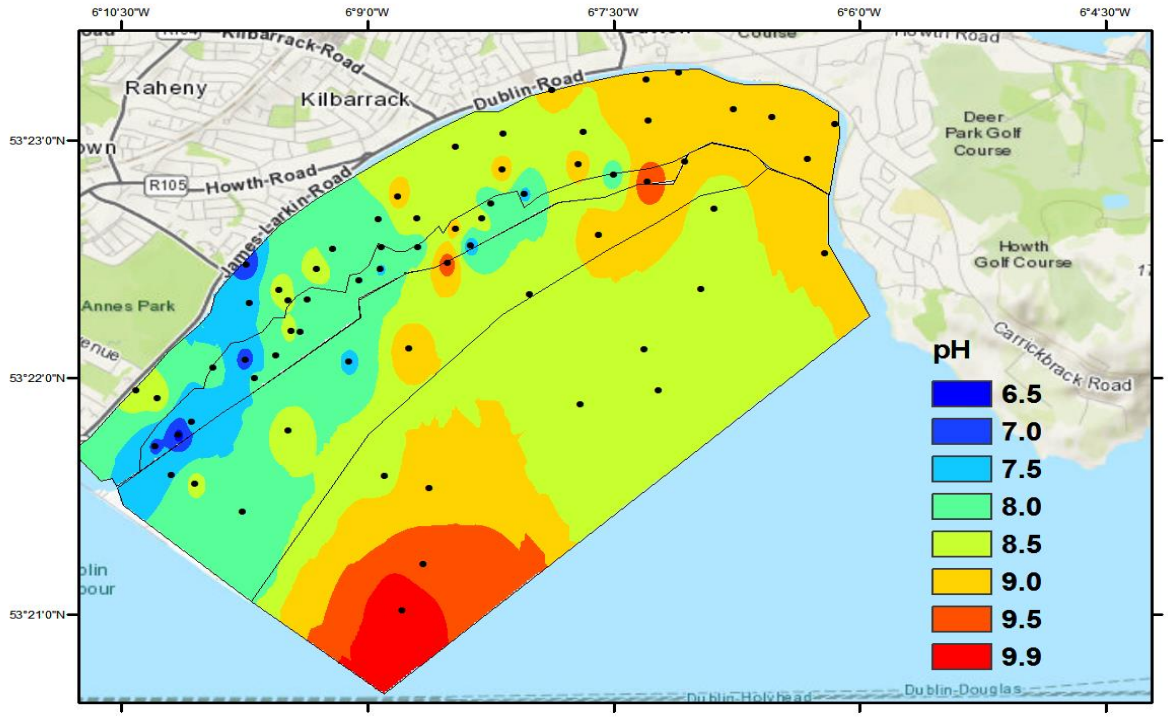

Figure 18: pH distribution map

4.2 Polycyclic Aromatic Hydrocarbon (PAH) Analysis of Dublin Bay Samples

The sum PAH concentrations and concentrations of 16 individual PAHs are shown in Table 3 and this distribution of PAH's is presented in Fig. 20 in ng/g. The sum concentrations (of 16 PAHs) in individual samples ranged from 32.0 - 8183.0 ng/g across the sampling area (see Appendix 5), which is below the sum PAH effect range medium (ERM) of 44,792 ng/g (Long et al, 1995). The lowest concentrations of PAHs occurred in samples taken from the intertidal zone, where samples ranged from <LOQ to 77.0 ng/g. The PAH content on the island was between <LOQ to 1595.0 ng/g. The island sample zone contains several dark blue circles which shows very low concentrations of PAHs. These circles are surrounded by a yellow colour, which is an interpolation of the results obtained from other samples in salt marsh and mudflat zones. As was seen with TOC and OM mapped results, the highest concentrations of PAHs were in salt marsh and mudflat zones. PAHs were consistently lower in samples of very

high sand content (≥97.5 % sand), with sample 14 (in the northern section of the mudflat, see Fig.6 for sample site) as an outlier, containing a value of over 8000 ng/g in an area over 97.5 % sand. Of the 16 PAHs that were quantified, fluoranthene, phenanthrene and pyrene occurred in the highest quantities (see Table 3).

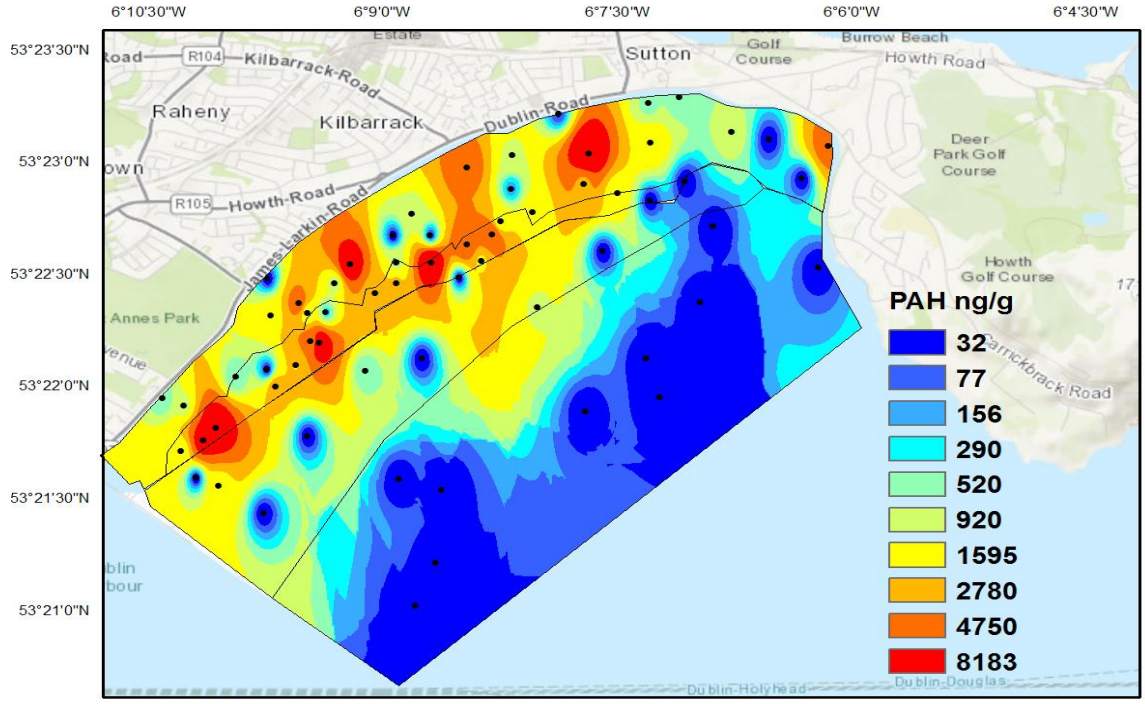

Figure 19: PAH distribution map (ng/g)

Although the PAH values have a wide range across the sampling area, the majority of single 16 PAHs were in concentrations between the effect range medium (ERM) and the effect range low (ERL). Three PAHs (acenaphthalene, acenaphthene and phenanthrene) existed above the ERM, thus showing a high risk of toxicity at various sites.

Table 3: Min and Max individual PAH values in sediments

PAH	range (ng/g)	max (ng/g)	LOQ (ng/g)	ERL (ng/g)	ERM (ng/g)
Naphthalene	33.8-775	775	33.8	160	2100
Acenanaphthylene	33.8-721	721	33.8	44	640
Acenaphthene	33.8-1213	1213	33.8	16	500
Fluorene	67.5-378	378	67.5	19	540
Phenanthrene	33.8-2771	2771	33.8	240	1500
Anthracene	33.8-653	653	33.8	853	1100
Fluoranthene	33.8-2715	2715	33.8	600	5100
Pyrene	22.5-2183	2183	22.5	665	2600
Chrysene	22.5-764	764	22.5	261	1600
Benz (a) anthracene	22.5-1005	1005	22.5	384	2800
Benzo (K) fluoranthene	22.5-555	555	22.5	320	1800
Benzo (b) fluoranthene	22.5-601	601	22.5	280	1620
Benzo (a) pyrene	22.5-622	622	22.5	430	1600
Indeno (123-cd) pyrene	22.5-554	554	22.5	n/a	n/a
Dibenz (ah) anthracene	22.5-119	119	22.5	63.4	260
Benzo (ghi) perylene	229.5-599	599	22.5	430	1600
∑PAH				4022	44792

Three isomer pair ratios, as defined by Yunker et al (2002) were first used in order to identify PAH source in river systems in British Columbia, Canada. The ratios include;

1. indeno[1,2,3-c,d]pyrene/(indeno[1,2,3-c,d]pyrene + benzo[g,h,i]perylene) (IP/IP+BghiP)

2. benzo[a]anthracene/ (benzo[a]anthracene + chrysene) (BaA/228)

3. anthracene/(anthracene + phenanthrene) (An/178),

These ratios were plotted against the parent PAH, Fluoranthene/(Fluoranthene + Pyrene) (Fl/Fl+Py) ratio to determine sources of PAHs in Bull Island as used by Oros & Ross (2004).

The PAH sources were determined as follows;

IP/IP+BghiP ratio <0.20 -petroleum, 0.20-0.50 petroleum combustion, >0.50 - combustion of coal, grasses and wood.

BaA/228 ratio <0.20 petroleum, 0.20-0.35 - petroleum and combustion, >0.35 –combustion, **An/178 ratio** <0.10 unburned petroleum sources, > 0.10 - combustion source.

Fl/Fl+Py ratio <0.40 - petroleum, 0.40-0.50 - petroleum combustion, >0.50 - combustion of coal grasses and wood.

Figure 20 shows the isomer ratio cross-plot for PAHs in Bull Island; the blue dots correspond to samples. It should be noted that many samples contained below LOQ concentrations of individual PAHs required for the isomer ratio calculation, so accurate sources could not be assessed for these specific samples, thus the source of PAHs in many samples could not be calculated.

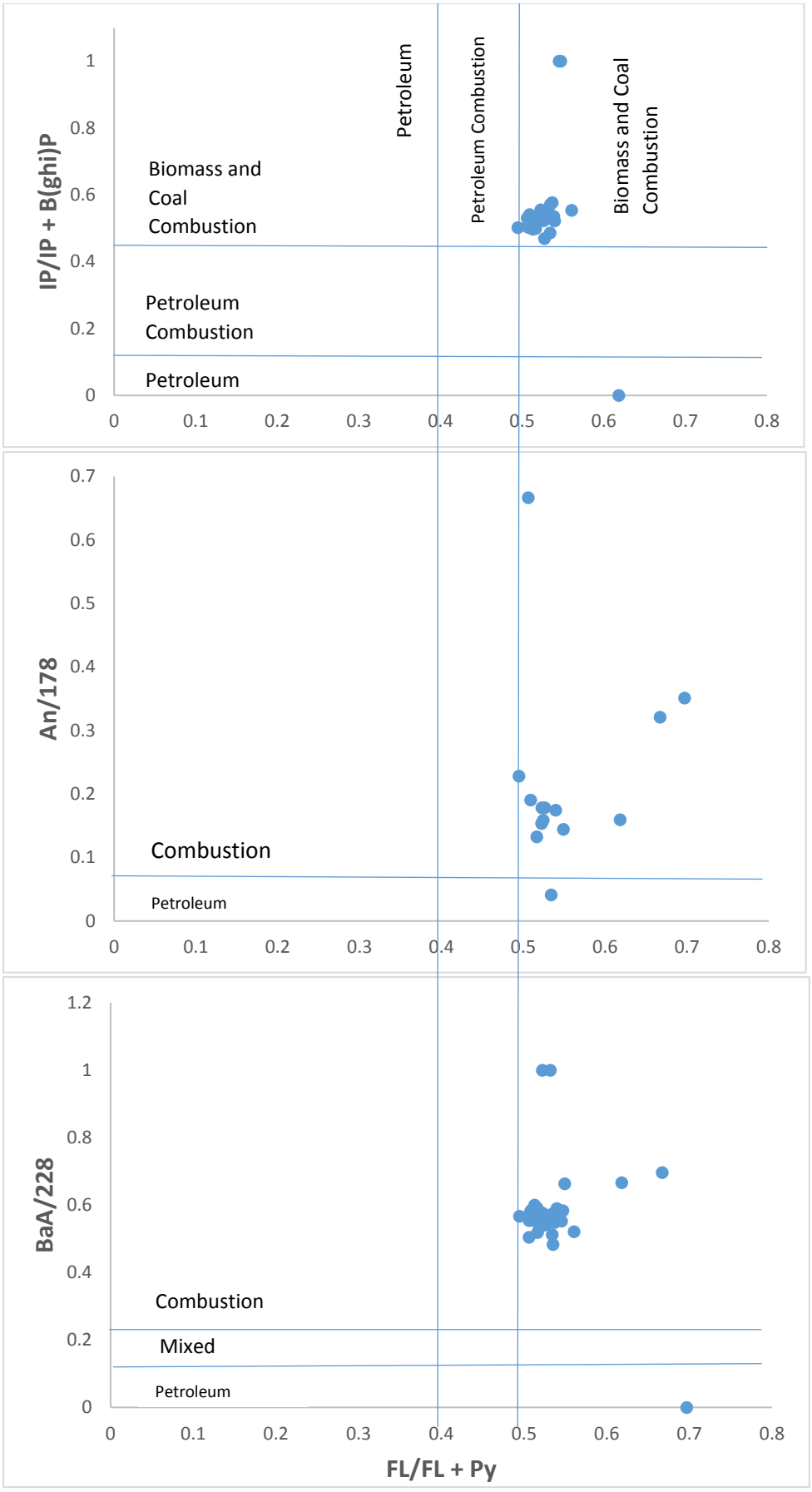

Figure 20: PAH isomer pair ratios cross-plot for source identification (Yunker et al. 2002; Oros & Ross 2004)

4.3 Comparative Study of Dublin Bay Sediments 2016/2017

Eight samples from the salt marsh area were analysed for PAHs using the same methods outlined above, one year after the initial sampling in 2016 (both sets of samples were taken during the summer months June and July) (Figure 21). These samples were taken from the same GPS points as the previous samples with a ±5m error diameter around a sampling site, to identify a change in concentration at selected sample points after one year. It must be noted that these sample sites are highly susceptible to environmental influences such as tidal effects, weather events, flooding and anthropogenic influences.

Figure 21: Sampling Map 2 with 8 sites resampled in 2017 for comparative analysis (samples 32, 33 36, 37, 38, 39, 41 and 44)

A clear change in PAH concentrations can be seen between 2016 and 2017 (see Table 4). Although there was no overall trend across all samples, there was an increase in PAHs in samples that are close together; 37, 33 and 44 after one year. In contrast, there was a decrease in concentration in samples 36, 32 and 38 which were also clustered close together.

Sample 39 contained no detectable PAHs in 2016 (all values below LOD) but contained 1696 ng/g PAH in 2017 indicating that PAHs were higher one year after the initial sampling period. The PAH content in sample 41 was much lower (2702.06 ng/g). There was also a higher abundance of high molecular weight (HMW) PAHs in the bay than their low molecular weight (LMW) counterparts. The isomer pair ratio calculation showed that these 8 salt marsh samples from 2017 have the common source of 'mixed fuel combustion', which is the same source as the previously taken samples in 2016. This indicates that the PAHs found in these 8 sample sites were most likely of the same source, yet more repetitive testing is needed to carry out a full assessment of the study area.

Table 4: Comparative sum PAH levels in sediment samples in 2016 and 2017, showing an increase in PAHs (+) between 2016 and 2017, or a decrease (-), including standard deviation of the triplicate samples.

Sample ID	**∑PAH (ng/g) 2016**	**∑PAH (ng/g) 2017**	**Change in concentration (ng/g) (2016-2017)**
37	786.4 ±0.31ng/g	3036.1 ±0.005ng/g	+2249.8
33	1658.0 ±0.06ng/g	2571.4 ±0.018ng/g	+913.4
44	1055.1 ±0.26ng/g	4425.1 ±0.004ng/g	+3369.9
36	5850.1 ±1.58ng/g	2485.0 ±0.05ng/g	-3365.1
32	7498.3 ±3.59ng/g	3170.5 ±0.016ng/g	-4327.8
38	4596.5 ±0.2ng/g	2469.0 ±0.008ng/g	-2127.5
39	<LOQ ±0.03ng/g	1696.6 ±0.004ng/g	+1696.6
41	6869.5 ±0.5ng/g	4167.4 ±0.04ng/g	-2702.1

4.4 Metal and Elemental results

Iron, calcium, aluminium, lead and chromium were analysed in samples from BI. Iron and calcium were the most abundant elements in all samples, with low concentrations of aluminium, lead and chromium across all samples. Average concentrations of these elements are displayed in Table 5. Figure 27 shows the relative abundance of iron, aluminium and calcium. Calcium, Iron and Aluminium are declared as percentages as the mapped data, where one percent equals 10,000 ppm. This unit is used as these elements occur naturally in the earth's crust, in very high concentrations (Fay et al, 2007).

Table 5: Average Heavy metal concentrations in DB samples (ppm)

ID	Fe ppm	Ca	Al	Pb	Cr	ID	Fe ppm	Ca	Al	Pb	Cr
2	17689.1	41198.4	2785.8	32.41	34.43	**35**	48635.54	16751.7	2770.44	113.5	44.01
4	23413.9	48036.4	3844.1	39.42	34.50	**36**	57980.48	8430.315	4052.47	439.7	58.09
06	33440.0	8039.6	3250.6	113.97	42.38	**37**	47388.27	9633.812	3196.44	122.0	47.32
7	18663.6	24936.3	3013.9	41.96	57.52	**38**	37031.28	20531.01	N/A	211.2	62.15
9	8930.3	69263.0	N/A	18.98	24.03	**39**	13283.88	19379.64	2154.83	24.8	29.91
10	13106.5	28076.3	2330.5	24.26	35.17	**40**	32432.31	13565.27	2235.46	174.5	50.51
12	22404.1	18514.8	2001.7	49.36	42.73	**41**	46435.86	11123.28	4079.28	143.2	37.71
14	7261.7	18419.8	N/A	N/A	30.06	**42**	31033.87	35835.89	N/A	146.3	65.07
15	27236.0	59182.1	4275.9	60.71	41.58	**43**	52136.46	13883.52	5252.86	137.5	38.10
16	37116.5	24188.6	2725.8	125.04	70.03	**44**	11317.02	35321.89	N/A	22.6	39.71
17	9768.4	18527.3	1705.0	31.57	49.72	**40**	31171.23	12449.45	2009.65	170.7	42.72
18	10541.5	21294.0	1793.4	21.78	32.26	**43**	55197.56	16620.11	4238.50	158.2	42.85
19	26816.8	20741.1	3971.9	56.90	39.62	**46**	14078.77	25439.76	2113.00	152.0	35.56
20	12650.1	25547.5	1968.9	29.83	35.08	**47**	7095.387	31269.79	N/A	N/A	35.40
21	6176.3	13171.9	N/A	18.55	27.92	**48**	7835.547	25921.54	N/A	32.4	46.38
22	21602.6	12293.9	3440.7	61.36	34.63	**49**	36687.22	8864.603	3515.24	129.2	38.99
23	42824.5	14589.1	5187.2	101.59	57.09	**50**	9240.397	27333.57	N/A	21.3	38.00
27	10087.8	26016.5	4896.3	30.12	38.49	**51**	10118.45	26620.62	N/A	17.7	46.45
29	12118.2	7049.5	1774.0	56.54	42.50	**53**	21053.35	20628.28	N/A	79.0	34.43
30	51314.1	17202.1	5711.3	115.80	45.29	**54**	6126.173	19279.99	N/A	20.6	41.22
31	48635.5	16751.7	2770.4	113.51	44.01	**61**	6156.09	19845.36	N/A	21.6	33.89
32	24328.7	11794.7	2384.7	119.02	44.68	**62**	7895.34	16789.14	N/A	19.4	29.9
34	37379.68	13654.87	3314.04	101.9	39.97	**63**	11742.49	14366.98	N/A	31.7	26.78

Calcium (Ca) had an overall range of 0.7-6.9 % Ca (7000- 69000 ppm) (Figure 22). Each zone shows a large variance in Ca content. The intertidal zone contained a variation of between 1.5 % and 6.9 % Ca, with the higher concentrations generally occuring to the north of the island. Samples 1, 9 and 24 in the mudflat zone contained a high Ca content of 6.0 - 6.9 % (60,000-69000 ppm), while there was a Ca content of 1.5 – 4 % (15000-40000 ppm) in the salt marsh zone and island.

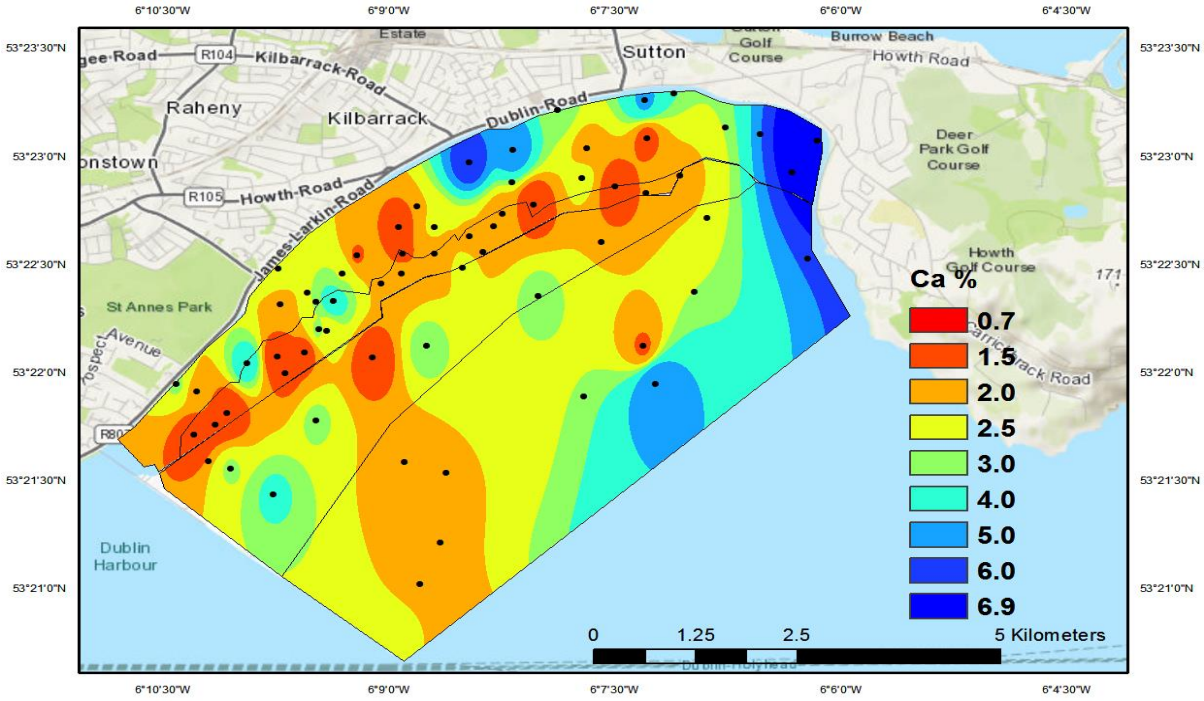

Figure 22: Calcium percentage distribution map

Iron (Fe) results show an overall range of 0.6 to 5.8 % (6000-58000 ppm) Fe, with the higher concentrations in the salt marsh and mudflats compared to the intertidal samples beyond the island (Figure 23). The iron content in the intertidal zone was ≤ 2.0 %, the island contained 1 - 4.5 %, but with only one sample containing the upper value of 4.5% and peak Fe is in the salt marsh zone in samples 26, 30, 31, 33, 35, 37 and 41. Sample 16 contained the highest Fe content in the mudflats at 3.71 %. Areas of high iron content between 4.5 and 5.8 % occur in the same places as high PAH content and coincide with the upper values of C: N in the sampling area.

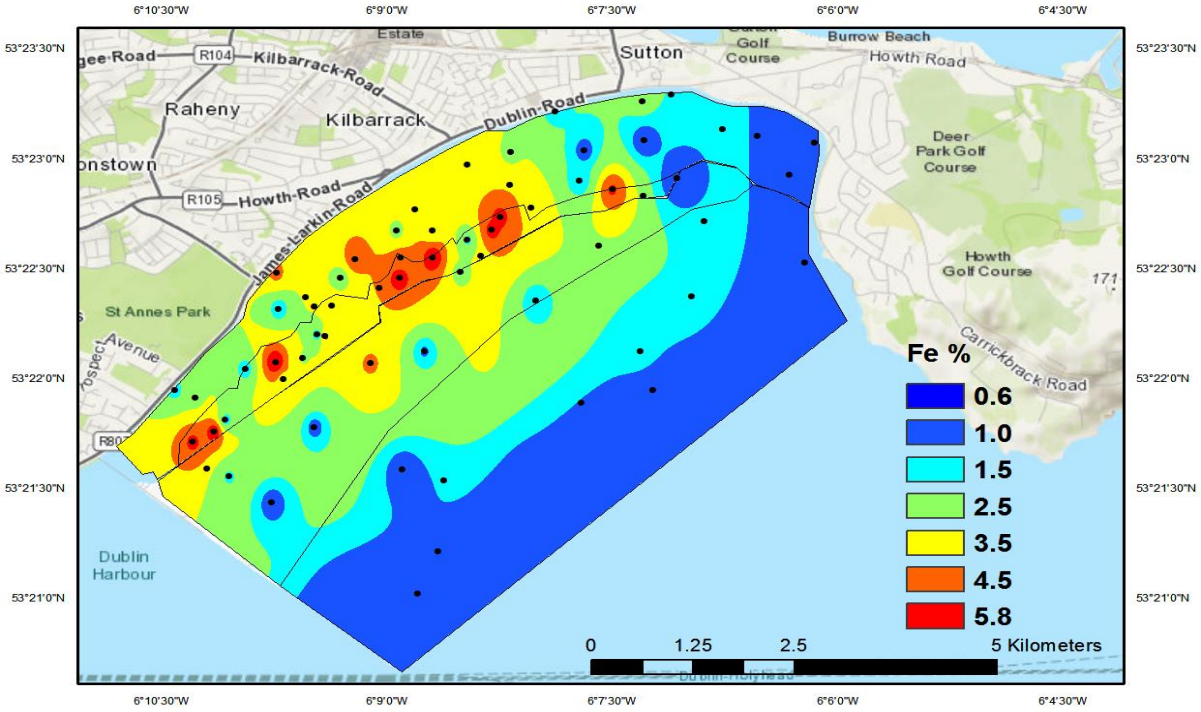

Figure 23: Iron percentage distribution map

Aluminium content varied between 2.0 and 5.70 % (20000-57000 ppm) (Figure 24). The lowest Al concentration was in the intertidal zone, with a range of 2.0 to 3.25 %. One sample from the island, sample number 48, contained a significantly higher Al content of 4.0 %, when compared to the other samples in this zone. The highest Al content was found in the salt marsh and mud flat samples. Sample numbers 04, 15, 19, 23, 27, 30, 36, 41 and 43

contained the higher percentages of Al when compared to all other sampling stations. Of these 8 samples, sample number 30 located in the mudflat zone contained the highest Al content at a value of 5.71 %.

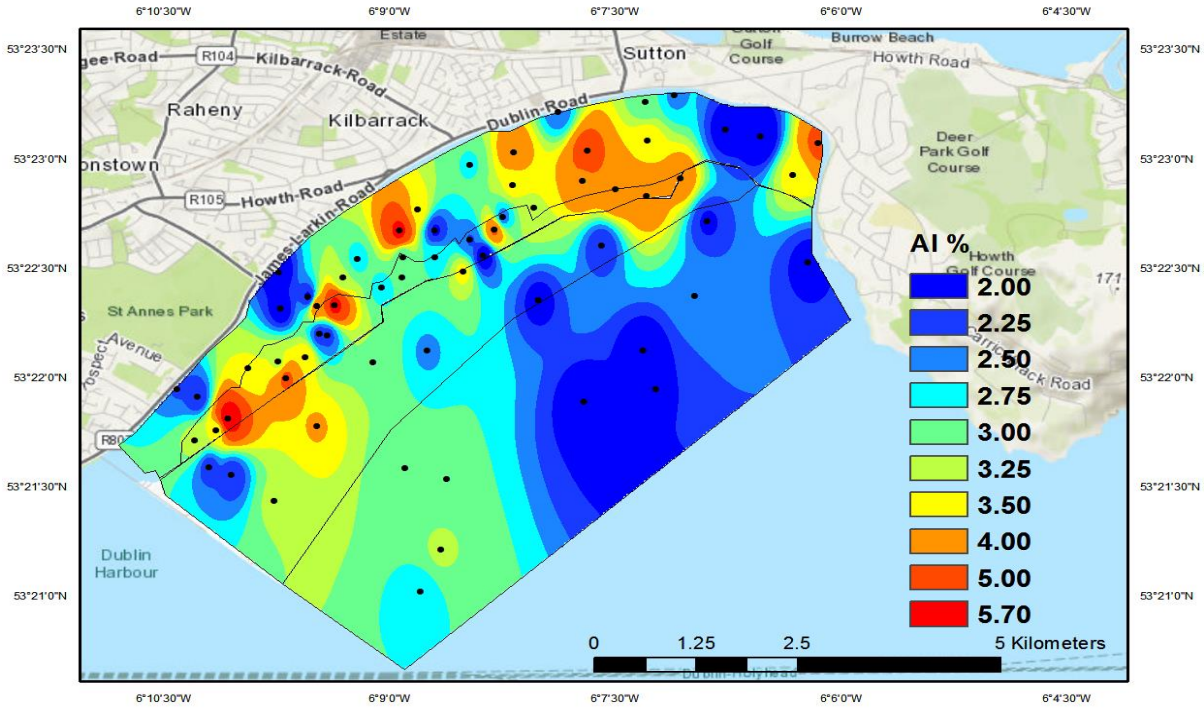

Figure 24: Aluminium percentage distribution map

Lead (Pb) distribution results are shown in Figure 25. The overall range of Pb is between 17.8 ppm to 440 ppm. It should be noted that average Pb values across the sampling area was 85.31 ppm, which is significantly lower than the max concentration of 440 ppm found at sample site 26. The red colour on the map below (Fig. 25) is sample number 26, in the salt marsh zone. This result is an outlier when compared to the average result of the sampling area of 85.31 ppm Pb.

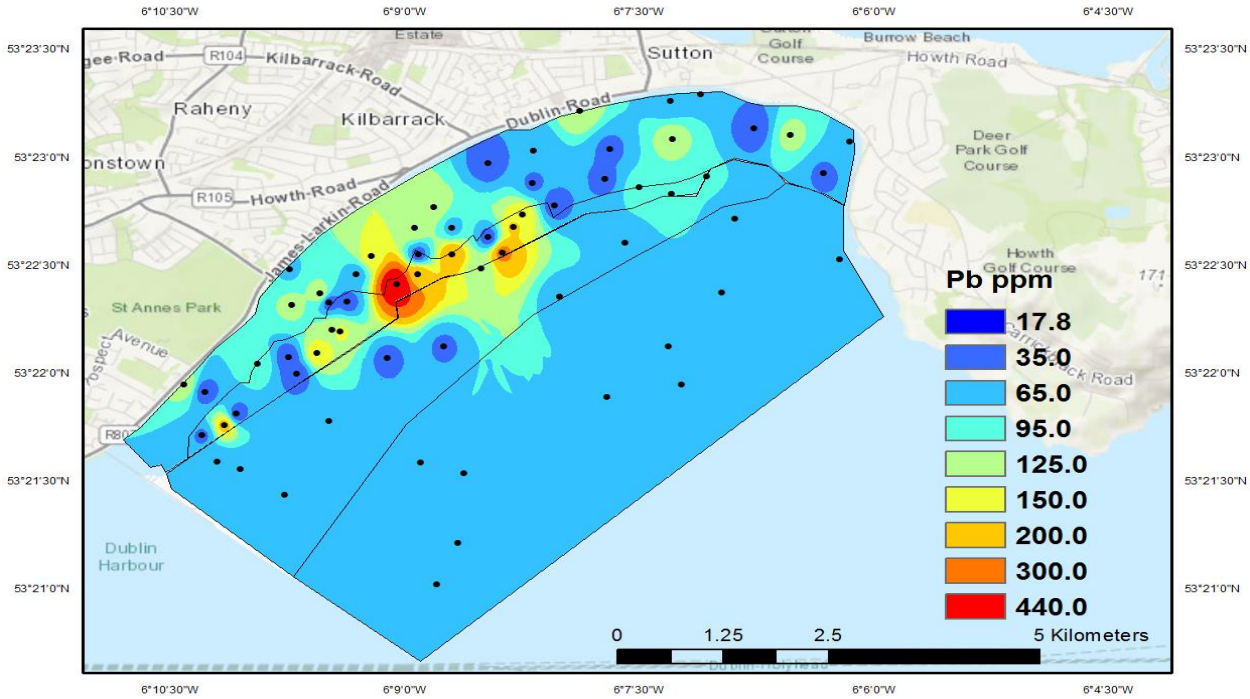

Figure 25: Lead distribution map (ppm)

Chromium was present between 27.5 ppm and 70.0 ppm, with higher concentrations occurring in the salt marsh and mudflat areas, and alongside the bridge that intersects into the middle of the island (Figure 26). As has been seen with Pb and Al, the maximum concentrations are seen in the salt marsh and mudflat areas which are the two zones with the lowest sand percentage. The areas of highest Cr concentration are samples 26, 28, 30, 32, 50 in the mudflat zone and samples 04, 10 and 17 in the mudflats. There is a large range in Cr concentration present in each of the four zones that were studied. The Cr content in the intertidal zone and island were from 35.0 ppm to 45.0 ppm, and from 30.0 ppm to 55 ppm respectively. Although

the Cr content on the island varied widely, some values are very low, or not detectable. The highest Cr content sites in the salt marsh, also contained high PAH values (see Fig. 19) which could indicate a common source for PAHs and chromium.

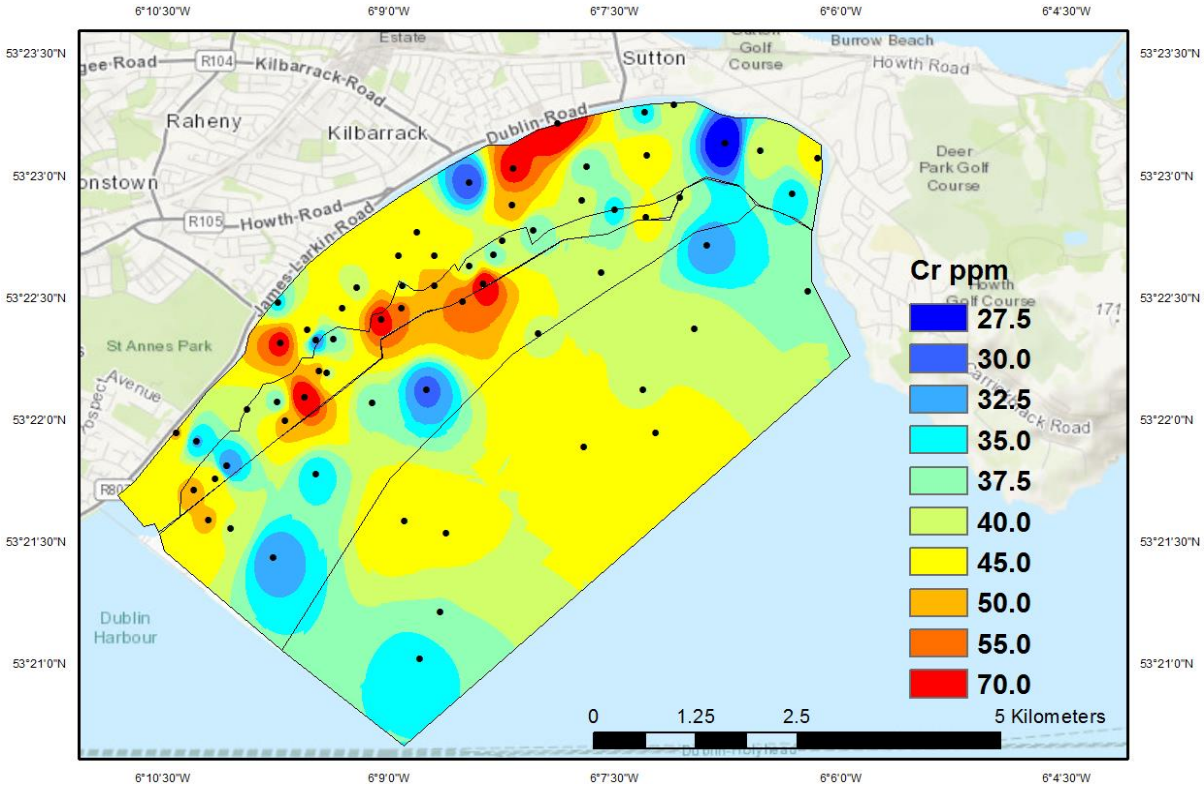

Figure 26: Chromium distribution map (ppm)

Toxicities of Pb and Cr can be discussed using the ERL and ERM values provided by Long et al (1995) as seen in table 6. Pb ranged from 17.8 ppm to 440 ppm, with this upper value of 440 ppm exceeding the ERM of 218ppm. This high value occurred only at one sample site, number 26 in the salt marsh zone. As seen in table 6, the average value was 85.3 ppm which lies below the ERM, and above the ERL. Many samples contained values between the ERL and ERM, indicating the possibility of toxicity and the necessity of further monitoring. In

this study, chromium fell below the ERL at all sites, indicating the unlikelihood of Cr induced toxicity at the time of sampling.

Table 6: Range and average concentrations of lead and chromium studied in BI, with ERL & ERM values from Long et al. (1995)

Element	Range in this study (ppm)	Mean (ppm)	ERL (ppm)	ERM (ppm)	Reference
Lead	17.8-440	85.3	46.7	218	Long et al 1995
Chromium	27.5-70.0	41.5	81	370	Long et al 1995

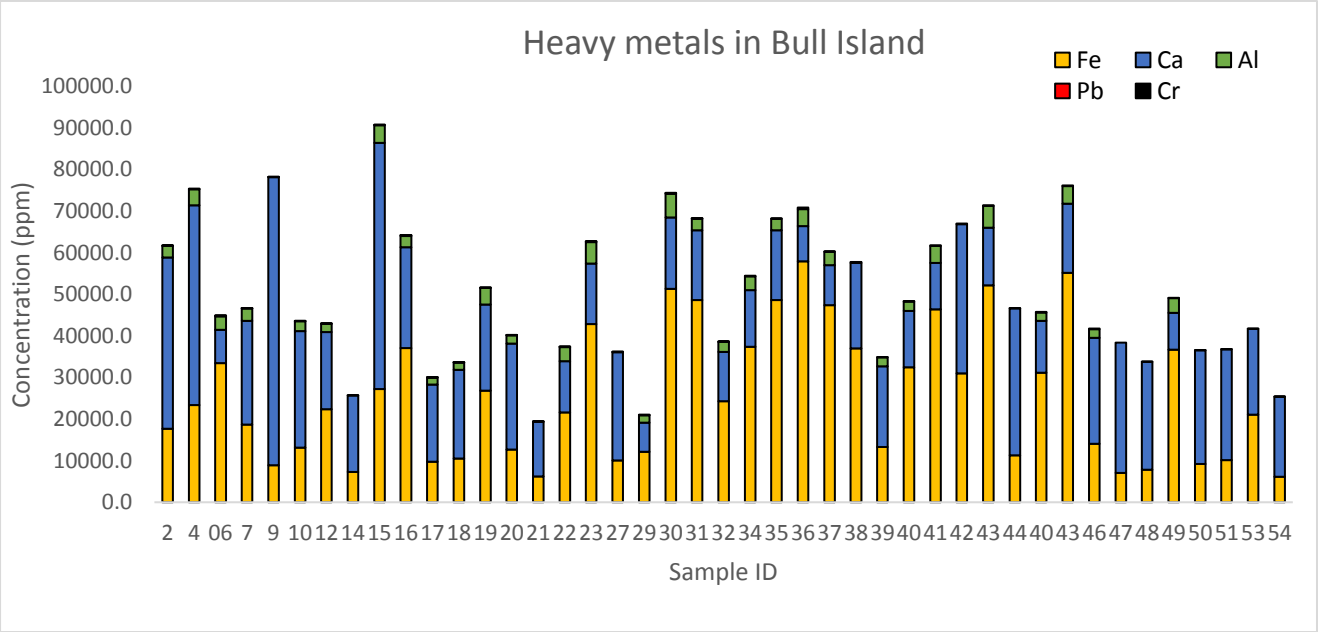

Figure 27: Relative concentrations of heavy metals Iron, Aluminium and Calcium in sediment samples

4.5 Statistical Testing

To identify possible relationships between PAHs, metals, TOC, C:N, %N, and %C a principle component analysis (PCA) plot (Figure 28) is used to provide information on the commonalities and differences in the study area. PCA was chosen as it relates many data sets with each other and also identifies the component that causes the most variance in a multi variate data set with a large amount of data (Clarke 1993, Vitko 1994). The principle loading

was PAH value, which accounted for 76.8 % of the variance (Appendix 6). This demonstrates that PAH content is the data set that has the most influence on the samples from Bull Island overall. This plot revealed that there are only small clusters of data points, (e.g. pH-OM and Pb-Cr) strongly associated with each other. All other variables in this data set seem to exist independently, without being directly influenced by another parameter. Thus, the PCA plot showed little relationship between parameters. On this plot, the position of the PAH ng/g is more isolated but grouped closer to the metals Al, Ca and Fe, which indicates that they relate to each other, statistically. Similarly, N, TOC and TOC:N were also grouped together.

This PCA was carried out using PAST software and conducted on the individual samples in order to provide meaningful relationships between variables in this data set. This statistical tool was used to determine whether PAHs and metals in particular influenced the sediment samples as a whole. This process highlighted how difficult it is to establish significant and meaningful relationships between the samples and their analysed variables. This was most likely due to the large variance in results and heterogeneous nature of the samples (e.g. sand vs muddy sediment). A further set of statistical tests were subsequently conducted where variability is reduced to identify any possible relationships that may exist between sample groups.

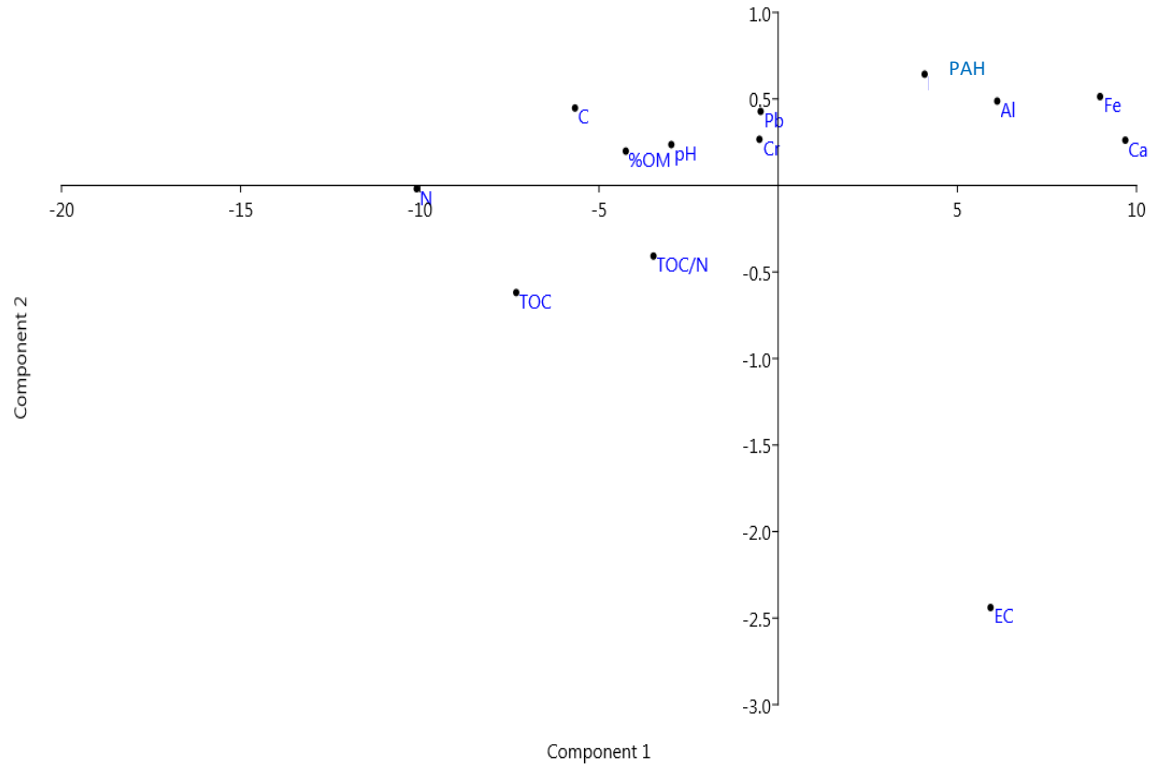

Fig. 28: PCA conducted on all variables analysed

Hierarchal cluster analysis was then carried on all individual characteristics of each sample in order to group samples together according to their geochemistry (pH, PAH, TOC etc.). A cluster plot (Fig. 29) of all samples shows six distinct clusters. The cluster on the top of the branch, including samples 61, 62 and 63 (circled green) is grouped together as all three samples have low concentrations of PAHs, all below the LOQ with the OM of this cluster between 0-2 %, and a 7.7 - 15 C:N ratio. Samples in this first cluster were also between 74.9 and 100 % sand. Overall, this cluster were samples with high sand content, low organic matter and low PAH content. Lead content varied between 31.13 - 41.3 % in these samples also. The next cluster (circled yellow) included samples 50, 51, and 54, which have low OM of 0.5 - 1.1 %, C:N ratio of 6.9 - 13.6 and low PAH content all below the LOQ. These three samples were of high sand content from 90 - 100 % and low TOC percentage of 0.16 - 0.68 %. The other two

large clusters (circled blue and red) showed no one specific commonality but had similar values for multiple parameters. They are closely related statistically, but it is difficult to confidently attribute a property that caused such clustering. This type of analysis proved to be very useful as it helped to group together heterogeneous samples with a large data set, according to their specific geochemistry.

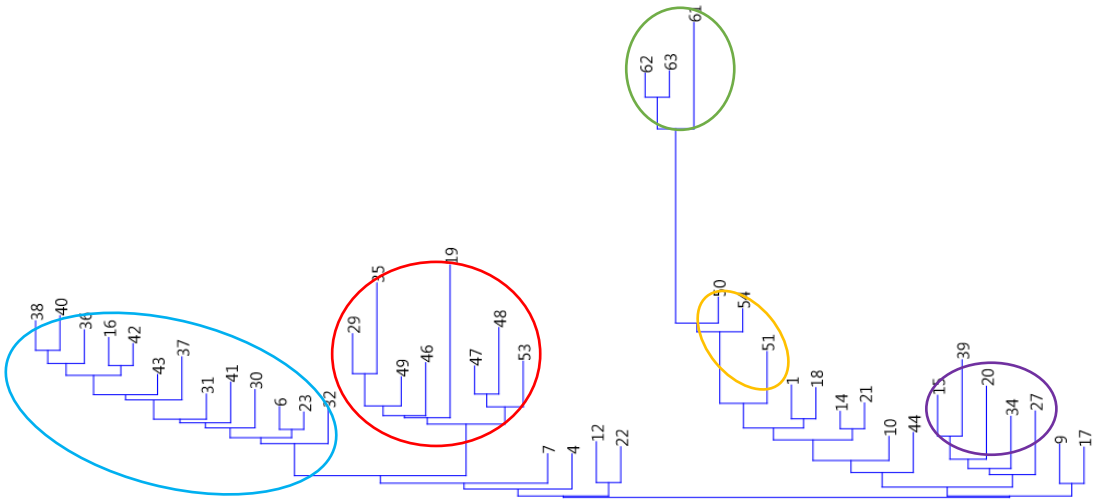

Fig 29. Cluster analysis conducted on individual samples from Dublin Bay based on the chemical characterisations

ANOVA was carried out on the clusters identified in Fig 29 and are tabulated in Table 6. This test further analyses the variance in a data set, to identify significance between clusters. The ANOVA test was conducted using the mean PAH value for each cluster to test for a significant difference within the clusters. This P value (<0.01) suggests there was a significant difference between the different clusters.

Table 7: ANOVA results conducted on grouping identified in PCA for PAH results

ANOVA

Source of Variation	*SS*	*df*	*MS*	*F*	*P-value*	*F crit*
PAH	78266237.64	5	15653247.53	8.913	0.00014	2.710
Error	35122942.41	20	1756147.12			
Total	116543442	29				

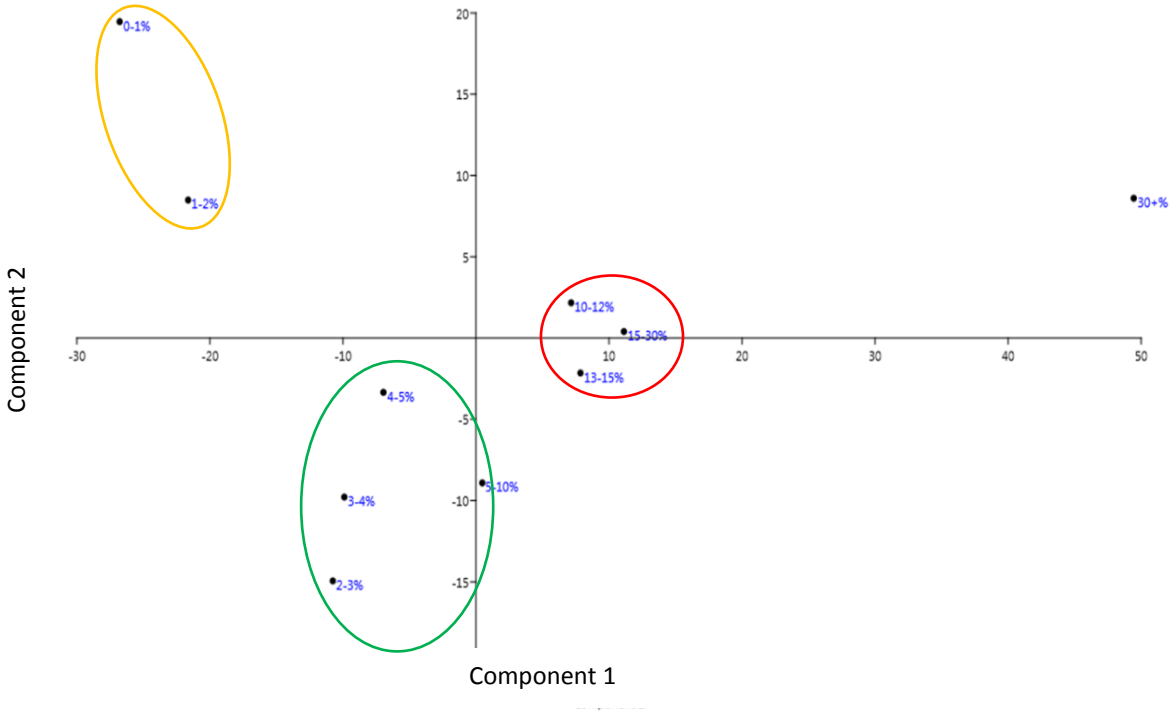

Figure 30: PCA according to OM content

An additional PCA was carried out (Fig. 30) to determine associations between samples when grouped according to organic matter content. This was carried out as the hierarchical cluster analysis (Fig. 29) identified that samples that were clustered together, had similar organic matter (OM) or organic carbon (TOC) contents. Samples were grouped into categories based on their OM content and those respective groups' mean variables were compared by PCA. A second set of loadings can be seen in Appendix 7, which shows that when the samples

are grouped by organic matter content, PAH and EC variables have the highest influences over the samples in general. This means that the PAH variable has less of an influence on samples when grouped according to organic matter content, whereas EC value now has a larger influence on the samples. Samples were grouped accordingly 0-1 %, 1-2 %, 3-4 %, 4-5 %, 5-10 %, 10-12 %, 13-15 %, 15-30 % and 30+ % OM. This was done specifically to investigate any relationship between OM content and PAH's and heavy metals (Murphy et al, 2016). The PCA plot (Figure 30) highlights the differences in the OM values and how they grouped together based on OM content. Samples with a lower OM (0-2 % circled orange), mid-range of OM (3-10 % circled green) and higher OM (10-30 % circled red) content grouping together. The samples with OM <30 % existed separate from all other groupings, showing that this set of data is in a class of its own, and it influenced independently.

One – way ANCOVA was then applied (with OM selected as the dependent variable and PAH the response as the independent variable) to grouped samples (Table 6). There is a trend in OM where 5 % or higher appears to be the level of significance where there is a difference in PAH and Pb concentration – PAH concentration at OM <5% = 942.05 ng/g and >5% = 2599.85 ng/g and Pb concentration at OM<5% = 41.93 ppm and OM >5% = 122.46 ppm. This suggests that the linear relationship between OM content and pollutant concentration (i.e. PAH and Pb) may be restricted to lower OM content i.e. between 0 - 5%. This linear relationship between PAH and Pb is shown graphically in Figure 31.

Table 8: One-way ANCOVA analysis (OM vs PAH).

Test for equal means, adjusted for covariate

	Sum of sqrs	df	Mean square	F	p (same)
Adj. mean:	3.37E+07	4	8.43E+06	4.207	0.01921
Adj. error:	2.80E+07	14	2.00E+06		
Adj. total:	6.17E+07	18			

Homogeneity (equality) of slopes:

F :	0.7059
p (same)	0.6059

The statistical tests show there is a significant relationship between OM and PAH/Pb concentration but there are large variances in some of the groups which are possibly caused by other environmental factors such as varying morphology and hydrology in the area. Pearson correlations were carried out on all data from Bull Island (Table 9). This test shows the linearity between sets of data in a large set. Each two variables have a calculated R^2 value showing the linearity of their relationship, with an R^2 value of 1 showing a direct proportionality between these two variables. Secondly, a P value is provided showing probability that you would have found the current result if the correlation coefficient were in fact zero (null hypothesis). A correlation coefficient (P) value less than 5 % ($P<0.05$) shows that the correlation coefficient is statistically significant.

A significant result is that PAH's have a strong positive correlation with the TOC content of sediment ($R^2 =0.59$, $P < 0.05$). Pb also correlated strongly with PAHs and TOC (see Fig 31, 32 and 33). The stepwise regression model in which PAH was the dependent variable identified OM, TOC and TOC/N as the three most related variables to PAH concentration. This highlights that OM and TOC may be used as potential predictors for ranges of PAH's that may be found in environmental samples. With PAH's and Pb a significant difference was seen above 5% OM. However, the same cannot be said for Cr which did not show a similar increase above

5% (Cr OM <5% = 36.25 OM >5% = 47.10). Pb and Fe also showed a strong linear relationship of $R^2 = 0.85$ and $P < 0.05$.

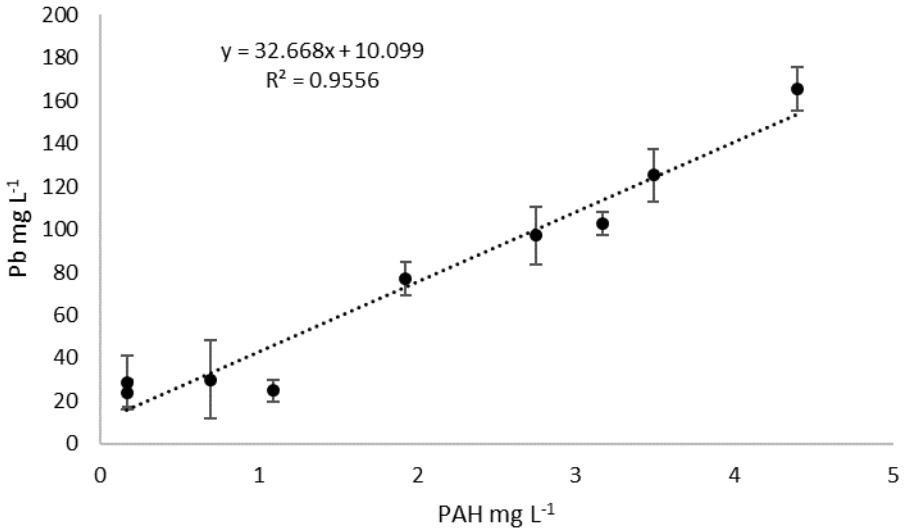

Figure 31: Total PAH concentration correlated with Pb concentration per organic matter group

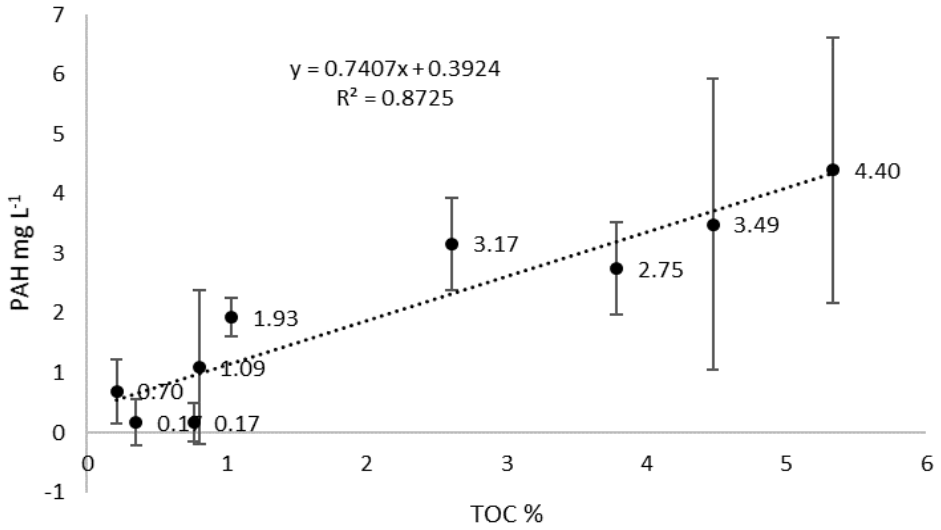

Figure 32: Total PAH concentration correlated with TOC

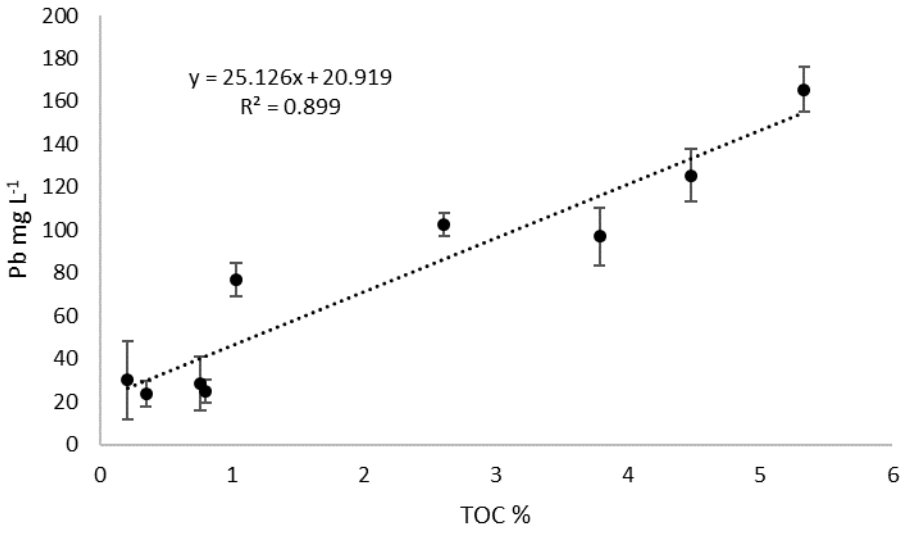

Figure 33: Pb correlation with TOC

The correlations shown in Figures 31, 32 and 33 show that there were strong linear relationships between lead and PAH content in sediment samples, along with a strong relationship between both lead and PAH with organic carbon content. These linear relationships could predict that the contaminants (Pb and PAH) could exist more commonly in areas of higher organic carbon.

Table 9: Pearson's correlation table of all chemical parameters with correlated R^2 (left) values and P figures (right)

	Fe	Ca	Al	Pb	Cr	pH	EC	% MC	% OM	N	C	TOC	TOC/N	PAH ng/g
Fe		0.020328	0.0059965	3.28E-13	0.0001321	4.90E-05	0.011605	0.0026243	2.31E-05	1.42E-06	4.45E-07	4.49E-06	0.49838	0.0002144
Ca	-0.34877		0.63626	0.0030891	0.28681	0.0014096	0.73721	0.18685	0.054181	0.11119	0.061045	0.05861	0.37656	0.84598
Al	0.40783	0.073312		0.022989	0.11613	0.45166	0.52163	0.57771	0.095238	0.40444	0.45148	0.50925	0.88942	0.17813
Pb	0.84907	-0.43604	0.34219		1.75E-05	6.94E-07	0.079039	0.0018904	9.44E-09	1.13E-07	5.21E-10	2.37E-09	0.07767	8.57E-05
Cr	0.54468	-0.16421	0.2403	0.59885		5.87E-06	0.023432	0.040716	0.0003946	0.0002464	1.90E-05	4.36E-05	0.16507	0.0023988
pH	-0.57247	0.4666	-0.11643	-0.66888	-0.62457		0.034134	2.69E-06	0.0002644	0.000266	1.94E-05	0.0001193	0.28463	0.0080521
EC	0.37719	0.05205	0.099228	0.26762	0.34116	-0.32013		0.022208	0.040878	0.0050856	0.047218	0.020592	0.87119	2.79E-06
% MC	0.44262	-0.20275	0.086258	0.45549	0.30979	-0.64161	0.34405		0.0001541	0.0005989	0.0004681	0.0019761	0.82852	0.0069333
% OM	0.59195	-0.2923	0.25468	0.74006	0.51089	-0.52368	0.30955	0.54013		2.93E-10	3.70E-12	1.17E-10	0.1936	3.43E-06
N	0.65483	-0.24351	0.12887	0.70155	0.52587	-0.52348	0.41506	0.49703	0.78461		4.92E-18	4.41E-13	0.71782	2.35E-05
C	0.67728	-0.28471	0.11648	0.77788	0.59685	-0.59637	0.30084	0.50529	0.82892	0.91379		5.65E-16	0.28048	1.34E-05
TOC	0.63055	-0.28732	0.10218	0.75899	0.57555	-0.54765	0.34808	0.45378	0.79488	0.84675	0.89074		0.0008812	2.27E-05
TOC/N	0.1048	-0.13661	-0.021581	0.26881	0.213	-0.16494	-0.025166	0.033612	0.19975	-0.05605	0.16635	0.48365		0.37431
PAH ng/g	0.53017	-0.030146	0.20675	0.5571	0.4462	-0.3945	0.64082	0.40133	0.6364	0.5915	0.60538	0.59247	0.13725	

5. Discussion

Obtaining all possible pieces of information about the environmental sediment samples was vital in understanding the chemistry and health of this manmade island and it's surrounds on the East coast of Ireland. Sediment characterisations such as particle size analysis, can tell so much about an environmental sample. An abundance of grains of a particular size can identify the availability of organic and inorganic matter, determine the effects of mechanical weathering or identify a depositional site within the study area (Unda-Calvo et al. 2019). The grain size in this study ranged from 106.9µm to 506.9µm and could be described as poorly sorted muddy sand to well sorted sand. 13 of the 31 samples sent away for PSA testing contained over 90 % sand, which is due to the island being formed from a sand spit (Gibson et al. 2012). The intertidal and island zones contained the highest sand content in their samples, when compared to the salt marsh and mudflat samples. This was expected as the island contains many sand dunes and the salt marsh and mud flat areas could be influenced by the rivers and streams entering the Irish Sea via this bay and transporting finer riverine sediments into these areas (Brooks et al. 2016).

The electrical conductivity (EC) (concentration of conductive ions) of a sample can provide some insight into the influence from either terrestrial or marine waters, with higher EC values indicating marine waters due to higher salinity. Varying EC can also influence cation exchange capacity, drainage conditions, organic matter content, salinity, and subsoil characteristics which all provide a bigger picture of the sediment health (Grisso et al, 2009). Figure 18 showed an EC range between 0.06 - 9.24 mS/cm. As expected, samples from the island showed lowest EC concentrations, where samples are not in direct contact with seawater. The intertidal zone EC values ranged from 1.0 to 6.0 mS/cm, whereas areas in the salt marsh and mudflats, specifically samples 15, 22, 32, 34, 35, 37, 39, 40 and 4 contained the highest values of 7.0 - 9.5 mS/cm. These 9 samples of higher EC content contained ≤85 % sand,

indicating that there is a trend between the finer sediments and a high EC content. This could be due to the larger surface area of smaller sediments and the likelihood of particles to attach to them physically.

The average global seawater pH is 8.1 (Ni Longphuirt, et al. 2010), and sediments that get covered in seawater are expected to have a similar pH to this. The range in pH values in the study area was from slightly acidic (6.30) to basic (9.9). The lower pH values occurred in the mudflat zone, near to where the Santry River and River Naniken enter the study area, there could be a riverine influence to the pH values here. In this area, low sand content (≤85 % sand) and higher OM contents were found. The organic matter content in the samples can indicate the content of living and decayed plant and animal materials, which is vital in understanding the overall chemistry occurring. The areas of lower sand content, with higher OM content could have occurred due to the lower surface area of these larger sand particles, compared to clay or mud, and also the available OM in the area.

Carbon to nitrogen ratio (C:N) and total organic carbon (TOC) are also useful tools in understanding the source of organic matter in a study area. A large variance in C:N was seen, between 2.0 – 43.0. As stated above, a C:N ratio between 4 - 10 indicates an algal or marine source, whereas a ratio over 15 indicates terrestrial plant content (Mayers 1997). Samples in the southern lagoon, specifically, contained C:N ratios over 15, indicating terrestrial input. The intertidal zone overall contains lower ratios (C:N <10) as expected, as this area is classed as marine waters. The highest ratio of C:N found in this study was 270 and this occurred across the mudflats, where the bridge enters the middle of the island. This indicates that the organic matter in this area had a much higher N content when compared to other samples. This could mean that sediments in this area could be derived from the coastal road adjacent to the island, due to coastal erosion (Gibson et al. 2012) or that the previously mentioned rivers and streams are bringing sediments into the study area. The successful storage of carbon in tidal wetlands

plays an important role in the global carbon cycle and with future influxes in stormy weather expected globally, protection of these wetlands is vital (Kelleway et al. 2017). The TOC assessment carried out in this study was carried out on the top 10 cm of sediment, thus providing only a small insight into the carbon stored in the leaves, stems and branches of plants, including some roots and dead organic matter. A higher carbon content is expected to be buried underneath this top-layer in the form of dead and decaying organic matter. As stated by Grimsditch et al. (2013), intertidal salt marsh zones have accumulation rates of around 18 g cm^{-2} yr^{-1}, and a healthy coastal salt marsh should continue to sequester carbon and increase sediment levels vertically as sea levels rise. An unhealthy coastal bay, as the latter, may not resist coastal changes and this could lead to the release of carbon dioxide through the oxidation of organic carbon present in sediments (McLeod et al. 2011).

In this study, PAH concentration decreased towards the Irish Sea, as did organic matter content and percentage clay. The average PAH concentration was 1751.0 ng/g, which is below the recommended ERL of 4,022 ng/g and ERM of 44,792 ng/g showing a low risk of toxicity (Long 1995). Although the samples contained sum PAH concentrations below the recommended toxicity limits, all 16 tested PAHs were present above their *individual* recommended effect range low (ERL) values at various sites, and three individual PAHs; acenaphthylene, acenaphthene and phenanthrene, were present above the individual effect range medium *(ERM)* values. Hydrocarbon pollution can be from natural or anthropogenic sources, yet PAHs are more commonly associated with human activities involving the burning of fossil fuels (Kvenvolden & Cooper 2003; Abdel-shafy & Mansour 2016; Sun et al. 2016; Murphy et al. 2016 Kim et al. 2017). Although the 16 PAHs are present in quanitities below the guidellined values for toxicity, they are persistent organic pollutants (POPs) and their monitoring is vital due to their ubiquitous and toxic nature in terrestrial and marine environments (Hung et al. 2008; Martinez et al. 2004; Raoux et al. 1999; Song et al. 2002;

Wilcke 2000). PAHs are a concern due to their carcinogenic, mutagenic and teratogenic properties (Abdel-shafy & Mansour 2016; Krasnoschekova 1979) and adverse influence on marine biota through bioaccumulation in fatty tissues, due to high lipid solubility (International Agency for Research in Cancer 1983; McCready et al. 2004; Woodhead et al. 1999).

There was an abundance of both high molecular weight (HMW) and low molecular weight (LMW) counterparts. HMW PAHs are more persistent in the environment, due to the higher volatility of the LMW compounds (Abdel-shafy & Mansour 2016; Wild et al. 1991). The beginning of industrialisation in the middle of the 19th Century, the peak of coal burning in the 1980's and the introduction of unleaded petrol in the 1980's (Glennon et al. 2014) are significant events that would have contributed to long-term effects on soils, including the release of HMW PAHs. Three single PAHs (acenaphthylene, acenaphthene and phenanthrene) were in quantities higher than the recommended ERM at several sites. This group of PAHs are LMW PAHs as they contain 3 aromatic rings. Acenaphthene in particular occurred at over twice it's ERM value of 500 ng/g, (Long et al, 1995) with a concentration of 1213 ng/g at one site. PAHs interact with the marine system by gaseous exchange at the air water interface, or via dry soot deposition or precipitation (Simoneit 1989). Once in the water they bind to particulate matter and accumulate in sediment over time (Oros & Ross 2004; Murphy et al. 2016). As these three PAHs are LMW, they are more likely to be lost via gaseous exchange, due to higher volatility, compared to the heavier counterparts. Yet, scenarios such as coastal erosion and mass sediment movements, could cause PAHs could to get buried and accumulate in sediments for long periods of time.

Three PAH isomer pair ratios were utilised to determine the source of PAHs in BI and showed a dominance of combustion sources, with few samples containing PAHs coming directly from petroleum. PAHs can come from the incomplete combustion of fossil fuels, road and industrial run off, contaminated sites and pyrolysis, along with natural seepage (Fleming

et al. 2005). These processes can release PAHs into the atmosphere, where they eventually settle into water bodies or sediments (Dat & Chang 2017). This could be one reason why PAH concentrations are higher near the roadsides. According to this ratio calculation, overall, PAHs in BI samples come from the combustion of biomass and fossil fuels, with a small input from direct petroleum sources. The first isomer ratio calculation (IP/IP+BghiP) revealed that many samples were likely to be from biomass and coal combustion sources. One sample, number 41 was an outlier, which can be seen on figure 20 as a blue dot on the x-axis (on the IP/(IP+BghiP) plot). This sample was taken from the salt marsh zone. The second isomer ratio calculation (BaA/228) also showed a large number of samples coming from combustion sources, the type of fuel combustion is not specified in this ratio calculation. The outlier of this graph was sample 46 taken from the island, which strongly suggests a petroleum source. The same result occurred for the final isomer ratio (An/178), with one more sample, number 49, showing petroleum as their source. This sample was also taken from the island. As there are only three samples indicating a petroleum source, it can be suggested that these are from localised point sources or due to activities on the island itself, such as fuel leaks from motor vehicles.

Sum PAH values exceeded 6000 ng/g in samples 16, 25, 32, 36, 41 and 46 (Appendix 5). These samples were described as ‘soil’ samples at the time of sampling, with some containing grass cover. These samples were generally light in colour with locations close to the roadside and/or on the golf course situated on BI. Sum PAH values over 6,000 ng/g are much higher than some similar studies in Libya and the USA on coastal bays (Kim et al. 2018; Bonsignore et al. 2018). However, higher PAH concentrations have been reported in many other studies in coastal bays, for example Viguri et al (2002) had a sum 16 PAH range of 20 - 25,800 ng/g in Santander Bay, Spain and Guanabara Bay, Brazil had a sum of 39 PAH range of 96.0 - 135,000 ng/g (Wagener et al. 2012). As stated by Glennon et al (2014) in the SURGE project, it is inaccurate to compare PAHs present in different countries as each country will

vary in its industrial activities, size and other environmental factors. Through a similar project, Andersson et al (2011) found peak concentrations of (∑ 16) PAHs in Dublin City of 63,000 ng/g. This large value is thought to be due to bituminous coal burning and considerable traffic congestion in the city centre. This study showed that Dublin City has much higher values of anthropogenic source PAHs, when compared to BI.

Three samples (15, 23 and 34) containing a sand content of ≤55 % contained higher PAH concentrations overall, with values between 884.84 – 1423.31 ng/g ∑PAH. This shows a link between samples of low sand, and high PAH content. Areas of high PAH concentration occur near known inlets of freshwater as seen in Figure 4. This is also where there was the highest C:N ratio, indicating that terrestrial sources are the dominant source of OM in this area (Mayers 1997). It has been estimated that 7.2 $x10^6$ m^3 d^{-1} of water is exchanged daily around Bull Island (Harris 1977). Seawater (Figure 4) enters from both the north and south of the island where it meets freshwater coming from inland rivers. The Naniken River flows into the southern lagoon, whereas the northern lagoon receives freshwater from Sutton Creek and Santry River (Figure 5) (Brooks et al. 2016). Dissolved and particulate material in these freshwater conduits may then concentrate and accumulate in the lagoon area.

PAH concentration is generally high in areas of high silt and clay content and were generally at lowest values in areas of ≥95 % sand. However, PAHs were high in areas of the salt marsh, which were low in clay possibly due to the presence of Salicornia salt marsh plants that have been shown to accumulate pollutants such as PAHs (Gonçalves et al. 2016). Plants that are commonly present in coastal salt marshes have recently been shown to efficiently phyto-remediate PAHs by assisting in the intake of PAHs. This occurs through roots and biodegradation through the rhizosphere, thus reducing the available PAHs in soils and sediments (Reddy et al. 2017; Gonçalves et al. 2016; Lu et al. 2011). Although studies have shown that whilst PAHs reduced in this scenario, metal concentrations did not decrease, some

became immobilized, yet it seems as though PAHs are more readily taken up by plants (Reddy et al. 2017.

There was a relatively high correlation (R^2 =0.76) between high PAH concentration and TOC content (Appendix 10), as seen in other studies (Arienzo et al. 2017; Simpson et al. 1996). Areas of high PAH and high C:N ratio over 20 can be seen in maps in Fig 17 and 20, along James Larkin road, to the right of the bridge which intersects the middle of the island. An opposite trend was seen at the north of the island, travelling towards Howth, where PAH concentration increased, as C:N decreased. Carbon to nitrogen ratio is important as it shows the likelihood of decomposition of organic matter in sediment, a wider C:N ratio shows that decomposition is less likely, and this directly relates to the possibility of breakdown of PAHs (Han et al. 2017).

The comparative PAH experiment between 2016 and 2017 showed that PAH content changes over time in the study area, according to the eight samples that were retested one year later. More specifically, samples 37, 33 and 44 from the southern lagoon showed an increase in PAH content between 2016 and 2017. These samples occur to the left of the bridge that intersects the island and close to the potential sources of riverine input, particularly from the Santry River and River Naniken. Samples 36, 32 and 38, also from the southern lagoon, showed a decrease in PAH content. Sample 39 and 41 from the northern lagoon showed an increase and a decrease respectively. This change in PAH content could be because of changes in deposition rates, either from water or the atmosphere or because the sample was not taken from exactly the same site with the same coordinates. If it was, the site would have been disturbed during sampling the year before and if it was not, PAH concentration may vary a lot even within a few meters. Alternative reasons for the change in concentration could be due to an increase in the motor vehicles used in the vicinity, coastal flooding or the opening of the Dublin

WtE plant, as previously mentioned. More temporal studies are required to investigate why these differences occurred.

Areas of highest iron concentration coincided with high lead and PAH concentrations, in the mudflat and salt marsh zones. Iron concentrations ranged from 0.6 - 5.8 % (6000 - 58000 ppm) in the study area, with a strong linear relationship between PAHs and Fe content (R^2 of 0.913) and also between Fe and TOC (R^2 of 0.697). Relatively high correlations have been reported in other studies between Fe and TOC (R^2 of 0.72 to 0.78), and Fe and Clay (R^2 of 0.64 to 0.83) (Wei-wei et al. 2018). Iron ranged from 0.58 – 4 % (5800-40000 ppm) in a study by Doyle & Otte (1997) in the wider Dublin Bay area, compared to the 0.6-5.8 % in this project, which shows similarities between the two surveys. The National Soil Database Project mapped iron concentrations across Ireland and found average concentrations of iron between 2.01 % and 2.5 % in Dublin (Fay. et al. 2007). This correlates with the map (Figure 25) of Fe in Bull island, with a range of 0.6 to 5.8 % Fe, with the higher concentrations being seen in the salt marsh and mudflats compared to the intertidal samples beyond the island.

The range of lead (Pb) in the sampling area was 17.8-440 ppm, with higher concentrations occurring in the salt marsh and mudflat areas. It should be noted that the average Pb concentration was much lower than the max value found (440 ppm), at 85.31 ppm, which only just exceeds the VROM recommended value of 85 ppm. However, this remains below the recommended ERM from Long et al. (1995) of 218 ppm (Table. 4), showing low chances of toxicity. The average Pb value lies larger than the recommended limit of Pb in China of 35 ppm (GB15618 Ministry of Environmental Protection of China 1995) and the recommended levels for soil of sustainable quality (85 ppm) (Dutch Ministry of Housing Spatial Planning and Environment (VROM) 2000). According to the Environmental Protection Agency Ireland (2006), the concentration of lead from ‘uncontaminated sites’ it a wide-scale study was between 30 -120 ppm. Both chromium and lead are listed as priority pollutants due to their

known toxicity carcinogenic properties over 0.015 ppm (US Department of health and human services. 2006). The area of highest Pb was along James Larkin Road, which is also the zone of highest PAH contamination. As previously stated, the C:N ratios indicate that this area is influenced mostly by materials coming from inland so it is reasonable to suggest that higher PAH and Pb concentrations would derive from terrestrial rather than marine sources. There is an indication of point source origin for Pb at sites alongside the road that intersects half way through BI, specifically in samples 26, 28, 30, 35 and 43, which could be influenced by the River Santry that feeds into the northern lagoon (Figure 5).

The concentration of lead generally decreases further away from the roadside, again indicating terrestrial sources (G.L.Wheeler & G.L.Rolfe 1979; Zupancic 1999). As also seen in the Dublin Soil Urban Geochemistry (SURGE) Project (the first in-depth baseline geochemical study of top soils in the greater Dublin area), Pb generally decreased with distance away from industrialised areas (Glennon et al. 2014).There is a recommended limit of 0.05 ppm Pb in water intended for drinking (S.I. No. 294/ European Union 1989) and an EQS (environmental quality standard) value of 0.0072 ppm for lead in transitional and coastal waters (Environmental Agency Germany 2011) and the average value of 85.31 ppm in this study exceeds these values greatly.

Average lead in Irish marine and terrestrial waters was at 7.2 ug/l in 2006 (EPA 2006). There is historic evidence of Pb pollution in the River Tolka (Buggy and Tobin, 2008), which feeds directly into the BI sampling zone and again suggests that this pollution in from inland sources carried to the study area through local rivers and streams. The higher concentrations of Pb are mostly contained to this salt marsh/mudflat area in the middle of the sample site. Reasoning for this containment of lead could be due to the transfer of metals, in a body of water. The Santry River and River Naniken enter the south lagoon close to where this

accumulation of lead is taking place. There could also be a depositional zone occurring in the centre of the south lagoon, where the bridge intersects the island (see Figure 5).

Chromium (Cr) is another metal that occurs naturally but high levels are linked to industrial activities that release different forms of Cr into the environment (Callender 2003). Cr was in concentrations between 27.5 to 70 ppm in Bull Island, with an average concentration of 41.5ppm. The higher concentrations, between 50 and 70 ppm were again in the salt marsh and mud flat zones, as seen with iron and aluminium. Long et al. (1995) set out ERL and ERM values for Cr (81 ppm and 370 ppm respectively), and the BI samples remained below both values showing low risk of toxicity to flora and fauna. However, the concentrations are notably above the median values for chromium (59 ppm) in European soils so it is important to continue to monitor this in the future (Luo et al. 2012). The average Cr value in this study is above the EPA recommended value of 0.015 ppm, with higher values showing signs of carcinogenicity (Environmental Protection Agency Ireland, 2006; U.S. Department of Health and Human Services 2002).

Aluminium (Al) has been used in past research as an indicator of source of metal pollution in marine sediments, as a representative metal (Weisberg et al. 1999). The Soil Geochemical Atlas of Ireland (Fay. et al. 2007) showed an Al range in greater Dublin of 4.1 - 5 % (41,000 – 50,000 ppm). Al in this BI study ranged between 2 - 5.7 %, with the highest concentrations occuring in the salt marsh and mudlflat zones, as seen with Fe and PAHs (Table 5). This suggests again that runoff from inland and rivers/steams has an influence on Al concentrations and that there may be an anthropogenic source. Although Al is present naturally, as the third most abundant metal on earth (Rosseland et al. 1990), it too has its negative impacts on the environment. Al induced toxicity affects marine life by way of reducing their capacity to uptake ions and carry out metabolic processes. Aluminium also has an antogonistic relatioship with calcium, where increasing Ca concentration decreases Al toxicity. This shows

the importance of monitoring all elements possible in an environmental study. Al also causes acidification of marine waters, so the pH value can show relate directly to the concentration of Al present also (Rosseland et al. 1990). No guidelines exist for the exposure limits of Al for humans for ingestion or overall exposure to the metal (Exley. 2013) but high levels of exposure have shown mild neurotoxic effects in a study in Italy (Polizzi et al. 2002) amongst workers exposed to alumiminium dusts. Al is another example of an element that needs to be monitored in the future, in protected areas such as Bull Island to ensure the health of the biosphere overall. Raised awareness about organic and inorganic groups of compounds is a necessity with regard to the future protection of this sand island and its surrounds in future years to come.

6. Conclusion

An aim of this study was to provide baseline information on the chemical and physical characteristics of soils and sediments from BI and to map these so that they are available for further use. Detailed surveys of ground properties are becoming even more important in an era of unprecedented environmental data generation from remote sensors on satellites and aircraft. Satellite-based environmental data is an important asset that can provide cost effective and timely information for mapping, monitoring, and managing coastal environments. It is therefore a major tool that can be used to address societal challenges such as coastal flooding, port security or marine pollution. A primary objective of this project was to provide information that can be used to validate, calibrate and extract as much information as possible from satellite earth observation data. A coordinated, long-term provision of such datasets is required to generate models that can be used to predict environmental change. These models will contribute to future planning in a diversity of areas such as coastal mapping, flooding prediction, marine habitats and fisheries, climate change, environmental protection and policy.

Another objective was to understand how anthropogenic activities are affecting the island through the study of organic and inorganic contaminants. The maps clearly indicate that there is a depositional zone in the salt marsh/mud flat area of Bull Island. PAH isomer ratios show that the primary source of PAHs is the combustion of fossil fuels and their distribution is dictated by dry and wet deposition. A short, comparative study of 8 sites showed that PAH concentration is not constant and that the level of contaminants is susceptible to changing over time. Total PAH levels remained below the concentrations of high chance of toxicity, with three 3-ringed PAHs showing high concentrations. According to these values, this site is not heavily contaminated by PAHs, but there is a presence of these compounds that should be monitored.

C:N ratios show that much deposition is through freshwater streams and inlets and suggests that the high PAH concentrations are mainly due to anthropogenic activity further inland. This is also true for the higher concentrations of Pb and Cr on Bull Island. Recent research also highlighted high concentrations of PAHs in greater Dublin Bay sediments and while this is not globally unique, it showed that microbial community structure can be perturbed in response to anthropogenic pollution (Murphy et al. 2016). Understanding the most basic chemistry of sediment samples is also vital in providing the overall picture of the health of Bull Island. The electrical conductivity, particle size and pH of samples shows the susceptibility of these sediments for cation-exchange, adherence of pollutants and transport of sediment particles.

Coastal systems such as BI are therefore dynamic and react and change constantly to natural and anthropogenic forcing. Prediction of change will be very important for the management of challenges such as rising sea level, acidification and erosion. Consistent monitoring of sediment and water properties in coastal areas will help to achieve this.

The study of the presence of a variety of flora and fauna in the study area is an important asset when discussing the impacts of global climate change on the health of a coastal wetland. Atlantic and Mediterranean Sea meadows (Grimsditch et al. 2013) cover large sections of the salt marsh, the roots providing strength and stability to ensure that the sediments are held tightly together to resist the effects of flooding. The effects of global climate change can be understood more efficiently when the knowledge of the basic environmental studies have been carried out on coastal bays and other vulnerable areas. Future work firstly includes the specific study of a wider range of PAHs, including alkylated and methylated compounds, to enhance the knowledge base of anthropogenic input into the study area, and secondly, the study of a number of coastal, manmade islands as a larger, comparative study to establish similarities and differences in these unique habitats.

7. Bibliography

Abdel-shafy, H.I. & Mansour, M.S.M., 2016. A review on polycyclic aromatic hydrocarbons : Source , environmental impact , effect on human health and remediation., pp.107–123.

Achterberg, E., Emerson, S.R. & Hedges, J.I., 2009. Chemical Oceanography and the Marine Carbon Cycle. *Marine Geophysical Researches*, 30(2), pp.135–135.

Al-Masri, M.S., Al-Kharfan, K. & Al-Shamali, K., 2006. Speciation of Pb, Cu and Zn determined by sequential extraction for identification of air pollution sources in Syria. *Atmospheric Environment*, 40(4), pp.753–761.

Alongi, D., 2002. Present State and Future of the World's Mangrove Forests. *Environmental Conservation*, 29(3), pp.331–349.

Andersson, M., Eggen, O., Finne T.E., Hoston, A., Jensen, H., O'Connor, P., Glennon, M., Scanlon, R., 2011. Arsenic, heavy metals, PAHs and PCBs in surface soils from Dublin, Ireland, Available at: http://www.ngu.no/upload/Publikasjoner/Rapporter/2011/2011_020.pdf.

Angelini, R., Contente, R. F., Rossi-Wongtschowski, .B. C., Soares, L., Schaeffer-Novelli, Y., Lopes, R., Mancini. L., Coll, M., Antonia, A., 2018. Ecosystem modeling as a framework to convert a multi-disciplinary research approach into a useful model for the Araçá Bay (Brazil). *Ocean and Coastal Management*.

Arienzo, M., Donadio, C., Mangoni, O., Bolinesi, F., Stanislao, C., Trifuoggi, M., Toscanesi, M., Natale, G., Ferrera, L., 2017. Characterization and source apportionment of polycyclic aromatic hydrocarbons (pahs) in the sediments of gulf of Pozzuoli (Campania , Italy). *Marine Pollution Bulletin*, 124(1), pp.480–487. Available at: http://dx.doi.org/10.1016/j.marpolbul.2017.07.006.

Aubert, H., and Pinta, M., 1978. Trace Elements in Soils. Bd. 7 der Reihe Developments in Soil Science. Elsevier, Amsterdam, New York 1977, Z. Pflanzenernaehr. Bodenk., 141: pp.252-253. doi:10.1002/jpln.19781410214

Barrington, S. et al., 2002. Effect of carbon source on compost nitrogen and carbon losses. *Bioresource Technology*, 83(3), pp.189–194.

Bevacqua, A., Yu, D. & Zhang, Y., 2018. Coastal vulnerability: Evolving concepts in understanding vulnerable people and places. *Environmental Science and Policy*, 82(January), pp.19–29.

Bonsignore, M. et al., 2018. Marine pollution in the Libyan coastal area : Environmental and risk assessment. *Marine Pollution Bulletin*, 128(November 2017), pp.340–352.

Bosch, A.T. & Cooper, M.J., 2009. Wetland Ecology and Management for Fish, Amphibians and Reptiles. *Earth Systems and Environmental Sciences*, pp.582–589.

Brooks, P.R. et al., 2016. *Dublin Port and Dublin Bay: Reconnecting with nature and people*, Elsevier Ltd. Available at: http://linkinghub.elsevier.com/retrieve/pii/S2352485516300305.

Callender, E., 2003. *Heavy metals in the environment historical trends. In: Treatise on Geochemistry (Editors; Holland. D, Turekian K. K.).* pp.67-105.

Candan, N. & Tarhan, L., 2005. Effects of Calcium, Stress on Contents of Chlorophyll and Carotenoid , LPO Levels , and Antioxidant Enzyme Activities in Mentha. *Journal of Plant Nutrition*, (November 2014), pp.127–139.

Costanza, R. et al., 1997. The value of the world's ecosystem services and natural capital. *Nature*, 387, pp.253–260.

Crowe, O. & Boland, H., 2004. Irish Wetland Bird Survey: Results of Waterbird Monitoring

in Ireland in 2001/02. *Irish Birds*, pp.313–326.

Crowe, O., Boland, H. & Walsh, A., 2012. *Irish Wetland Bird Survey: results of waterbird monitoring in Ireland in 2010/11*,

Dat, N. & Chang, M.B., 2017. Review on characteristics of PAHs in atmosphere, anthropogenic sources and control technologies. *Science of the Total Environment Review*. 609, pp.682–693.

Doyle, M.O. & Otte, M.L., 1997. Organism-induced accumulation of Iron, Zinc and Arsenic in Weltand soils. *Environmental Pollution*, 96(1).

Dublin City Council (DCC), 2013. *Environmental Report of the Naas Road Lands Local Area Plan – Strategic Environmental Assessment (SEA)*.

Dutch Ministry of Housing Spatial Planning and Environment (VROM), 2000. *Circular on Target Values and Intervention Values for Soil Remedia- tion Annex a: Target Values, Soil Remediation Intervention Values and Indicative Levels for Serous Contamination.*,

Dwyer, N., 2012. *The Status of Ireland' s Climate , 2012*, Johnstown Castle, Ireland.

Environmental Agency Germany, 2011. *Environmental quality standards (EQS) for priority substances and other substances relating to chemical status. Surface Waters Ordinance 2011*, Available at: https://www.umweltbundesamt.de/sites/default/files/medien/376/dokumente/environmental_quality_standards_eqs_for_priority_substances_and_other_substances_relating_to_chemical_status.pdf.

Environmental Protection Agency Ireland, 2006. Authors; Clenaghan, C., O'Neill, N., Page, D., Dangerous substances regulations national implementation report, 2005. Wexford, Ireland

EPA, 2006. *EPA Water Framework Directive EU Water Framework Directive Monitoring*

Programme - EPA. Prepared to meet the requirements of the EU Water Framework Directive (2000/60/EC) and National Regulations implementing the Water Framework Directive (S.I. No. 722).

EU, 1976. *Council directive, 76/464/EEC pollution caused by certain dangerous substances discharged into the aquatic environment of the community. Off. J. Eur. Union*,

EU, 1980. *Council directive 80/778/EEC of 15 July 1980 relating to the quality of water intended for human consumption. Off. J. Eur. Union*.

European Union and European Parliament, 2000. Directive *2000/60/EC of the European Parliament and of the council of 23 October 2000, establishing a framework for Community action in the field of water policy*, Available at: http://eur-lex.europa.eu/resource.html?uri=cellar:5c835afb-2ec6-4577-bdf8-756d3d694eeb.0004.02/DOC_1&format=pdf.

Exley, C. 2013. Human Exposure to aluminium. *Environmental Science Processes & Impacts. 15 (10) pp. 1785–1970.*

Fay., D., Kramers., G. & Zhang, C., 2007. *Soil Geochemical Atlas of Ireland*, Wexford.

Fleming, N., Edger, M. & O'Keeffe, C., 2005. *Greater Dublin Strategic Drainage Study Regional Drainage Policies - Volume 3. Environmental Management 3. 3.1 water quality*,

Fourqurean, J.W. et al., 2012. Seagrass ecosystems as a globally significant carbon stock. *Nat. Geosci*, 5(7), pp.505–509.

Friedel, J.K. & Gabel, D., 2001. Microbial biomass and microbial C:N ratio in bulk soil and buried bags for evaluating in situ net N mineralization in agricultural soils. *Journal of Plant Nutrition and Soil Science*, 164(6), pp.673–679.

G.L.Wheeler & G.L.Rolfe, 1979. The relationship between daily traffic volume and the

distribution of lead in roadside soil and vegetation. *Environmental Pollution (1970)*, 18(4), pp.265–274.

Gibson, P.J., Caloca-Casado, S. & Jiménez-Martín, D., 2012. *Integrated Coastal Mapping of Dublin Bay Geomorphology based on geophysical data, satellite inferred bathymetry and 3D integration with INFOMAR datasets.*, Available at: http://infomar.ie/documents/Research/INF-11-07-GIB.pdf.

Glennon, M.M. et al., 2014. The Dublin SURGE Project: Geochemical baseline for heavy metals in topsoils and spatial correlation with historical industry in Dublin, Ireland. *Environmental Geochemistry and Health*, 36(2), pp.235–254.

Gonçalves, C. et al., 2016. PAHs levels in Portuguese estuaries and lagoons : Salt marsh plants as potential agents for the containment of PAHs contamination in sediments. *Regional Studies in Marine Science*, 7, pp.211–221. Available at: http://dx.doi.org/10.1016/j.rsma.2016.05.004.

Gunnell, J.R., Rodriguez, A.B. & Mckee, B.A., 2013. How a marsh is built from the bottom up. *Geological Society of America Bulletin*, pp.1–4.

Grimsditch, G., Alder, J., Nakamura, T., Kenchington, R. Ambrose. & Tamelander, J. (2013). The blue carbon special edition – Introduction and overview. Ocean and Coastal Management, 83 1-4.

Grisso, R., Alley, M., Holshouser, D., Thomason, W. (2009) Precision Farming Tools: Soil Electrical Conductivity. *Virginia Polytechnic Institute and State University.*

Hammer, O., Harper, D, A, T., and Ryan, P. 2001. *Paleotonlogical statistics sotfware package for education and data analysis*.

Han, X., Hu, H., Shi, X., Zhang, L., He, J. 2017. Effects of different agricultural wastes on

the dissipation of PAHs and the PAH-degrading genes in a PAH-contaminated soil. *Chemosphere*, 172, https://doi.org/10.1016/j.chemosphere.2017.01.012. pp 286-293

Harris, C.R., 1977. North Bull Island Dublin Bay - A Modern Coastal Natural History Chapter 2: Sedimentology and Geomorphology. In D. W. Jeffrey, ed. *North Bull Island Dublin Bay - A Modern Coastal Natural History*. Dublin, pp. 13–25.

Harris, M., Eakin, M., Farrell, M., Moore, L., Clabby, G., NiCholmain, N., Casey, S., (2014). North Bull Island UNESCO Biosphere Periodic Review Report 2014. 10.13140/RG.2.1.3069.2089.

Heemken, O., Theobald, N., Wenclawiak, B. N., 1997. Comparison of ASE and SFE with Soxhlet, Sonication, and Methanolic Saponification Extractions for the Determination of Organic Micropollutants in Marine Particulate Matter. *Analytical Chemistry*. 69 (11), 2171-2180. DOI: 10.1021/ac960695f.

Hoogsteena, M.J.J. et al., 2015. Estimating soil organic carbon through loss on ignition : effects of ignition conditions and structural water loss. *European Journal of Soil Science*, 66(March), pp.320–328.

Hung, C. et al., 2008. Enhancement of particulate organic carbon export flux induced by atmospheric forcing in the subtropical oligotrophic northwest Pacific Ocean. *Marine Chemistry*.

ICH, 2005. *Validation of Analytical Procedures: Test and Methodology*, Q2 (R1). From; International conference on haromonisation of technical requirements for registration of pharmaceuticals for human use.

International Agency for Research in Cancer, 1983. *Monographs on the Evaluation of the Carcinogenic Risk of Chemical to Humans Polycyclic Aromatic Compounds, Part I*

Chemical, Environmental and Environmental Data, Lyon. Available at: http://monographs.iarc.fr/ENG/Monographs/vol1-42/mono32.pdf.

IPCC, 2012. Managing the risks of extreme events and disasters to advance climate change adaptation*: Special Report of the Intergovernmental Panel on Climate Change*, Available at: https://www.ipcc.ch/pdf/special-reports/srex/SREX_Full_Report.pdf.

IPPC, 2014. *Climate Change 2014: Impacts, Adaptation, and Vulnerability. Part A: Global and Sectoral Aspects. Contribution of Working Group II to the Fifth Assessment Report of the Intergovernmental Panel on Climate Change*, Cambridge University Press, Cambridge.

Ishiwatari, R. & Uzaki, M., 1987. Diagenetic changes of lignin compounds in a more than 0.6 million-year-old lacustrine sediment (Lake Biwa, Japan). *Geochimica et Cosmochimica Acta*, 51(2), pp.321–328.

ISO (the International Organization for Standardization), 2005. *ISO 10390:2005. Soil quality - Determination of pH*, Available at: www.iso.org/obp/ui/#iso:std:iso:10390:ed-2:v1:en.

Kähler, P. & Koeve, W., 2001. Marine dissolved organic matter: Can its C:N ratio explain carbon overconsumption? *Deep Sea Research Part I Oceanographic Research Papers*, 48, pp.49–62.

Kantamaneni, K. Phillips, M., Thomas, T., Jenkins, R., (2018). Assessing coastal vulnerability: Development of a combined physical and economic index. *Ocean and Coastal Management*, 158 (April 2017), pp.164–175.

Kelleway, J.J. et al., Saintilan, N., Macreadie, P., 2017. Baldock , J. A., Heijnis, H., Zawadzki, A., Gadd, P., Jacobsen, G., Ralph, P.J. Geochemical analyses reveal the importance of environmental history for blue carbon sequestration. *J. Geophys. Res. Biogeosci*, (122),

pp.1789–1805.

Kennedy, H., J. et al., Beggins, J., Duarte, C. M., Fourqurean, J.W., Holmer, M., Marbà, N., Middelburg, J.J., 2010. Seagrass sediments as a global carbon sink: Isotopic constraints. GB4026. *Global Biogeochem. Cycles*, 24.

Killops, Stephen., Killops, V., 2005. Anthropogenic carbon and the environment. Chapter 7. In *Introduction to Organic Geochemistry*. Victoria, Australia: Blackwell Publishing, pp. 295–317.

Kim, A.W.,Vane, C., Moss-Hayes, V., Engelhart, S., Kemp, A.C., (2017). PAH, PCB, TPH and mercury in surface sediments of the Delaware River Estuary and Delmarva Peninsula, USA. *Marine Pollution Bulletin.* 129. 10.1016/j.marpolbul.2017.10.008. pp.788–793.

Koutsogiannopoulou, V. & Wilson, J., 2007. The fish assemblage of the intertidal salt marsh creeks in North Bull Island, Dublin Bay: seasonal and tidal changes in composition, distribution and abundance. , 588, pp.213–224. Available at: http://link.springer.com/article/10.1007/s10750-007-0664-z/fulltext.html.

Krasnoschekova, R., 1979. Changes in Hydrophobicity of Carcinogenic Polycyclic Arenes Influenced by Phenols. *Acta hydrochimica et hydrobiologica (Weinheim an der Bergstrasse, Germany)*, 7(4), pp.453–457.

Kristensen, E., Bouillon, S., Dittmar, T., Marchand, C., 2008. Organic carbon dynamics in mangrove ecosystems: A review. *Aquatic Botany*, 89, pp.201–219.

Kvenvolden, K.A. & Cooper, C.K., 2003. Natural seepage of crude oil into the marine environment. *Geo-Mar Lett*, (23), pp.140–146.

Lalor, B., 1989. *Dublin Bay: From Killiney to Howth* 1st ed., Dublin: O'Brien Press Ltd.

Long, E.R., Macdonald, D. D., Smith, S. S., Calderet, F.D., 1995. Incidence of Adverse

Biological Effects Within Ranges of Chemical Concentrations in Marine and Estuarine Sediments. *Environmental Management*, 19, pp.81–97.

Lu, H., Zhang, Y., Liu, B., Liu, J., Ye, J., Yan, C., 2011. Rhizodegradation gradients of phenanthrene and pyrene in sediment of mangrove (Kandelia candel (L.) Druce). *Journal of Hazardous Materials*, 196, pp.263–269.

Luo, X. Yu, S., Zhu, Y.G., Li, X., 2012. Science of the Total Environment Trace metal contamination in urban soils of China. *Science of the Total Environment*, 421–422, pp.17–30.

Martinez, E., Gros, M., Lacorte, S., Barcelo, D., 2004. Simplified procedures for the analysis of polycyclic aromatic hydrocarbons in water, sediments and mussels. *Journal of Chromatography A*, 1047(2), pp.181–188.

Mayers, P., 1997. Organic geochemical proxies of paleoceanographic, paleolimnologic, and paleoclimatic processes. *Organic Geochemistry*, 27(5–6), pp.213–250.

McBreen, F. & Wilson, J.G., 2006. The Pollution Status of North Dublin Bay. In *ESAI COLLOQUIUM PROCEEDINGS 2005*. Citeseer, p. 38.

McCready, S., Spyrakis, G., Greely, C. R., Birch, G.F., Long, E.R., 2004. Toxicity of Surficial Sediments from Sydney Harbour and Vicinity, Australia. *Environmental Monitoring and Assessment*, 96(1–3), pp.53–83. Available at: https://link.springer.com/article/10.1023/B:EMAS.0000031716.34645.71.

Mcleod, E., Chmura, L., Bouillon, S., Salm, R., Björk, M., Duarte, C. M., Lovelock, C. M., Schlesinger, W. M., Silliman, B.R., A blueprint for blue carbon: toward an improved understanding of the role of vegetated coastal habitats in sequestering CO 2 In a nutshell : *Front Ecol Environ*, 9(10), pp.552–560.

Meyers, P.A., 1997. Organic geochemical proxies of paleoceanographic, paleolimnologic, and paleoclimatic processes. *Organic Geochemistry*, 27(5), pp.213–250.

Ministry of Environmental Protection of China, B., 1995. *GB15618 Soil Environmental Quality Standards in China.*, Beijing.

Molamohyeddin, N., Ghafourian, H. & Sadatipour, S.M., 2017. Contamination assessment of mercury, lead, cadmium and arsenic in surface sediments of Chabahar Bay. *Marine Pollution Bulletin*, 124(July), pp.521–525.

Mossor-pietraszewska, T., 2001. *Effect of aluminium on plant growth and metabolism*,

Murad., E. & Fischer., W.R., 1988. The Geobiochemical Cycle of Iron. In *Iron in Soils and Clay Minerals.* pp. 1–18.

Murphy, B.T., O'Reilly, S. S., Monteys, X., Reid, B. F., Szpak. M., McCaul, M. M., Jordan, S. F., Allen, C. R., Kelleher, B.P., 2016. The occurrence of PAHs and faecal sterols in Dublin Bay and their in fl uence on sedimentary microbial communities. *Marine Pollution Bulletin*, 106(1–2), pp.215–224. Available at: http://www.sciencedirect.com/science/article/pii/S0025326X16301163.

Neathery, W., Miller, W.J. & Science, D., 1975. *Metabolism and Toxicity of Cadmium , Mercury , and Lead in Animals : A Review. Journal of Dairy Science. 58(12), December 1975, pp. 1767-1781.*

Ni Longphuirt, S., Stengel, D., Dowd, C., Mcgovern, E., (2010) Ocean Acidification : An Emerging Threat to our Marine Environment. Marine Institute, Sea Change, NUIG.

Nixon, S.W., 1980. *Between coastal marshes and coastal waters: A review of twenty years of speculation and research on the role of salt marshes in estuarine productivity and water chemistry*. Marine Science book series (MR, volume 11).

NPWS (National Parks and Wildlife Services), 2014. *North Bull Island Special Protection Area (Site Code 4006) & 1358 South Dublin Bay and River Tolka Estuary Special Protection Area (Site Code 4024) - Conservation 1359 Objectives Supporting Document (Version 1)*.

Oros, D. R., Ross, J. R. M., 2004. Polycyclic aromatic hydrocarbons in San Francisco Estuary sediments. 86, pp.169–184.

Polizzi, S., Pira, E., Ferrara, M., Bugiani, M., Papaleo, A., Albera, R., Palmi, S. 2002. Neurotoxic Effects of Aluminium Among Foundry Workers and Alzheimer's Disease, *NeuroToxicology,* 23(6), pp 761-774. https://doi.org/10.1016/S0161-813X(02)00097-9.

Raoux, C., Boyona, J.M., Miquel, J.C., Teyssie, J.L, Fowler, S.W., Albaigés, J., (1999) Particulate Fluxes of Aliphatic and Aromatic Hydrocarbons in Near-shore Waters to the Northwestern Mediterranean Sea, and the Effect of Continental Runoff. *Estuarine, Coastal and Shelf Science*, 48(5), pp.605–616.

Rashdi, A.S., Arabi, A., Howari, F., Siad, A., (2015). Distribution of heavy metals in the coastal area of Abu Dhabi in the United Arab Emirates. Marine pollution bulletin. 97. 10.1016/j.marpolbul.2015.05.052.Distribution of heavy metals in the coastal area of Abu Dhabi in the United Arab Emirates. *Marine Pollution Bulletin*, 97(1–2), pp.494–498.

Reddy, K., Amaya-Santos, G., Yargicoglu, E., Cooper, D., Negri, C. (2017). Phytoremediation of heavy metals and PAHs at slag fill site: three-year field-scale investigation. International Journal of Geotechnical Engineering. 10.1080/19386362.2017.1318231.

Reimann, C. & Caritat, P. de., 2000. Chemical Elements in the Environment. Factsheets for the Geochemist and Environmental Scientist. *Geological Magazine*, pp.593–598.

Rengarajan, T. Peramaiyan, R. Natarajan, N., Lokeshkumar, B., Rajendran, P., Nishigaki, I

(2015). Exposure to polycyclic aromatic hydrocarbons with special focus on cancer. *Asian Pacific Journal of Tropical Biomedicine*, 5(3), pp.182–189. Available at: http://dx.doi.org/10.1016/S2221-1691(15)30003-4.

Rosseland, B.O., Eldhuset, T.D., Staurnes, M., 1990. Environmental effects of aluminium. Environmental Geochemistry and Health. 12(1-2), pp17-27.

Rumolo, P., Barra, M., Gherardi, S., Marsellaa, E., Sprovier, M., 2011. Stable isotopes and C/N ratios in marine sediments as a tool for discriminating anthropogenic impact. *Journal of Environmental Monitoring*, 13(12), pp.3399–3408.

Saim, N. Dean, J. R., Abdullah, M. P., Zakaria, Z., 1998. An Experimental Design Approach for the Determination of Polycyclic Aromatic Hydrocarbons from Highly Contaminated Soil Using Accelerated Solvent Extraction. , 70(2), pp.420–424.

Sedman, R.M. Beaumont, J., McDonald, T.A., Reynolds, S., Krowech, G., Howd, R., 2006. Review of the evidence regarding the carcinogenicity of hexavalent chromium in drinking water. *J Environ Sci Health C Environ Carcinog Ecotoxicol Rev*, 24(1), pp.155–182.

Sharma, P. & Dubey, R., 2005. Lead toxicity in Plants. *Braz. J Plant Physiol*, 17(1), pp.35–52.

Simoneit, B.R.T., 1989. Organic matter of the troposphere — V: Application of molecular marker analysis to biogenic emissions into the troposphere for source reconciliations. *Journal of Atmospheric Chemistry*, 8(3), pp.251–275.

Simpson, C.D. Mosi, A. A., Cullen, W. R., Reimer. K, J., 1996. Composition and distribution of polycyclic aromatic hydrocarbon contamination in surficial marine sediments from Kitimat Harbor, Canada. 9697(95).

Sivaperuman, C. & Venkatraman, C., 2015. Marine Faunal Diversity in India. Chapter 7: Coastal and Marine Bird Communities of India. In *Marine Faunal Diversity in India*.

Kolkata, West Bengal, India: Elsevier, pp. 261–281.

Song, Y., Jing, X., Fleischmann, S., Wilke, B. M., 2002. Comparative study of extraction methods for the determination of PAHs from contaminated soils and sediments. *Chemosphere*, 48(9), pp.993–1001.

Sun, R., Lin, Q., Ke, C.L., Du, F. Y., Gu, Y. G., Cao, K., Luo, X. J., Mai, B. X., 2016. Polycyclic aromatic hydrocarbons in surface sediments and marine organisms from the Daya Bay , South China. *Marine Pollution Bulletin*, 103(1–2), pp.325–332. Available at: http://dx.doi.org/10.1016/j.marpolbul.2016.01.009.

Tanaka, A. & Tsuji, H., 1980. Effects of Calcium on Chlorophyll Synthesis and Stability in the Early Phase of Greening in Cucumber Cotyledons. *Plant Physiol.*, pp.1211–1215.

Tiwari, S., Tripathi, I. P., Tiwari, H.L., 2013. Effects of Lead on Environment. *International Journal of Emerging Research in Management &Technology*, 2(6).

Tollefston, J., 2018. Climate scientists unlock secrets of "blue carbon." *Nature*, (553), pp.139–140.

U.S. Department of Health and Human Services, 2002. NTP (National Toxicology Program)10th Report on carcinogens. Available at: https://ntp.niehs.nih.gov/pubhealth/roc/index-1.html#toc1.

Unda-Calvo, J., Ruiz-Romera, E., Fdez-Ortiz de Vallejuelo, S., Martínez-Santos, M., Gredilla, A (2019). Evaluating the role of particle size on urban environmental geochemistry of metals in surface sediments, *Science of The Total Environment*, (646), pp 121-133, Available at: https://doi.org/10.1016/j.scitotenv.2018.07.172.

UNESCO, 1995. *The seville strategy for biosphere reserves. Biosphere Reserves: The first Twenty Years*.

UNESCO, 2015. The Seville strategy for biosphere reserves: The first Twenty years, UNESCO. Available at: http://www.unesco.org/mab/doc/brs/Strategy.pdf.

Union, E., 1989. *S.I. No. 294/1989 - European Communities (Quality of Surface Water Intended For The Abstraction of Drinking Water) Regulations, 1989.*, Available at: http://www.irishstatutebook.ie/eli/1989/si/294/made/en/print#.

Vajpayee, P. Sharma, S.C., Tripathi, R. D., Rai, U. N., Yunus, M., 1999. Bioaccumulation of chromium and toxicity to photosynthetic pigments, nitrate reductase activity and protein content of Nelumbo nucifera gaertin. *Chemosphere*, 39(12), pp.2159–2169.

Viguri, J., Verde, J. & Irabien, A., 2002. Environmental assessment of polycyclic aromatic hydrocarbons (PAHs) in surface sediments of the Santander Bay , Northern Spain. *Chemosphere*, 48, pp.157–165.

Wagener, A. L., Meniconi, M, F., Hamacher, C., Farias, C.O, DaSilva, G.C., Gabardo, I.T., Scofield, I. L., 2012. Hydrocarbons in sediments of a chronically contaminated bay : The challenge of source assignment. , 64, pp.284–294.

Wallace, M.A.G., Pleil, J. D., Mentese, S., Oliver, K. D., Whitaker, D.A., Fent, K.W.,2017. Calibration and performance of synchronous SIM/scan mode for simultaneous targeted and discovery (non-targeted) analysis of exhaled breath samples from firefighters. *Journal of Chromatography A*, 1516, pp.114–124.

Wei-wei, M., Zhu, M., Yang, G., Li, T., 2018. Iron geochemistry and organic carbon preservation by iron (oxyhydr) oxides in surface sediments of the East China Sea and the south Yellow Sea. *Journal of Marine Systems*, 178(May 2017), pp.62–74.

Weisberg, S.B., Wilson, T., Heimbuch, D., Windom, H., Summers,. 1999. Comparison of sediment metal:aluminum relationships between the eastern and gulf coasts of the united

states. *Environmental Monitoring and Assessment*, 61, pp.373–385.

WILD, S.R., Obbard, J.B., Munn, C. I., Berrow, M.L., Jones, K.C., 1991. THE LONG-TERM PERSISTENCE OF POLYNUCLEAR AROMATIC HYDROCARBONS (PAHs) IN AN AGRICULTURAL SOIL AMENDED WITH METAL-CONTAMINATED SEWAGE SLUDGES. *The Science of the Total Environment*, 101, pp.235–253.

Wilson, J.G., 2003. Diffuse Pollution Conference Dublin 2003 DIFFUSE INPUTS OF NUTRIENTS TO DUBLIN BAY Diffuse Pollution Conference Dublin 2003. *Zoology*, (1962), pp.105–110.

Wilson, J.G., 2005. Difuse Inputs of Nutrients to Dublin Bay. In; *Diffuse Pollution Conference Dublin 2003*. Dublin 2, Ireland, pp. 105–110.

Wilson, J.G., 1982. The Littoral Fauna of Dublin Bay. *Irish Fisheries Investigations. Series B (Marine)*, 26.

Wolfgang & Wilcke, 2000. SYNOPSIS Polycyclic Aromatic Hydrocarbons (PAHs) in Soil — a Review. *Journal of Plant Nutrition and Soil Science*, 163(3), pp.229–248.

Woodhead, R. J., Law, R. & Matthiessen, P., 1999. Polycyclic Aromatic Hydrocarbons in Surface Sediments Around England and Wales, and Their Possible Biological Significance. *Marine Pollution Bulletin*, 9(38), pp.773–790.

Yan, Jian., Wanga, Lei., Fub, Peter., and Yua., H., 2009. Photomutagenicity of 16 polycyclic aromatic hydrocarbons from the US EPA priority pollutant list. *Mutation research*, 557(1), pp.99–108.

Yang, M., Luo, J., Li, K., Hu, S., Ding, T., Liu, H., Sheng, P., Yang, M., 2018. Determination and pharmacokinetic study of guaiol in rat plasma by gas chromatography – mass spectrometry with selected ion monitoring. *Journal of Chromatography B*, 1085(March),

pp.30–35.

Yunker, M.B. Macdonald, R. W., Vingarzan, R., Mitchell, R. H., Goyette, D., Sylvestre, S., 2002. PAHs in the Fraser River basin : a critical appraisal of PAH ratios as indicators of PAH source and composition. , 33, pp.489–515.

Zupancic, N., 1999. Lead contamination in the roadside soils of slovenia. *Environmental Geochemistry and Health*, 21(1), pp.37–50.

8. Appendices

Appendix 1: Sample GPS coordinates and description

Sample ID	x cord	y cord	Sample appearance/description
DB201601	-6.105289	53.382057	Muddy sand
DB201602	-6.105289	53.382057	Heavy black mud
DB201603	-6.105289	53.382057	Heavy mud
DB201604	-6.105289	53.382057	Golf course sandy soil
DB201605	-6.105289	53.382057	Sandy mud
DB201606	-6.105289	53.382057	Salt marsh sandy mud
DB201607	-6.105289	53.382057	Sandy mud
DB201608	-6.105289	53.382057	Heavy sand, green algae cover
DB201609	-6.105289	53.382057	Black mud with sea shells
DB201610	-6.105289	53.382057	Sandy mud, near wall
DB201611	-6.105289	53.382057	Heavy black mud & green algae
DB201612	-6.105289	53.382057	Sand
DB201614	-6.128129	53.383901	black mud
DB201616	-6.162209	53.374592	Soil with grass cover
DB201617	-6.16158	53.371876	Dark mud with decayed seaweed
DB201618	-6.128608	53.38162	Heavy mud
DB201619	-6.144935	53.377827	Heavy black mud
DB201620	-6.173817	53.36571	Sand with black decayed seaweed
DB201621	-6.121488	53.3847	Heavy back mud
DB201622	-6.148964	53.377916	Heavy mud
DB201623	-6.15356	53.375668	Mud with seaweed cover
DB201624	-6.108865	53.384971	mud flats, sandy mud
DB201625	-6.159454	53.372631	Soil from road side
DB201626	-6.150846	53.373457	Salt marsh mud
DB201627	-6.157725	53.369912	Very wet soil
DB201629	-6.139616	53.37467	Heavy mud
DB201630	-6.148636	53.374222	Soil
DB201631	-6.144898	53.375845	Muddy soil
DB201632	-6.159283	53.368198	Soil
DB201633	-6.169153	53.362579	Soil
DB201634	-6.148519	53.375783	Mud flat mud with algae
DB201635	-6.138389	53.377894	Soil

DB201636	-6.162354	53.367846	Heavy muddy soil
DB201637	-6.171565	53.361769	Soil
DB201638	-6.156835	53.369829	Soil
DB201639	-6.14114	53.37709	Salt marsh channel, heavy black mud
DB201640	-6.161467	53.366599	Soil
DB201641	-6.125037	53.380938	salt marsh mud
DB201642	-6.159034	53.3721	Soil
DB201643	-6.144906	53.37578	Soil with bush vegetation
DB201644	-6.16557	53.36733	Mud at edge of salt marsh
DB201645	-6.166561	53.358872	Soil in dunes
DB201646	-6.167405	53.359752	Sandy soil, golf course
DB201647	-6.162428	53.357208	Soil, sand dunes
DB201648	-6.159008	53.361311	Soil, sand dunes
DB201649	-6.15121	53.367011	Soil, sand dunes
DB201650	-6.145856	53.368803	Sand dunes
DB201651	-6.133967	53.37271	Beach sand
DB201653	-6.13648	53.375996	Golf course sandy soil
DB201654	-6.117753	53.381827	Sand dune
DB201655	6.121541	53.380431	salt marsh soil

Appendix 2: PSA results for Bull Island samples

Sample ID	Mean (µm)	Sorting	Clay (%)	Silt (%)	Mud (%) [cl+silt]	Sand (%)	Description
Sample 1	272.04	1.28	0.94	4.13	5.07	94.93	poorly sorted sand
Sample 02	198.20	1.72	2.56	16.35	18.91	81.09	poorly sorted muddy sand
Sample 3	372.94	1.73	1.36	7.71	9.08	90.92	poorly sorted sand
Sample 5	283.06	1.54	1.15	8.84	9.99	90.01	poorly sorted sand
Sample 6	214.10	2.57	8.99	27.22	36.21	63.79	very poorly sorted muddy sand
Sample 7	144.34	1.67	3.15	19.64	22.79	77.21	poorly sorted muddy sand
Sample 10	197.41	0.72	0.34	0.28	0.61	99.39	moderately sorted sand
Sample 14	178.52	0.41	0.00	0.00	0.00	100.00	well sorted sand
Sample 15	188.43	2.70	11.55	37.73	49.28	50.72	very poorly sorted muddy sand
Sample 17	155.81	1.59	3.06	12.61	15.67	84.33	poorly sorted muddy sand
Sample 19	161.08	1.91	4.55	20.28	24.82	75.18	poorly sorted muddy sand
Sample 23	106.86	2.52	14.14	43.75	57.89	42.11	very poorly sorted sandy mud
Sample 25	225.06	2.17	4.35	27.56	31.91	68.09	very poorly sorted muddy sand
Sample 28	122.20	2.08	6.92	28.70	35.62	64.38	very poorly sorted muddy sand
Sample 30	464.23	3.07	9.25	24.05	33.30	66.70	very poorly sorted muddy sand
Sample 32	186.21	2.35	8.13	18.71	26.84	73.16	very poorly sorted muddy sand
Sample 34	107.59	2.31	10.58	34.11	44.69	55.31	very poorly sorted muddy sand
Sample 36	506.90	2.04	2.54	10.19	12.72	87.28	very poorly sorted muddy sand
Sample 37	330.61	2.81	8.20	26.90	35.11	64.89	very poorly sorted muddy sand
Sample 39	169.22	1.34	1.73	8.71	10.45	89.55	poorly sorted muddy sand
Sample 41	238.25	2.66	9.09	31.22	40.31	59.69	very poorly sorted muddy sand
Sample 44	168.11	1.34	2.15	6.70	8.85	91.15	poorly sorted sand
Sample 45	198.44	0.86	0.68	0.56	1.25	98.75	moderately sorted sand
Sample 47	190.43	0.84	0.57	0.55	1.12	98.88	moderately sorted sand
Sample 45	172.32	0.44	0.00	0.02	0.02	99.98	well sorted sand
Sample 49	156.45	0.42	0.00	0.16	0.16	99.84	well sorted sand
Sample 53	184.92	0.45	0.00	0.00	0.00	100.00	well sorted sand
Sample 54	190.99	0.41	0.00	0.00	0.00	100.00	well sorted sand
Sample 55	319.04	2.49	6.12	18.98	25.10	74.90	very poorly sorted muddy sand
Sample 56	234.43	2.00	4.39	12.32	16.71	83.29	very poorly sorted muddy sand
Sample 60	172.26	0.41	0	0.00	0.00	100.00	well sorted sand

Appendix 3: Organic matter (OM), nitrogen (N), Carbon (C), C: N ratio and TOC results for Bull Island samples

ID	%OM	%N	%C	C:N ratio	%TOC	ID	%OM	%N	%C	C:N ratio	%TOC
01	0.93	0.046	0.359	4.43	0.20	**32**	7.07	0.153	2.977	12.02	1.84
02	3.64	0.061	0.826	12.66	0.77	**33**	48.14	1.096	15.775	0.16	0.17
03	4.05	0.020	0.480	37.13	0.74	**34**	6.49	0.120	2.370	1.28	0.15
04	7.48	0.067	2.803	10.99	0.73	**35**	32.65	0.757	10.154	8.81	6.67
05	3.20	0.074	1.493	18.08	1.34	**36**	23.48	1.013	10.733	9.19	9.31
06	9.24	0.264	4.682	10.05	2.65	**37**	13.85	1.308	17.676	2.97	3.89
07	5.76	0.133	1.910	9.38	1.25	**38**	61.5	1.340	16.759	9.49	12.72
08	2.32	0.045	0.610	7.57	0.34	**39**	3.2	0.856	1.880	0.68	0.58
09	3.43	0.054	0.870	10.81	0.58	**40**	53.9	1.970	25.480	8.09	15.95
10	3.16	0.095	1.026	7.77	0.74	**41**	13.9	0.290	4.030	14.38	4.17
11	0.83	0.036	0.599	14.19	0.51	**42**	14.4	1.343	17.680	4.71	6.32
12	1.95	0.023	0.809	18.72	0.43	**43**	14.78	0.659	6.667	8.15	5.37
14	1.50	0.043	0.509	5.39	0.23	**44**	2.15	0.065	0.480	3.85	0.25
15	8.69	0.370	2.982	0.68	0.25	**45**	10.89	0.060	2.127	28.22	1.69
16	11.73	1.001	16.134	9.40	9.41	**46**	4.95	0.176	3.472	10.48	1.84
17	3.86	0.033	1.250	12.00	0.40	**47**	13.26	0.093	3.580	28.18	2.63
18	2.03	0.086	0.621	2.33	0.20	**48**	11.14	0.151	4.450	23.55	3.56
19	2.75	0.046	2.002	1.62	0.08	**49**	12.05	0.189	4.430	10.85	2.05
20	4.19	0.693	15.837	1.88	1.30	**50**	1.10	0.023	0.730	6.96	0.16
21	2.06	0.049	0.623	3.86	0.19	**51**	1.30	0.029	0.600	9.66	0.28
22	7.38	0.033	1.380	10.20	0.34	**52**	0.95	0.050	0.970	13.60	0.68
23	10.90	0.178	3.334	12.43	2.21	**53**	18.28	0.130	2.980	15.62	2.03
24	0.31	0.039	0.968	269.74	10.52	**54**	0.75	0.030	0.597	7.33	0.22
25	30.31	0.659	9.531	12.83	8.45	**56**	0.85	0.024	0.810	15.00	0.36
26	1.39	0.026	0.403	175.64	4.57	**57**	1.30	0.026	0.660	3.85	0.10
27	22.00	0.102	0.788	1.96	0.20	**60**	1.78	0.030	0.500	5.33	0.16
28	3.20	0.698	9.433	1.72	1.20	**61**	0.56	0.005	0.100	2.00	0.00
29	55.99	0.817	10.983	5.23	4.27	**62**	0.88	0.040	0.900	7.75	0.31
30	4.98	0.355	4.492	11.76	4.17	**63**	1.30	0.022	0.460	7.27	0.16
31	4.97	0.408	5.468	12.22	4.98						

Appendix 4: pH and EC values in BI samples

ID	pH	EC (mS/cm)	ID	pH	EC (mS/cm)
01	8.88	3098.67	**32**	7.58	4706.67
02	8.95	3536.67	**33**	6.33	6650.00
03	8.85	2690.33	**34**	7.83	6470.00
04	7.99	4253.33	**35**	8.24	9.255
05	8.93	4386.67	**36**	6.69	6663.33
06	7.42	6173.33	**37**	6.92	5426.67
07	8.26	3164.33	**38**	7.57	6880
08	8.08	2769.67	**39**	8.66	3786.67
09	8.71	3456.67	**40**	7.58	7360.00
10	8.69	3660	**41**	7.68	6700
11	8.91	2993.67	**42**	7.6	8910
12	8.39	4790	**43**	7.75	6090.00
14	8.33	2701.33	**44**	7.74	2452.33
15	8.08	5883.33	**45**	7.50	79.00
16	6.56	7890.00	**46**	8.22	105.57
17	7.34	3530.00	**47**	7.76	175.87
18	8.65	2869.67	**48**	8.37	111.30
19	8.17	5.19	**49**	7.41	141.83
20	8.46	3006.33	**50**	8.92	52.27
21	8.76	2836.67	**51**	8.13	3090.00
22	7.65	4176.67	**52**	8.40	77.36
23	7.84	6943.33	**53**	9.40	100.57
24	8.59	3326.67	**54**	8.91	56.57
25	8.26	257.53	**56**	8.38	3.70
26	7.86	3966.67	**57**	8.00	4.18
27	8.36	3229.33	**60**	8.43	3.20
28	8.25	3002.02	**61**	8.10	5.00
29	7.07	138.3	**62**	8.25	3.85
30	7.43	1217	**63**	8.40	4.11
31	7.47	5870			

Appendix 5: Sum PAH values in BI samples

Sample	Sample appearance	∑PAH ng/g	Sample	Sample appearance	∑PAH ng/g
01	Mudflats muddy sand	<LOQ	**30**	Soil	3027.934
02	Heavy mud, black organic matter	453.780	**31**	Muddy soil	1499.869
03	Heavy mud	758.341	**32**	Soil	7498.320
04	Golf course sandy soil	868.386	**33**	Soil	1658.012
05	Sandy mud	630.619	**34**	Mud flat mud with algae	884.840
06	Salt marsh sandy mud	1130.510	**35**	Soil	1587.805
07	Sandy mud	763.385	**36**	Heavy muddy soil	5850.058
08	Heavy sand, green algae cover	838.791	**37**	Soil	786.357
09	Mud flat heavy mud with sea shells	3462.117	**38**	Soil	4596.529
10	Mud flat, sandy mud, near wall	27.469	**39**	Heavy black mud	<LOQ
11	Heavy black mud and green algae	113.358	**40**	Soil	1103.608
12	Sand	800.369	**41**	salt marsh mud	6869.458
14	black mud	386.206	**42**	Soil	4156.845
16	Soil with grass cover	8182.542	**43**	Soil with bush vegetation	1964.965
17	Dark mud with decayed seaweed	3621.907	**44**	Mud at edge of salt marsh	1055.119
18	heavy mud	<LOQ	**45**	Soil, sand dunes	240.090
19	Heavy mud, black organic matter	1139.025	**46**	Sandy soil, golf course	7621.404
20	Sandy with black decayed seaweed	2587.463	**47**	Soil, sand dunes	304.972
21	Heavy back mud	25.380	**48**	Soil, sand dunes	4.605
22	Heavy mud	290.444	**49**	Soil, sand dunes	1234.448
23	Mud with seaweed cover	1423.313	**50**	Sand dunes	<LOQ
24	mud flats, sandy mud	<LOQ	**51**	Beach sand	<LOQ
25	Soil from road side	6367.384	**53**	Golf course sandy soil	352.906
26	Salt marsh mud	<LOQ	**54**	Sand dune	<LOQ
27	Very wet soil	3530.959	**55**	salt marsh soil	889.534
29	Heavy mud	2213.753	**61**	intertidal sand	<LOQ
			62	intertidal sand	<LOQ

Appendix 6: Loading scores for all tested variables for component 1 and 2.

	PC 1	PC 2
pH	-0.00783	-0.01166
EC	0.45404	-0.71072
%OM	0.20103	0.32013
N	0.23841	0.33252
C	0.20818	0.3793
C/N Ratio	-0.03022	0.046743
TOC	0.23711	0.34276
TOC/N	-0.00102	0.008987
PAH ng/g	0.76841	0.017584
Fe	0.073542	0.090093
Ca	-0.00793	-0.06335
Al	0.008786	-0.00185
Pb	0.005744	-0.01048
Cr	0.005388	-0.07426

Appendix 7: Loadings scores for component 1 and 2, with variables grouped by organic matter content (OM)

	PC 1	PC 2
pH	-0.00022	1.37E-05
EC	0.83886	-0.5349
%Moistur	0.005458	-5.19E-05
%OM	0.005797	0.002226
N	0.000174	3.89E-05
C	0.002297	0.000766
C/N Ratio	-0.0006	-0.001
TOC	0.00104	0.000943
TOC/N	-0.00463	-0.00104
PAH ng/g	0.52957	0.76
Al	0.12375	0.36773
Pb	0.021495	0.032333
Cr	0.002589	0.001791